Investigation of peripheral blood immune cell subsets and cytokine levels in females living with breast cancer before and after first-phase chemotherapy

Nicole Ambrin Chicken

A dissertation submitted to the Faculty of Health Sciences, University of Pretoria, Tshwane, in fulfilment of the requirements for the degree Master of Science

Tshwane, 2025

Declaration

I, Nicole Ambrin Chicken, declare that this dissertation is my own work. It is being submitted for the degree of Master of Science at the University of Pretoria, Tshwane. It has not been submitted before for any degree or examination at this or any other university.

_____

Signature

On this day the 10th of January 2025 in Tshwane

Executive summary

Introduction: Breast cancer is the most frequently diagnosed cancer in females in sub-Saharan Africa and up to 80% of cases are stage 3 or 4 tumours. Triple-negative breast cancer (TNBC) accounts for up to 20% of all breast cancer cases and is aggressive, highly metastatic, tends to be diagnosed in younger women, and has a 5-year survival rate of 60%. This breast cancer subtype has limited treatment options due to its hormone insensitivity and heightened proliferative potential. The tumour microenvironment is a key driver of tumourigenesis and consists of different cancer cell clones, normal stromal cells, cytokines, chemokines, growth factors, and immune cells. Manipulation of the tumour microenvironment by cancer cells to promote tumour progression and metastasis has been observed in both breast and other cancer types and affects treatment response and patient prognosis. Immune cells and cytokines within the tumour microenvironment and the circulation may play a pro- or anti-tumourigenic role in TNBC and therefore act as potential surrogate biomarkers. The aim of this study was to compare immune cell subsets and cytokine levels in peripheral blood between healthy donors and TNBC patients, and in patients before and after first-phase (at least 3 cycles) of chemotherapy.

Methods: Twenty-three patients recently diagnosed with TNBC and ten healthy donors consented to participate in this study. Patients were recruited from a private clinic in Johannesburg, Gauteng with their consent. Blood was collected prior to treatment and after first-phase chemotherapy. Full blood counts, patient demographics, and treatment response were recorded. The percentage of circulating $CD4^+$ and $CD8^+$ T-cells, B-cells, natural killer (NK) cells, monocytes, and regulatory T-cells (Tregs) as well as the expression of various cell markers was evaluated by flow cytometry and compared between participant groups. The concentrations of vascular endothelial growth factor (VEGF), granulocyte-macrophage colony stimulating factor (GM-CSF), growth and differentiation factor 15 (GDF-15), Interleukin-6, -8, and -10 (IL-6, -8, -10) and interferon gamma-induced protein (IP-10) were evaluated in participant plasma by enzyme-linked immunosorbent assays (ELISAs) and the results were compared between participant groups. These were also compared to treatment outcomes.

Results: This study showed an increase in the percentage of $CD14^+$ monocytes and $CD56^{high}$ NK cells, and a decrease in $CD19^+$ B-cells after first-phase chemotherapy, while no significant differences in cell percentages were seen between healthy donors and treatment-naïve patient

groups. The expression of CD206 was increased in B-cells and monocytes, while HLA-DR expression was increased on NK cells after first-phase chemotherapy. While little difference in the median Treg percentage was observed between patient groups, changes in the number of Tregs were observed after first-phase treatment when looking at individual patients, suggesting that observations may be patient-specific. An increase in expression of CD39, CD45RA, Helios, and CD127 was observed in Tregs after first-phase treatment. The concentrations of VEGF and GM-CSF were similar between patient and healthy donor groups, while IL-6, -8, and -10, and IP-10 and GDF-15 were increased in the post first-phase treatment plasma.

Conclusion: This study provides valuable insights into the dynamic changes in immune cell subsets and cytokine levels in TNBC patients undergoing chemotherapy. The observed alterations in T-cells, B-cells, NK cells, monocytes, and Tregs, along with their associated markers, suggest a complex interplay between the immune system and cancer progression. The increased levels of specific cytokines post-treatment highlight potential biomarkers for monitoring treatment response and disease progression. These findings contribute to our understanding of the immune landscape in TNBC and may inform future strategies for immunotherapy and personalized treatment approaches. Further research is warranted to elucidate the functional implications of these changes and their potential as prognostic indicators or therapeutic targets in TNBC management.

Key words: breast cancer, TNBC, flow cytometry, ELISA, immune cells, cytokines, chemotherapy, biomarkers, TME, Tregs.

Acknowledgements

I would like to express my sincere gratitude to my supervisor, Dr. CM Worsley, and my co-supervisor, Professor PWA Meyer, for all the support and guidance they have given me since my enrolment in the Department of Medical Immunology. I would also like to thank them for their patience as I have learnt and adapted to the postgraduate world and for answering all of my many, many questions.

I would like to thank my whole family, especially my Mom, Dad, and brother, Tristan, for all the support they have given me not only during this degree but also during my entire academic career. I would never have been able to get to where I am today without them pushing me onward. I would also like to acknowledge my dog, Bella, whose cuddles were key to my survival.

I would like to thank Shududfhadzo Singo for all the laughs, walks, and “hai’s”. Even though we had to fight our respective battles on our own, having someone get grey eyebrows in the trenches next to you makes things just a little bit easier.

I would like to thank the National Research Foundation and the University of Pretoria for funding me during this degree.

Finally, I would like to thank our Heavenly Father for all He has done and for holding my hand each step of the way.

Proverbs 3:5-6 “Trust in the Lord with all your heart, And lean not on your own understanding; In all your ways acknowledge Him, And He shall set your path straight”.

Table of Contents

List of abbreviations and symbols

µl	microlitre
ADP	adenosine diphosphate
AF647	Alexa Fluor 647
AF700	Alexa Fluor 700
AJCC	American Joint Committee on Cancer
AMP	adenosine monophosphate
APC	allophycocyanin (reference to fluorophore)
APC	antigen presenting cell (reference to cell type)
APC-AF750	allophycocyanin-Alexa Fluor 750
ATP	adenosine triphosphate
BMI	body mass index
Breg	regulatory b-cell
BV780	Brilliant Violet 780
CAF	cancer associated fibroblast
CCL5	chemokine (C-C motif) ligand 5
CCR7	C-C motif receptor 7
CD	cluster of differentiation
CD45RA	cluster of differentiation molecule 45 residues on exon A
CXCL-12	C-X-C motif chemokine ligand 12
CXCL-8	C-X-C motif chemokine ligand 8
CXCR3	C-X-C motif receptor 3
DNA	deoxyribonucleic acid
DOX	Docetaxel and Cyclophosphamide
ECD	R-Phycoerythrin-Texas Red-X energy-coupled dye

ECM	extracellular matrix
ECOG	Eastern Cooperative Oncology Group
EDTA	ethylenediaminetetraacetic acid
EGF	epidermal growth factor
ELISA	enzyme-linked immunosorbent assay
ELISPOT	enzyme-linked immunospot
EMT	epithelial-mesenchymal transition
ER	oestrogen receptor
FBC	full blood count
FBS	foetal bovine serum
FCS	flow cytometry standard
FITC	fluorescein isothiocyanate
FoxP3	forkhead box protein P3
FSC-A	forward scatter area
FSC-H	forward scatter height
G-CSF	granulocyte-colony stimulating factor
GDF-15	growth and differentiation factor 15
GM-CSF	granulocyte-macrophage colony stimulating factor
HER2	human epidermal growth factor receptor 2
HGF	hepatocyte growth factor
HIV	human immunodeficiency virus
HLA-DR	human leukocyte antigen - DR isotype
HRP	horseradish peroxidase
IDO	indoleamine 2,3-dioxygenase
IGF	insulin-like growth factor
IL-10	interleukin-10
IL-13	interleukin-13

IL-17	interleukin-17
IL-2	interleukin-2
IL-4	interleukin-4
IL-5	interleukin-5
IL-6	interleukin-6
IL-8	interleukin-8
IL-9	interleukin-9
IM	immunophenotyping
IP-10	interferon gamma-induced protein 10
Ki-67	antigen kiel 67
KrO	Krome Orange
M-CSF	macrophage colony-stimulating factor
MDSC	myeloid-derived suppressor cell
MFI	mean fluorescence intensity
min	minutes
ml	millilitre
NCAM	neural cell adhesion molecule
NK	natural killer
NKT	natural killer T-lymphocyte
NLR	neutrophil-lymphocyte ratio
OD	optical density
ODU	optical density units
PB	Pacific Blue
PBS	phosphate buffered saline
PC5.5	R-Phycoerythrin-Cyanine 5.5
PC7	Phycoerythrin-Cyanine 7
PCR	pathological complete response

PD1	programmed cell death protein 1
PDGF	platelet-derived growth factor
PD-L1	programmed cell death ligand 1
PE	phycoerythrin
pg/ml	picograms per millilitre
pH	potential of hydrogen
pHe	extracellular potential of hydrogen
pHi	intracellular potential of hydrogen
PIC	persistent invasive carcinoma
PR	progesterone receptor
PS	performance status
QC	quality control
RCF	relative centrifugal force
ROS	reactive oxygen species
RT	room temperature
RTU	ready to use
s	seconds
SARS-CoV-2	Severe-Acute Respiratory Syndrome Coronavirus 2
SCID	severe combined immunodeficiency disease
SSA	sub-Saharan Africa
SSC-A	side scatter area
TAC	Taxotere-Adriamycin-Cyclophosphamide
TAM	tumour associated macrophage
TAN	tumour associated neutrophil
TAP 1	transporter associated with antigen processing 1

TAP 2	transporter associated with antigen processing 2
TCR	t-cell receptor
TGF-β	transforming growth factor beta
Th0	naïve helper T-cell
Th1	T helper 1
Th17	T helper 17
Th2	T helper 2
TIL	tumour infiltrating lymphocyte
TME	tumour microenvironment
TNBC	triple-negative breast cancer
TNF-α	tumour necrosis factor alpha
Treg	regulatory T-cell
USA	United States of America
VEGF	vascular endothelial growth factor

List of Figures

List of Tables

Chapter 1: General introduction

1.1 Cancer

Cancer is a disease in which cells proliferate uncontrollably[1]. This uncontrolled growth is caused by genetic instability and selective pressures in the tumour microenvironment (TME) that affect how cells respond to proliferative and apoptotic signals[1]. Several risk factors influence cancer initiation including infections from pathogens (such as *Helicobacter pylori*, and the Hepatitis B and C viruses), exposure to alcohol, aflatoxin, tobacco smoke, radiation, and ultraviolet rays, as well as sedentary lifestyle, poor diet, and high levels of stress[2, 3]. Cancer can arise in different cell types, tissues, and organs, and are described based on their origins (Fig. 1.1).

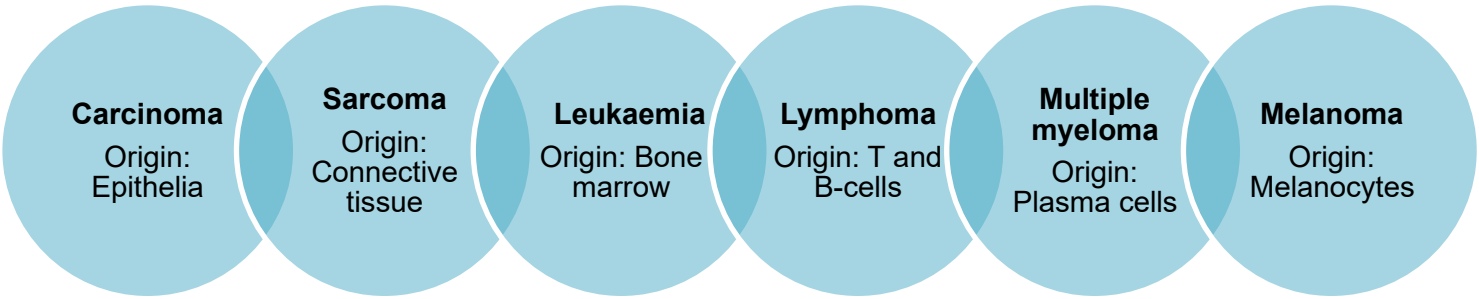

Figure 1.1: **The main cancer classes.** Cancer can arise from many different cell types and tissues and is therefore described based on its origin[1]. For example, cancer of the epithelia is referred to as a carcinoma, whereas lymphomas originates from lymphocytes[1].

Cancer caused approximately 10 million deaths in 2022, with breast cancer being the second most commonly diagnosed cancer with 2.31 million newly diagnosed cases globally (Fig. 1.2)[4]. Approximately 665 000 breast cancer-related deaths occurred in the same year giving it the fourth highest cancer mortality rate in the world[4]. In South Africa, 111 321 cancer cases were diagnosed in 2022[5]. In the same year, 64 547 cancer-related deaths occurred[5]. Breast cancer had the highest incidence in South Africa, followed by prostate and cervix uteri cancers (Fig. 1.3)[5]. The incidence of cancer in South Africa is expected to double by 2030[6].

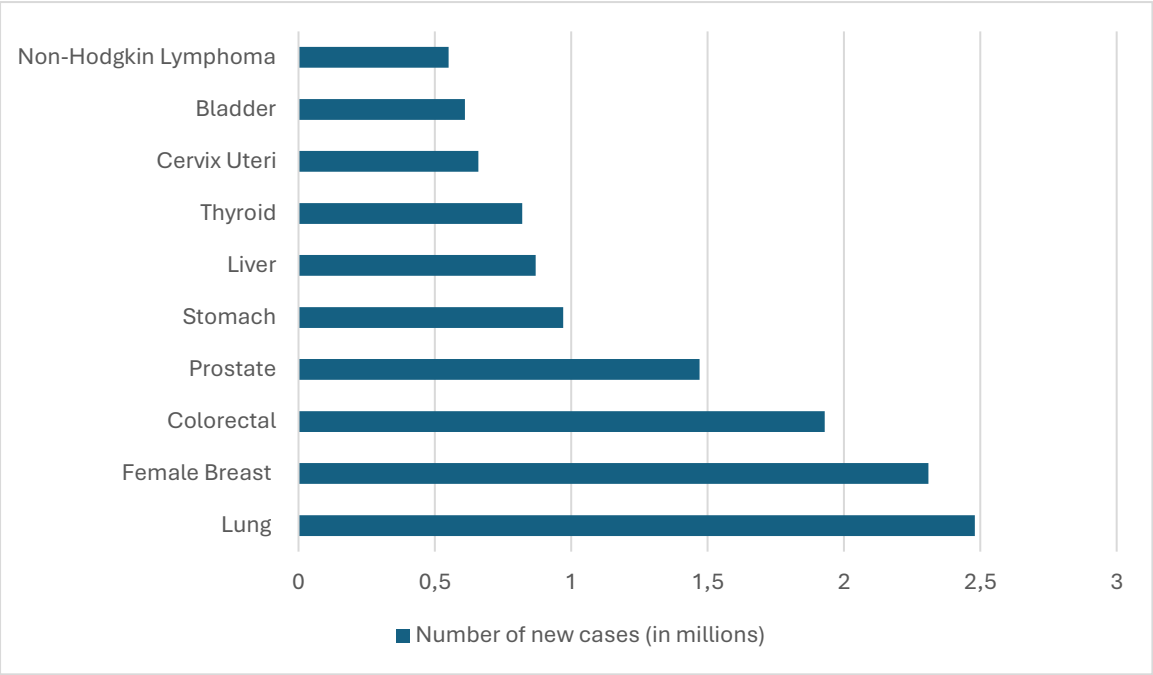

Figure 1.2: The ten most commonly diagnosed cancers worldwide. Cancer caused approximately 10 million deaths in 2022, with the top 10 most commonly diagnosed types of cancer being lung, female breast, colorectal, prostate, stomach, liver, thyroid, cervix uteri, and bladder cancer [4].

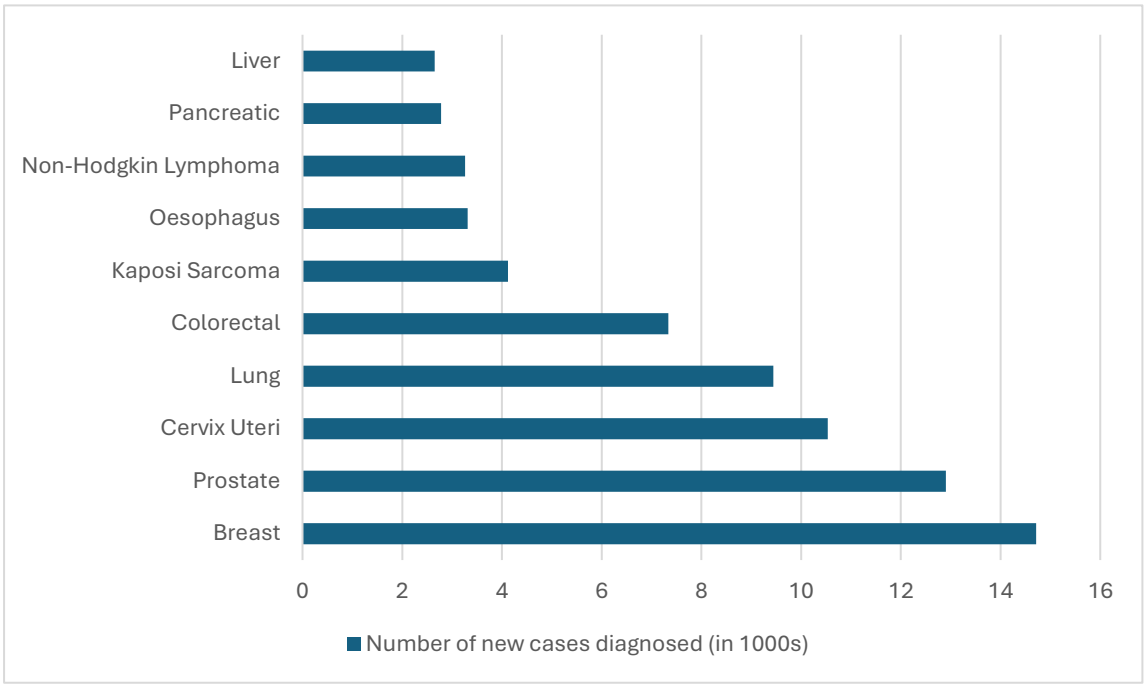

Figure 1.3: The most commonly diagnosed cancers in South Africa. In South Africa, 111 321 cancer cases were diagnosed in 2022[5]. The top 10 most frequently diagnosed cancers in South Africa are breast, prostate, cervix uteri, lung, colorectal, Kaposi Sarcoma, oesophageal, non-Hodgkin Lymphoma, pancreatic, and liver cancer[5].

As the incidence and mortality rates of breast cancer are rapidly increasing both locally and globally, a better understanding of tumourigenesis and immune surveillance is needed to improve the diagnosis and treatment of patients with this cancer type.

1.2 Breast cancer

Breast cancer is the most frequently diagnosed cancer in females in sub-Saharan Africa (SSA), with up to 80% of women diagnosed with stage 3 or 4 breast cancer compared to 15% of women in high-income countries[7]. SSA women also tend to be diagnosed at a younger age[7]. One in 26 South African women is at risk of developing breast cancer in their lifetime, with breast cancer accounting for 16% of all cancer-related deaths in South Africa[8]. The 5-year survival rates are better in high-income countries (up to 90%) than in poorer countries such as India (66%) and South Africa (40%)[9].

Although the incidence of breast cancer in SSA is lower than that of other regions, the mortality rates are significant[10]. A lack of disease awareness and access to adequate screening means that patients are diagnosed at an advanced disease stage, making treatment more difficult[6]. Several risk factors influence susceptibility to breast cancer, including sex, ancestry, age, lifestyle (exercise and eating habits, smoking, alcohol consumption), the presence of comorbidities, pregnancy and breastfeeding, as well as genetics[9].

Most breast cancers are adenocarcinomas which mostly occur in the ducts (85%) or lobular epithelium (15%)[11]. Breast cancer often presents as a painless lump along with changes in the appearance of the breast[11]. It is classified based on histology, anatomical origin (ductal or lobular), and the presence or absence of hormone receptors, such as oestrogen receptors (ER), progesterone receptors (PR), and human epidermal growth factor receptor 2 (HER2). The four main subtypes of breast cancer are luminal A (ER^+, PR^+, $HER2^-$), luminal B (ER^+, PR^+, $HER2^{\pm}$), HER2 positive, and triple-negative[12, 13].

Normal tissue homeostasis is maintained when cells cooperate with one another to promote the survival of the tissue or organ over that of individual cells[14]. These cooperative behaviours include maintaining a balance between cell proliferation and apoptosis, establishing

communication networks, suppressing mutations, and removing old or damaged cells[14]. Cancer develops when there is a breakdown in this cooperation and cells develop common characteristics that contribute to tumourigenesis[14].

1.3 The Hallmarks of Cancer

Hanahan and Weinberg (2000) described six hallmarks that characterize cancer cells, namely, continuous proliferation, insensitivity towards growth suppressor signals, avoidance of cell death, the ability to replicate continuously, the stimulation of angiogenesis, and the induction of invasion and metastasis (Fig. 1.4)[15, 16]. They later included two more hallmarks, namely, metabolic alterations and the avoidance of immune-mediated destruction (Fig. 1.5)[17].

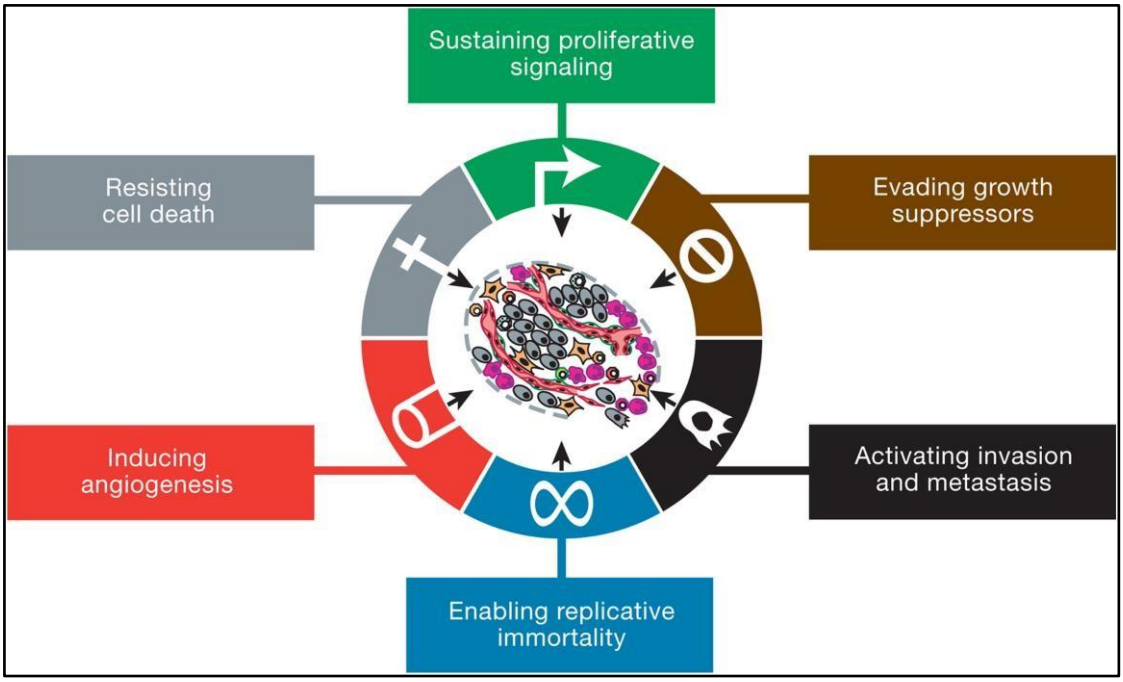

Figure 1.4: The hallmarks of cancer. All cancer cells possess the following six hallmarks: evasion of growth suppression, sustained proliferative signalling, resistance to cell death, induction of angiogenesis, enablement of replicative immortality, and activation of invasion and metastasis[14]. Illustration taken from reference [17]. Permission to use the published figure can be found in Appendix A, Figure 1.

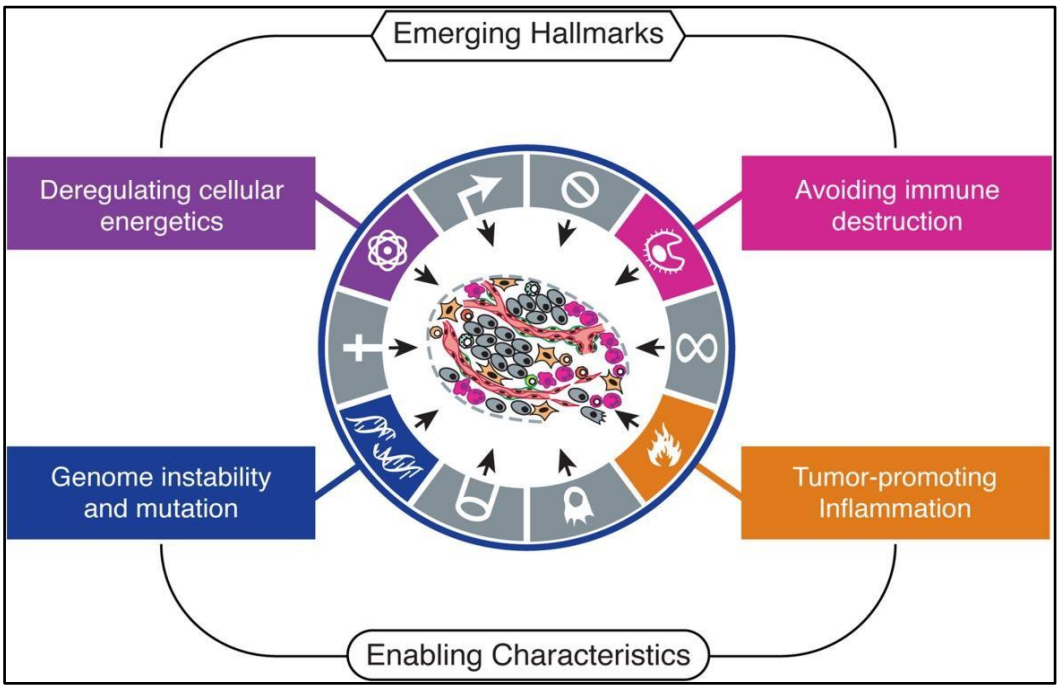

Figure 1.5: Additional hallmarks of cancer. Hanahan and Weinberg proposed another two hallmarks of cancer in addition to the original six to include deregulating cellular energetics and avoiding immune destruction with the enabling characteristics of tumour-promoting inflammation and genome instability and mutation[17]. Illustration taken from reference[17]. Permission to use the published figure can be found in Appendix A, Figure 1.

While normal cells require exogenous mitogenic signals to stimulate growth and proliferation, cancer cells are less dependent on these signals, as they can secrete growth factors in an autocrine manner and promote their own growth and survival (Fig. 1.4 and 1.5)[15, 16]. Normal cells undergo a form of programmed cell death termed apoptosis, which occurs in response to deoxyribonucleic acid (DNA) damage to prevent malignancy[15, 16]. The apoptotic pathways of a cell contain sensors that monitor both the external and internal environments for abnormalities such as DNA damage, insufficient quantities of survival factors, hypoxia, or oncogene gene products, while effectors mediate the release of pro-apoptotic enzymes and intracellular molecules such as proteases[15]. In contrast, cancer cells frequently upregulate oncogenes and downregulate tumour suppressor genes, enabling uncontrolled growth and proliferation[1, 15, 16]. They also evade apoptosis by disrupting anti-growth signal receptors and intracellular pathways[15, 16]. Tumour cells maintain their telomeres which allows for continuous cell division and expansion of the tumour[15, 16]. They also promote tumour growth and survival by stimulating angiogenesis, thereby securing the supply of nutrients and oxygen and the removal of waste products[15, 16].

As cancer cell proliferation increases and apoptosis is suppressed, the lack of space and resources within the TME becomes a challenge for growing tumours. To overcome this challenge, tumour cells invade surrounding tissues using extracellular proteases to degrade the extracellular matrix (ECM)[15, 16]. As cells migrate, they intravasate into the blood or lymphatic vessels and are transported to distant sites, where they form secondary tumours or metastases[15, 16].

While a cancer cell-centric view has dominated cancer research, recent work has focused on the TME as a key component driving tumour cell evolution and disease progression. Intra-tumoural heterogeneity is caused by genetic and epigenetic changes as well as factors within the TME[18]. A better understanding of the TME could help identify key targets to improve treatment outcomes.

1.4 The tumour microenvironment

The TME is a key factor that drives tumourigenesis[19, 20]. It is heterogeneous and comprised of different cancer cell clones, normal stromal cells, signalling molecules, such as cytokines and chemokines, and immune cells (Fig. 1.6)[19, 20]. Normal cells within the TME include fibroblasts, endothelial cells, and adipocytes[19, 20].

Fibroblasts within the TME support tumour growth and development through ECM remodelling and secretion of growth factors and inflammatory molecules. Cancer-associated fibroblasts (CAFs) also regulate epithelial-mesenchymal transition (EMT) in breast cancer through the secretion of molecules such as C-X-C motif chemokine ligand 12 (CXCL-12)[21]. Endothelial cells promote angiogenesis by releasing vascular endothelial growth factor (VEGF) and support the invasion of breast cancer cells through Jag1/Notch signalling[22]. Adipocytes drive tumour progression through the release of inflammatory molecules, such as interleukin-6 (IL-6) and tumour necrosis factor α (TNF-α), as well as by suppressing cytotoxic T-cells[23]. Bi-directional signalling occurs between tumour cells and stromal components, with the tumour driving the reprogramming of normal cells to promote tumourigenesis[19, 20]. As components of the TME affect clinical outcomes, they provide possible therapeutic targets.

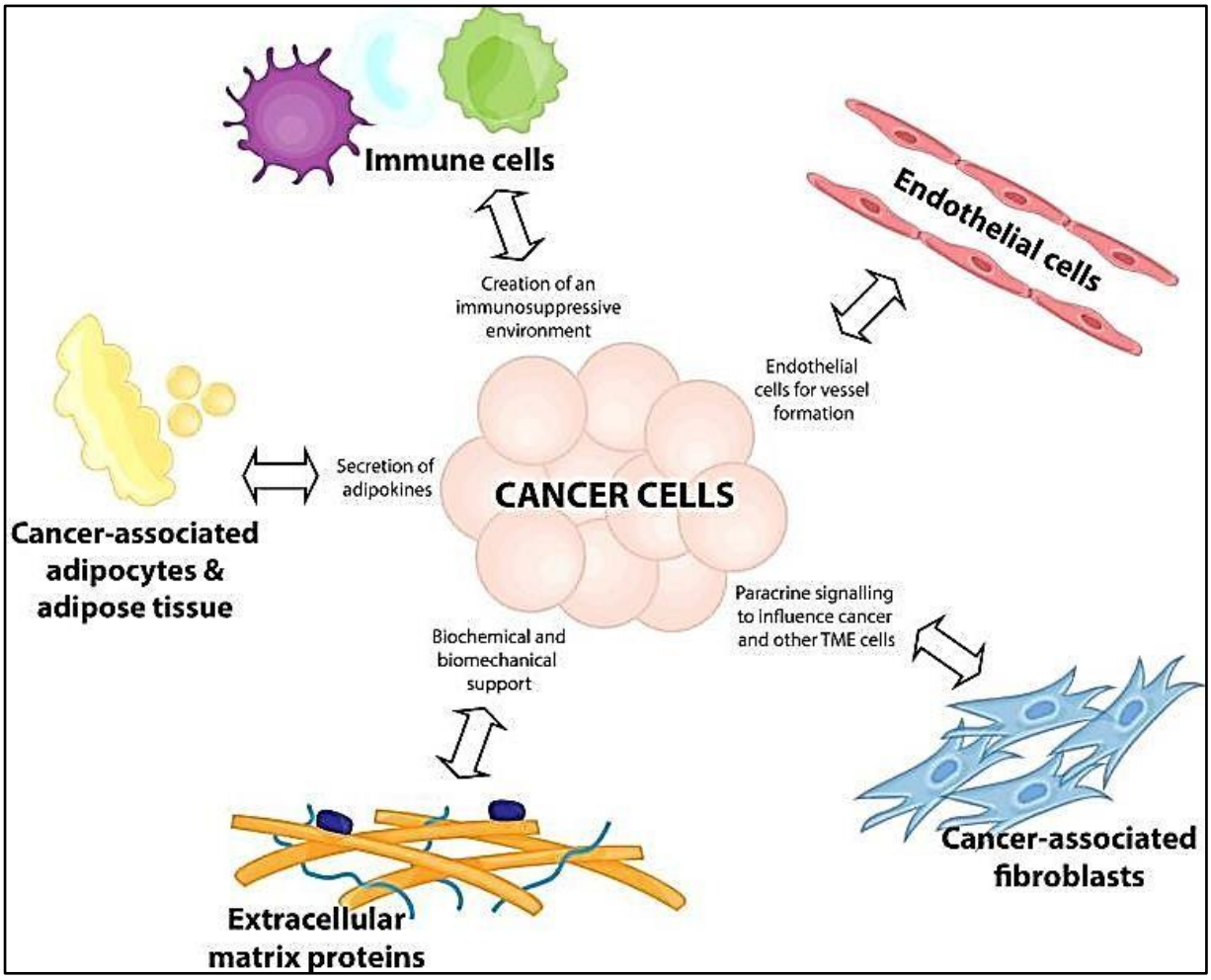

Figure 1.6: The tumour microenvironment. The TME is a key driver of tumourigenesis. It is highly heterogeneous and is composed of various cancer cell clones, normal stromal cells, such as fibroblasts and endothelial cells, signalling molecules, such as cytokines and chemokines, and immune cells[19, 20]. Illustration taken from reference[24]. Refer to Appendix A, Figure 2 for permission to use the published figure.

Although tumour cells stimulate angiogenesis, it is often an inefficient process with the formation of suboptimal blood vessels. This creates hypoxic areas within the tumour mass. Under low-oxygen conditions, tumour cells switch metabolic strategies and favour aerobic glycolysis over oxidative phosphorylation, known as the Warburg effect, which has been documented in many cancer types[17]. Aerobic glycolysis, which is inefficient in producing adenosine triphosphate (ATP), converts large amounts of glucose into lactate and generates metabolic intermediates that can be used in the synthesis of cell components[25]. This allows for rapid cellular and population growth in cancer cells[25].

Aerobic glycolysis generates metabolic by-products such as hydrogen ions and lactate which increase intracellular acidity. Normal cellular functioning requires an intracellular potential of hydrogen (pHi) of 7.2-7.4, while a low potential of hydrogen (pH) prevents normal cell functioning. Cancer cells adapt by upregulating molecules that export protons and lactate to maintain pHi. This results in a decrease in the extracellular pH (pHe) of the TME to a pH of 6.5 – 6.9. Normal cells, particularly immune cells, are inhibited by the extracellular acidity in the TME. Hydrogen ions within the TME also stimulate tissue remodelling and promote cell detachment from the tumour[26]. Overall, aerobic glycolysis promotes the survival and expansion of tumours[17].

The immune system plays an important role in cancer prevention. Many immune cells are present in the TME, some of which are inhibited, while others are pro-tumourigenic. The presence of T and B-lymphocytes, and natural killer (NK) cells is linked to good prognosis, while immunosuppressive cells such as regulatory T-cells (Tregs), myeloid derived suppressor cells (MDSCs), and M2 macrophages are linked to tumour progression[19, 20, 27-29].

As the tumour develops, an immunosuppressive TME can be created through the release of immunosuppressive factors and checkpoint molecules by cancerous and non-cancerous cells of the TME[28, 29]. Several factors released by cancer cells and stromal cells promote the evasion of immune-mediated cancer cell destruction. Transforming growth factor-β (TGF-β) is secreted by tumour cells specifically to promote tumour cell growth and also regulates lymphocyte, NK, macrophage, and dendritic cell proliferation, differentiation, survival, and activation[30]. Interleukin-10 (IL-10) impairs dendritic cell function and downregulates the expression of transporters associated with antigen processing 1 and 2 (TAP 1 and 2), which helps cancer cells evade destruction by cluster of differentiation molecule (CD) 8 positive T-cells[31].

Tumour cells also evade immune-mediated death by upregulating the expression of checkpoint molecules, programmed cell death protein 1, and programmed cell death ligand 1 (PD-1/PDL1). In breast cancer, this promotes $CD8^+$ T-cell apoptosis and tumour development[31]. Autocrine and paracrine TGF-β signalling can delay the progression of breast cancer if it is activated in premalignant lesions, but if present in later stages of the disease, it promotes angiogenesis, immune evasion, and metastasis, and can be immunosuppressive by activating MDSCs and Tregs[32]. The release of the enzyme indoleamine 2,3-dioxygenase (IDO) from tissue macrophages promotes T-cell anergy and Treg differentiation which allows cancer cells to evade and escape immune detection and desruction[33, 34]. High levels of reactive

oxygen species (ROS) produced by tumour-associated macrophages (TAMs), tumour-associated neutrophils (TANs), MDSCs, and cancer cells in the TME serve as immunosuppressive molecules, because the high levels of ROS frequently found in the TME are not conducive to the functioning of anti-tumourigenic immune cells[33]. Cancer cells can adapt to high levels of ROS by upregulating their antioxidant cellular pathways[33].

IL-6 and interleukin-8 (IL-8) levels are elevated in patients with breast cancer and correlate with breast cancer stage and mortality[32]. Interleukin-4, -10, and -7 promote the development of breast cancer cells, and increased levels are associated with increased breast cancer related mortality[32]. TNF-α enhances the migratory potential of breast cancer cells, and co-expression with IL-6 is associated with reduced survival and greater nodal involvement[32]. A previous study conducted in the Department of Immunology of the University of Pretoria found that immune checkpoints and immunomodulatory proteins were dysregulated in breast cancer patients[35]. While the reasons for this are unclear, elevated levels of macrophage colony-stimulating factor (M-CSF) and chemokine (C-C motif) ligand 5 (CCL5) suggest the involvement of suppressor immune cells such as M2 macrophages[35].

While acute inflammation can create a hostile environment for tumour growth, persistent and misdirected inflammation can drive tumourigenesis through the formation of an immunosuppressive niche. This has implications for the treatment of the disease, with a large emphasis placed on driving appropriate immune responses to control tumour growth.

1.5 Cancer treatment and relapse

Cancer treatment focuses on either preventing tumour cell proliferation or promoting apoptosis. Common treatment strategies include surgery, chemotherapy, and radiation therapy, with the inclusion of hormone therapy and stem cell or bone marrow transplantation, depending on the type of cancer[36-40]. Breast cancer is typically treated using a combination of surgery, radiation therapy, chemotherapy, and hormone therapy[41]. Conventional cancer treatment kills both tumour and bystander stromal cells, including immune cells. Neutropenia and leukopenia is often reported in patients post chemotherapy[42]. While the white blood cell count eventually recovers, different immune cells may recover at different rates. Which cell types do or do not recover, as well as the activity of these cells, may influence treatment success and long-term patient outcomes.

Obtaining greater insight into the effect of cancer treatments, such as chemotherapy, on circulating immune cell subsets, treatment success, and disease outcomes in patients with breast cancer may feed forward into the improvement of existing diagnostic and treatment procedures and act as a sturdy foundation for the development of new techniques.

1.6 Study Aims and Objectives

The aim of this study was to compare the immune cell subsets and cytokine levels in the peripheral blood of healthy controls and triple-negative breast cancer (TNBC) patients, and of patients before and after first-phase chemotherapy.

The first objective was to recruit treatment-naïve patients with TNBC and to develop and evaluate a flow cytometric method to perform immunophenotyping of the circulating immune cells. The second study objective was to compare immunophenotypic profiles of healthy controls to treatment-naïve TNBC patients, and of patients before and after first-phase chemotherapy using flow cytometry. The final objective of this study was to measure pro- and anti-tumourigenic cell function by detecting cytokines in healthy controls and TNBC patients before and after first-phase chemotherapy using enzyme-linked immunosorbent assays (ELISAs).

Chapter 2: Development of a flow cytometric method to characterise immune cell subsets in the peripheral blood of triple-negative breast cancer patients before and after first-phase chemotherapy

2.1 Introduction

The first fluorescence-based flow cytometer was developed in 1968 in Germany and subsequently commercialised[43-45]. Initially, flow cytometry allowed researchers to analyse a limited number of cell populations simultaneously owing to constraints in fluorophore and laser technology[43-45]. At present, flow cytometry enables the analysis of numerous cell populations within a single sample owing to advancements in laser and detector technology, fluorophore optimisation, and improvements in data analysis software[43-45]. Flow cytometers, when integrated with a cell sorter, facilitate the separation of distinct cell populations for further investigation[43, 44].

The use of appropriate antibodies is necessary to identify and distinguish between the different cell populations present in different sample types. In peripheral blood samples, erythrocytes must be lysed to prevent non-specific binding of antibodies, and the remaining cells are incubated with fluorophore-labelled antibodies against the markers of interest[43-45]. As the labelled cells pass through the flow cell of the flow cytometer, the fluorophores are activated by a laser, and the emitted light is collected, quantified, and converted into an electrical signal, which is subsequently plotted onto graphs for analysis[43-45]. Emitted and scattered light is captured by various detectors and information on cell size, internal complexity, cell surface markers, and intracellular markers is acquired[43-45]. Flow cytometry can be conducted on liquid samples (for example, blood, serum, plasma, and pleural effusions), bone marrow aspirates, or on mechanically and enzymatically digested solid tissues[43, 44].

Flow cytometry has advanced the discovery of disease biomarkers and has particular utility in the diagnosis of haematological malignancies. In addition, it aids in monitoring immune cell phenotypes in autoinflammatory and autoimmune disorders, and provides information regarding the immune response to infectious diseases[44].

Understanding and characterising the immune cell subsets present in the peripheral blood of patients with breast cancer is relevant to this study. Comparison of markers analysed by flow cytometry between healthy control subjects and patients with cancer may identify valuable prognostic biomarkers. T-cells, B-cells, NK cells, monocytes, and Tregs play important roles in breast cancer and may be identified using appropriate markers (Table 2.1.)

Table 2.1: Cellular markers to identify different immune cell subsets

Cell types	Defining cellular markers	Markers for further characterisation	References
$CD8^+$ cytotoxic T-cells	CD45, CD3, CD8	CXCR3, CD194, CD196	46-49
$CD4^+$ helper T-cells	CD45, CD3, CD4	CXCR3, CD161	46-49
Tregs	CD45, CD3, CD4, CD25, Forkhead Box Protein P3 (FoxP3) (intracellular)	CD127, Helios, CD39, CD45RA	46-49
Natural Killer T-cells (NKTs)	CD45, CD3, CD56, CD16	Neural cell adhesion molecule (NCAM), CD161	46-49
Monocytes	CD45, CD14, CD16	CD56, CD206, HLA-DR	46-48, 50
NK Cells	CD45, CD16, CD56	HLA-DR, CD69	46-48, 51, 52
B-lymphocytes	CD19, CD20, CD45, CD38, CD138 (plasma cells)	CD206, C-C motif chemokine receptor 7 (CCR7)	46-48, 53
Tregs: regulatory T-cells. NK cells: natural killer cells.			

The TME contains both innate and adaptive immune cells that contribute to either driving or preventing tumour progression (Table 2.2)[19, 20]. The presence of immune cells within the TME, including T-lymphocytes, NK cells, dendritic cells, neutrophils, B-lymphocytes, MDSCs, and macrophages, influences disease progression and prognosis[19, 20]. The presence of tumour infiltrating lymphocytes (TILs), which include T and B-lymphocytes, and NK cells is associated with good treatment responses in patients with TNBC or $HER2^+$ breast cancer as these cells mediate tumour cell destruction[19, 20, 54]. However, tumour cells may use several mechanisms to block TIL recruitment or activation and avoid immune-mediated killing, while simultaneously creating an immunosuppressive environment. Tumour cells can directly prevent dendritic cell maturation, causing decreased neoantigen presentation and blocking T-cell activation[19, 20]. Tumour cells release cytokines that recruit MDSCs and Tregs which further drive immunosuppression within the TME[19, 20]. Increased Treg levels in breast cancer biopsies are

associated with a more invasive phenotype and poorer prognosis[19, 20]. Tumours also drive the polarisation of neutrophils and macrophages towards N2 and M2 tumour-promoting phenotypes, respectively which promote resistance to chemotherapy in ER^- breast cancer patients[37].

Table 2.2: The roles of immune cell subsets in the tumour microenvironment

Innate Immune cells		**Pro- or anti-tumourigenic**	**References**
Macrophages	Normal function: Antigen presentation to $CD4^+$ and $CD8^+$ T-cells. When activated, can be divided into M1 and M2 phenotypes. Function in cancer: The acidity of the TME drives M2 phenotype polarisation with further release of immunosuppressive factors.	M2: Pro-tumourigenic	19, 20, 29, 55
Neutrophils	Normal function: Phagocytosis of pathogens and other foreign bodies at sites of infection and inflammation. Function in cancer: The TME drives polarisation of the N2 phenotype. A higher neutrophil-to-lymphocyte ratio is associated with a poorer prognosis and increased mortality.	N2: Pro-tumourigenic	19, 20, 29, 56
NK Cells	Normal function: Kill cells directly by inducing apoptosis or by compromising cell membrane integrity. Function in cancer: Their function is inhibited by the acidity of the TME and by immunosuppressive cytokines released by cancer cells.	Anti-tumourigenic	18, 19, 29, 54
Dendritic cells	Normal function: Presentation of antigens to $CD4^+$ and $CD8^+$ T-cells which go on to destroy the target cell. Function in cancer: The acidity of the TME prevents their maturation and causes them to become tolerogenic.	Pro-tumourigenic and/or tolerogenic	19, 20, 29, 57
Adaptive Immune Cells			
$CD4^+$ T-lymphocytes	Normal function: Assist in the activation and function of $CD8^+$ T-cells. Function in cancer: The TME alters their metabolism and hinders their anti-tumourigenic ability.	Anti-tumourigenic	19, 20, 29

CD8⁺ T-cells	Normal function: Kill their target by inducing apoptosis or compromising cell membrane integrity. In cancer: The TME reduces their cytotoxic ability and alters their metabolism.	Anti-tumourigenic	19, 20, 29
Tregs	Normal function: Moderates CD4⁺ and CD8⁺ activity to prevent excessive immune activation. Function in cancer: The acidic TME favours Treg activity which supresses anti-tumourigenic immune cells such as CD8⁺ T-cells.	Pro-tumourigenic	19, 20, 29
NKTs	Normal function: Exhibit both T-cell and NK cell-like effector mechanisms to destroy their target. Function in cancer: The acidic TME inhibits NKT cell function by disrupting intracellular signalling mechanisms.	Anti-tumourigenic	19, 20, 29, 58, 59
B-cells	Normal function: Act as professional antigen presenting cells (APCs), produce antibodies, can differentiate into memory B-cells, and release pro-inflammatory and anti-inflammatory molecules. Function in cancer: Produce antibodies against cancer cells and present tumour antigens to T-cells. However, TME conditions can favour regulatory B cell subsets which are immunosuppressive.	Pro- or anti-tumourigenic	18, 19, 27, 29

NK cells: natural killer cells. Tregs: regulatory T-cells. NKT: natural killer T-cell.

Alterations to the immune cell components in and around the TME due to manipulation by cancer cells have been documented in numerous cancer types[19, 28, 29]. A more comprehensive understanding of the impact of solid tumours on circulating immune cell populations and the effects of chemotherapy on these cells is relevant for patient prognosis and treatment. As obtaining a tumour biopsy can be an invasive procedure, less intrusive procedures are needed to assess the response to treatment[19, 28, 29]. In this study, a multi-colour flow cytometric panel was developed to conduct immunophenotyping of immune cell subsets in the peripheral blood of patients with TNBC.

2.2 Materials and Methods

2.2.1 Participant selection

Twenty-three newly diagnosed TNBC patients were recruited from the Medical Oncology Centre of Rosebank in Johannesburg. All participants were female and over 18 years old. All the inclusion and exclusion criteria can be found in Appendix B, Table 1. Ten healthy female volunteers were recruited from the Health Sciences campus of the University of Pretoria, Tshwane, as the healthy donor group.

2.2.2 Specimen collection

Peripheral blood was collected in two 5 ml ethylenediaminetetraacetic acid (EDTA) tubes prior to the initiation of chemotherapy and after the first phase of chemotherapy (at least three cycles of chemotherapy). Blood samples were transported to the laboratory at room temperature (RT) and upon arrival, one 5 ml EDTA tube of participant blood was used for flow cytometric analysis and the other was used to store plasma for later use.

2.2.3 Ethical considerations and approval

Each participant completed a written informed consent form and was assigned a depersonalised study number to ensure confidentiality. Ethical approval was obtained from the University of Pretoria Faculty of Health Sciences Research Ethics committee (approval number 302/2023) (Appendix B, Figure 1).

2.2.4 Antibodies

Immune cell subsets were identified using DURAClone Immunophenotyping (IM) Basic and Treg kits from Beckman Coulter (California, United States of America (USA)). These kits contain a panel of dried-down antibodies. The DURAClone IM Basic kit (Beckman Coulter, USA) contained CD45-Krome Orange (KrO), CD16-Fluorescein isothiocyanate (FITC), CD56-Phycoerythrin (PE), CD19-R-Phycoerythrin-Texas Red-X energy coupled dye (ECD), CD14-Phycoerythrin-Cyanine 7 (PC7), CD4-Allophycocyanin (APC), CD8-Alexa Fluor 700 (AF700), CD3-Allophycocyanin-Alexa Fluor 750 (APC-AF750) that allowed for the characterisation of monocytes, macrophages, B-cells, $CD4^+$ T-cells, $CD8^+$ T-cells, and NK cells. A CD206-Pacific Blue (PB) (BioLegend, USA) and human leukocyte antigen-DR isotype (HLA-DR)-Brilliant

Violet 780 (BV780) (BioLegend, USA) liquid antibody drop-in were added to this panel. The DURAClone IM Treg kit (Beckman Coulter, USA) and a CD127-AF700 (BioLegend, USA) liquid antibody drop-in were used to obtain more detailed information on circulating $CD4^+$ T-cells and $CD25^+FoxP3^+$ Tregs from each participant. This kit contained Helios-PB, CD45-KrO, cluster of differentiation molecule 45 residues on exon A (CD45RA)-FITC, CD25-PE, CD39-R-Phycoerythrin-Cyanin 5.5 (PC5.5), CD4-PC7, FoxP3-Alexa Fluor 647 (AF647), and CD3-APC-AF750 antibodies.

2.2.5 Compensation

Colour compensation was performed by adding two drops of positive and negative VersaComp (Beckman Coulter, USA) antibody capture beads to an unstained tube and to tubes containing single colour fluorophores. The DURAClone IM Basic Immunophenotyping Compensation kit contained CD4-FITC, CD4-PE, CD19-ECD, CD14-PC7, CD4-APC, CD8-A700, CD3-APC-A750, and CD8-KrO, and separate tubes were prepared with 10 µl of CD206-PB (BioLegend, USA) and HLA-DR-BV780 (BioLegend, USA). The DURAClone Treg compensation kit contained CD4-FITC, CD4-PE, CD39-PC5.5, CD4-PC7, FoxP3-A647, CD3-APC-A750, CD4-PBE, and CD8-KrO, and a separate tube was prepared with 10 µl of CD127-AF700 (BioLegend, USA). After vortexing and incubating the tubes in the dark at RT for 15 minutes, 3 ml of 1x Phosphate buffered saline (PBS) (ThermoFisher Scientific, USA) was added and the tubes centrifuged at 500 relative centrifugal force (RCF) for 5 minutes (brake off) using an Allegra® X-12R centrifuge (Beckman Coulter, USA). The pellet was resuspended in 600 µl 1x PBS (ThermoFisher Scientific, USA), the results were acquired on the CytoFlex flow cytometer (Beckman Coulter, USA), and H-gates were placed over the positively stained bead populations for each tube before recording. The results were saved in a compensation library for each respective assay.

2.2.6 Daily quality control and standardisation

Daily quality control (QC) was performed using CytoFlex Ready to Use (RTU) Daily QC fluorospheres (Beckman Coulter, USA)[60]. After ensuring that the target value file for the specific lot of QC beads was loaded, the fluorospheres were thoroughly vortexed and 10 drops were added into a sterile tube. Once the QC passed, standardisation was performed to ensure assay accuracy and reproducibility. Flow-set pro fluorospheres (Beckman Coulter, USA) were used for daily assay standardisation, and after vortexing, 10 drops were added into a sterile tube, which was then acquired on the CytoFlex flow cytometer (Beckman Coulter, USA), and the results were imported into the gain acquisition settings.

2.2.7 Basic immunophenotyping flow cytometry panel

A volume of 5 µl of CD206-PB (BioLegend, USA) and HLA-DR-BV780 (BioLegend, USA) liquid antibodies were added into a labelled DURAClone IM basic kit (Beckman Coulter, USA) reagent tube, and the tube vortexed. To minimise the formation of staining artefacts, 30 µl of Brilliant Violet stain buffer (BD Biosciences, USA) was added to the reagent tube along with 100 µl of whole blood. The tube was vortexed and incubated in the dark at RT for 15 minutes (min). VersaLyse solution (Beckman Coulter, USA) (2 ml) was added after the incubation period, and the tube contents were mixed and incubated in the dark for another 15 min at RT. The tube was then centrifuged at 200 RCF for 5 min (brake off) using an Allegra® X-12R centrifuge (Beckman Coulter, USA), and the pellet was resuspended in 3 ml 1x PBS (ThermoFisher Scientific, USA). After centrifuging at 200 RCF for 5 minutes (brake off) using an Allegra® X-12R centrifuge (Beckman Coulter, USA), the pellet was resuspended in 500 µl PBS (ThermoFisher Scientific, USA) and the results acquired on the CytoFlex flow cytometer (Beckman Coulter, USA).

2.2.8 Treg immunophenotyping flow cytometry panel

Five microlitres (µl) of CD127-AF700 (BioLegend, USA) liquid antibody and 50 µl of whole blood were added to a labelled DURAClone IM Phenotyping Treg kit tube 1 (Beckman Coulter, USA), and the tube was vortexed and incubated in the dark for 15 min at RT. After adding 3 millilitres (ml) 1x PBS (ThermoFisher Scientific, USA), the tube was centrifuged at 500 RCF for 5 min (brake off) using an Allegra® X-12R centrifuge (Beckman Coulter, USA). The pellet was resuspended in 50 µl of foetal bovine serum (FBS) (ThermoFisher Scientific, USA). Permeabilisation buffer (PerFix-nc buffer 1, Beckman Coulter, USA) (5 µl) was incubated with the sample for 15 min before 400 µl of fixation buffer (PerFix-nc buffer 2, Beckman Coulter, USA) was added. The contents of tube 1 were transferred to reagent tube 2 and incubated in the dark for 60 min at RT. After adding 3 ml PBS (ThermoFisher Scientific, USA) and incubating in the dark for 5 min at RT, the tube was centrifuged at 500 RCF for 5 min, and the supernatant was discarded. After adding 3 ml diluted Perfix-nc buffer 3 wash buffer (diluted 1 in 10 with deionised water) (Beckman Coulter, USA), the tube was centrifuged at 500 RCF for 5 minutes (brake off) using an Allegra® X-12R centrifuge (Beckman Coulter, USA), and the pellet resuspended in 500 µl of diluted Perfix-nc buffer 3 (diluted 1 in 10 with deionised water) (Beckman Coulter, USA). Finally, the results were acquired using a CytoFlex flow cytometer (Beckman Coulter, USA).

2.2.9 Data analysis

Following data acquisition using the CytoFlex flow cytometer (Beckman Coulter, USA), the flow cytometry standard (FCS) files were imported into Kaluza Analysis software version 2.2.1 (Beckman Coulter, USA). A standard cleanup protocol was created for the basic and Treg immunophenotyping panels, as well as the standardised compensation dataset. Doublets were excluded, scaling was adjusted to ensure that all cell populations were adequately visualised, and the compensation was adjusted. These files were then imported into FlowJo™ software version 10.9.0 (Beckton Dickenson, USA) for further analysis.

2.3 Results

Immune cell populations of interest were detected using a basic and Treg immunophenotyping panel and liquid antibody drop-ins on the CytoFlex flow cytometer (Beckman Coulter, USA). To correctly identify and define cell populations of interest using the collected data, a gating strategy was developed and visualised using FlowJo™ software v10.9.0 (Beckton Dickenson, USA). The gating strategy presented here was performed using peripheral blood obtained from a healthy donor.

2.3.1. Identification of T-cell, B-cell, NK cell, and monocyte subsets in peripheral blood

A forward scatter height (FSC-H) vs. forward scatter area (FSC-A) plot was created to eliminate cell debris and doublets from the analysis (Fig. 2.1 A). Next, to identify leukocytes, a CD45 vs. granularity by side scatter area (SSC-A) dot plot was created, and the $CD45^+$ events were gated (Fig 2.1 B). Monocytes were identified based on CD14 expression using a CD14 vs. SSC-A plot and lymphocytes were identified using a CD45 vs. SSC-A (Fig. 2.1 C, D) plot. Monocyte subsets were further classified based on CD14 and CD16 expression as follows: classical ($CD14^+$ $CD16^-$), intermediate ($CD14^+$ $CD16^+$), and non-classical ($CD14^{dim}$ $CD16^+$) (Fig. 2.1 E). B-lymphocytes were identified based on a lack of CD3 expression and positive CD19 expression (Fig. 2.1 F). Natural killer cells were identified by CD56 expression (Fig. 2.1 G, H), whereas $CD3^+$ T cells were subdivided into $CD4^+$ or $CD8^+$ subsets (Fig 2.1 G, I). The percentage of parent population and mean fluorescence intensity (MFI) of each gated population were determined. To further characterise the cell populations detected using this panel, the MFI of CD206 on B-cells, CD56, CD206, and HLA-DR on monocytes, and CD16 and HLA-DR on NK cells were determined. This gating strategy was first established using healthy donor flow cytometry data before being applied to that of the recruited patients.

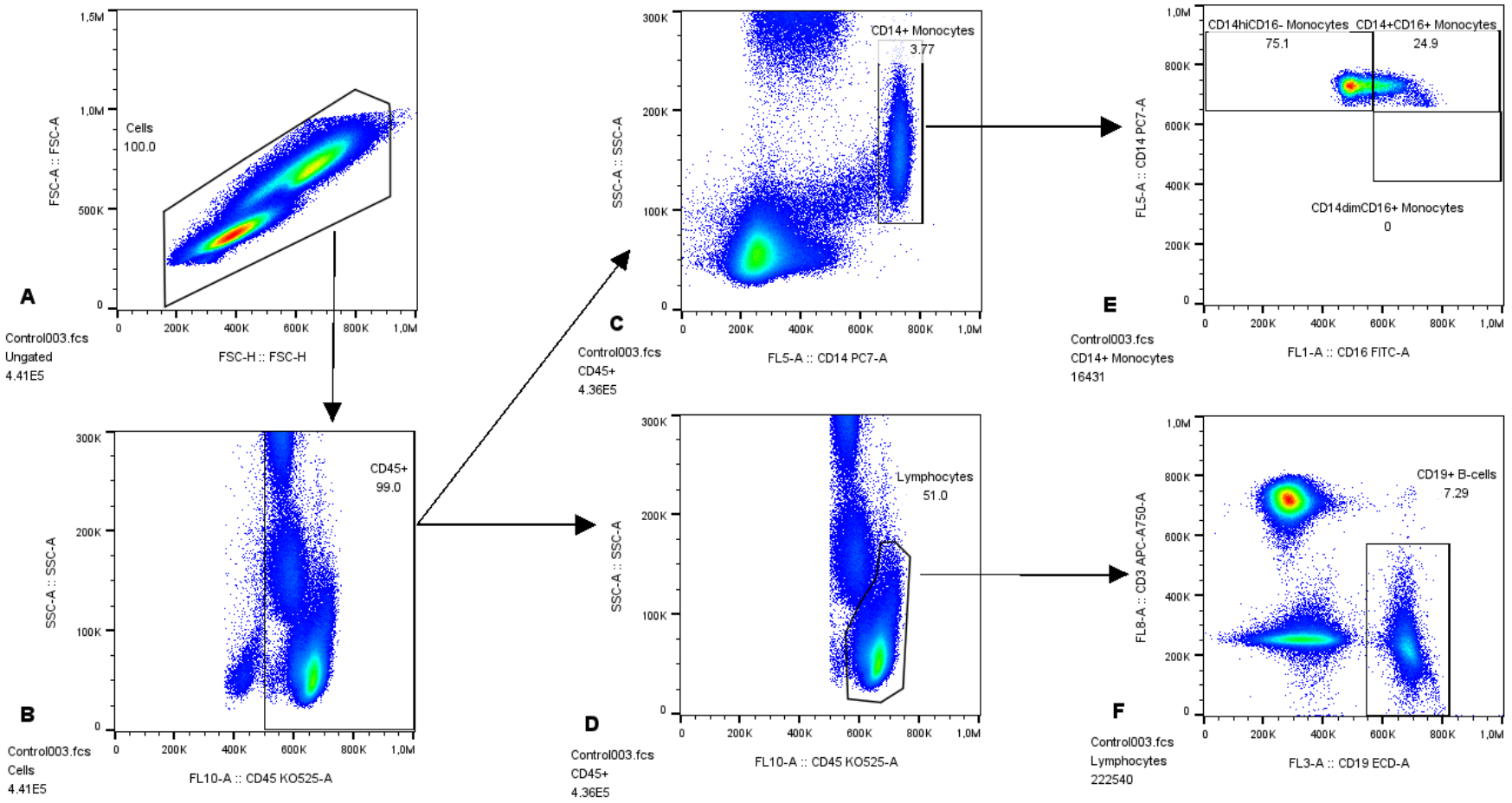

Figure 2.1: Gating strategy used to identify T-cell, B-cell, NK cell, and monocyte subsets in healthy donor whole blood. Singlets were gated using a FSC-H vs. FSC-A plot (A) and $CD45^+$ leukocytes were identified using a CD45 vs. SSC-A plot (B). Using gated $CD45^+$ leukocytes, $CD14^+$ monocytes (C) and lymphocytes (D) were identified. Monocyte subsets were evaluated using a CD16 vs. CD14 plot (E). Using events gated in D, $CD19^+$ B-cells were identified in plot F. NK cell: natural killer cell. FSC-H: forward scatter height. FSC-A: forward scatter area. SSC-A: side scatter area.

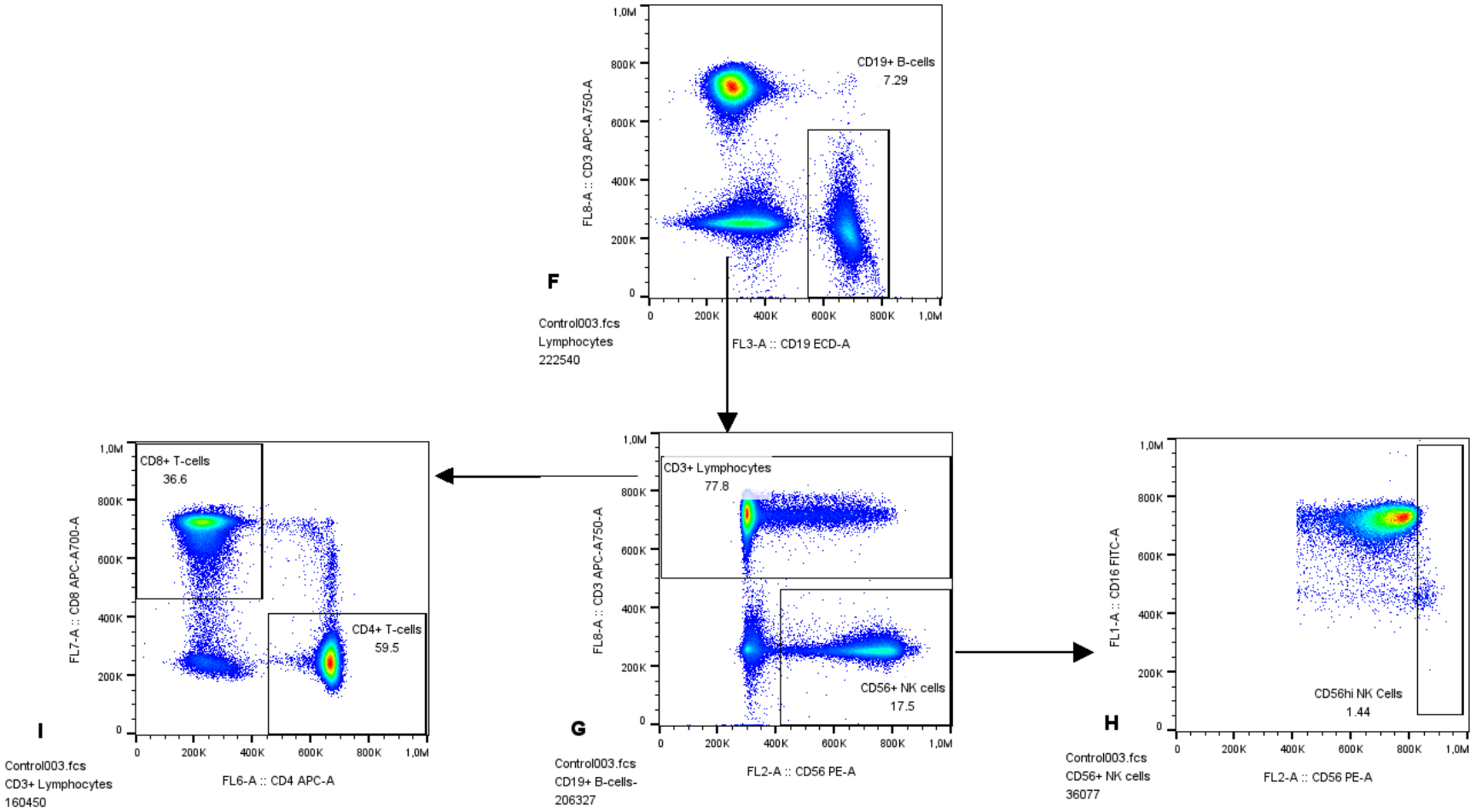

Figure 2.1 continued: Natural killer cells and $CD3^+$ lymphocytes were identified using a CD3 vs. CD56 plot (G). $CD56^{high}$ NK cells were identified using a CD56 vs. CD16 plot (H), whereas $CD4^+$ helper T-cells and $CD8^+$ cytotoxic T-cells were identified using a CD4 vs. CD8 plot (I). NK cell: natural killer cell.

2.3.2 Identification of $CD4^+CD25^+FoxP3^+$ Tregs in peripheral blood

To identify singlets, a FSC-H vs. FSC-A plot was generated (Fig. 2.2 A). Next, the $CD45^+$ lymphocytes were gated (Fig. 2.2 B), and helper T-cells ($CD3^+$ $CD4^+$) were identified (Fig. 2.2 C). A CD4 vs. CD25 plot was used to identify the $CD25^+$ and $CD25^{dim}$ helper T-cell populations (Fig. 2.2 D). Next, a FoxP3 vs. CD25 plot was used to identify $CD25^+FoxP3^+$ Tregs (Fig. 2.2 E). To improve the characterisation of participant $CD25^+FoxP3^+$ Tregs, the MFI of CD39, CD127, CD45RA, and Helios in these cells was evaluated. This gating strategy was first established using healthy donor flow cytometry data before being applied to that of the recruited patients.

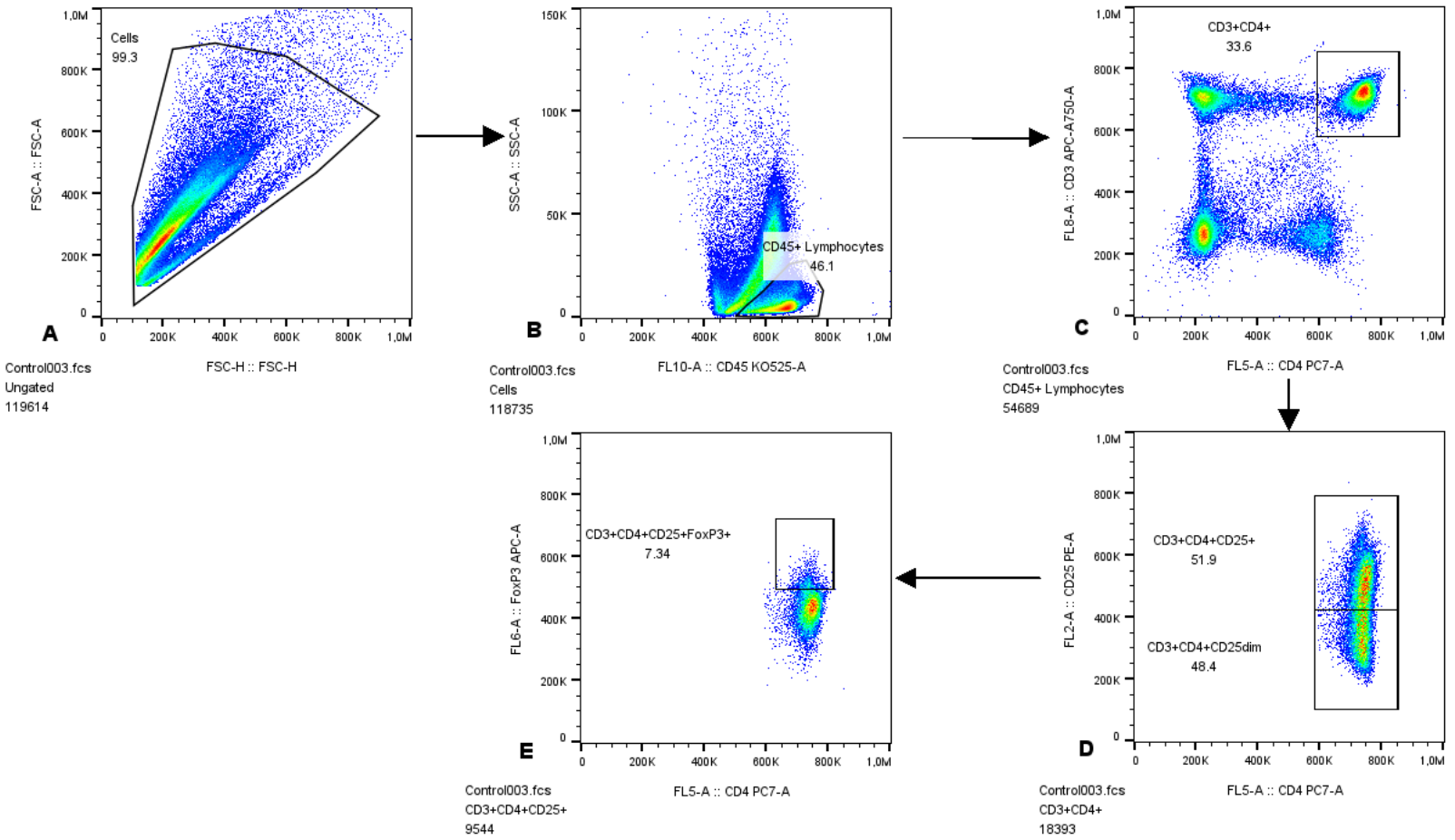

Figure 2.2: **Gating strategy used to identify CD4$^+$CD25$^+$FoxP3$^+$ Tregs in healthy donor whole blood.** Singlet cells (A) and CD45$^+$ lymphocytes (B) were identified. Helper (CD3$^+$CD4$^+$) T-cells were gated (C), and CD25$^+$ and CD25^{dim} helper T-cell populations were identified using a CD4 vs. CD25 plot (D). Finally, CD25$^+$FoxP3$^+$ Tregs were identified using a FoxP3 vs. CD25 plot (E). FoxP3: Forkhead Box Protein P3. Tregs: regulatory T-cells.

2.4 Discussion

Breast cancer is the second most frequently diagnosed cancer with the fourth highest mortality rate worldwide, making it a healthcare priority[4]. TNBC, accounting for 10-20% of diagnosed invasive breast cancers, is more aggressive, has greater proliferative potential, metastasises earlier, and has fewer treatment options than other breast cancer types[61]. Accurate biomarkers to track and monitor the progression and response to treatment are important for developing better treatment strategies for patients with TNBC. Surrogate biomarkers present in peripheral blood assist in monitoring tumour progression or response to treatment, negating the need for invasive biopsies in longitudinal testing[62].

The aim of this study was to detect and characterise circulating immune cell subsets in healthy volunteers and patients with TNBC using flow cytometry. This technique was selected because it is a well-established tool for identifying and distinguishing between different immune cells present within a sample[43-45]. Owing to their crucial roles in tumour growth and progression, circulating T and B-lymphocytes, NK cells, monocytes, and $CD25^{+}FoxP3^{+}$ Tregs in both healthy individuals and those with TNBC were detected using a flow cytometric protocol and gating strategy developed specifically for this purpose. The protocol and gating strategy developed were published online on protocols.io (DOI: https://dx.doi.org/10.17504/protocols.io.14egn379ml5d/v3) (Appendix B, Figure 2).

By establishing this gating strategy using blood from healthy donors, immunophenotypic comparisons can be made in patients with TNBC. In addition, monitoring these immune cell subsets during treatment may provide clinical data and help predict treatment outcomes.

Chapter 3: Immunophenotyping of T-cells, B-cells, NK cells, and monocytes in healthy donors and TNBC patients before and after first-phase chemotherapy

3.1 Introduction

Breast cancer was the second most commonly diagnosed cancer in 2022 with 2.31 million new cases diagnosed globally and the fourth highest cancer mortality rate in the world, making it a healthcare priority[4]. TNBC does not express any hormone receptors, accounts for 10-20% of diagnosed invasive breast cancer cases, and has a 5-year survival rate of 60%[63, 64]. The hormone insensitivity and heightened proliferative and metastatic potential of TNBC limit the range of treatment strategies that can be used to chemotherapy, radiation, surgery, and immunotherapy[61, 63].The TNBC TME, including the immune cell component, differs from that of other breast cancer subtypes, and T-cells, B-cells, NK cells, monocytes, and other immune cells both within the TME and the circulation may play a pro- or anti-tumourigenic role in TNBC[30, 31, 65].

Cytotoxic $CD8^+$ T-cells destroy infected and malignant cells[66, 67]. $CD8^+$ T-cells require exposure to an antigen specific to their T-cell receptor (TCR) and the presence of interleukin 2 (IL-2) (produced by activated $CD4^+$ T-cells) to become actiavted[66, 67]. $CD8^+$ T-cells secrete anti-microbial and anti-tumourigenic cytokines, such as TNF-α and IFN-γ, release cytotoxic granules containing perforin and granzymes, and use FAS/FAS ligand signalling to activate the caspase cascade within target cells to trigger apoptosis[66, 67]. The degree of $CD8^+$ T-cell infiltration into the TME can be used to classify tumours as ‘hot’ and ‘cold’ tumours[66, 67]. ‘Hot’ tumours contain large amounts of non-exhausted $CD8^+$ T-cells, respond well to immunotherapy and are associated with a more favourable prognosis[66, 67]. Inhospitable conditions within the TME however, are a mechanism by which malignant cells manipulate $CD8^+$ T-cell function[66, 67].

$CD4^+$ T-cells are activated in response to antigenic presentation by cells such as dendritic cells, and subsequently release IL-2[68-70]. Newly activated $CD4^+$ (Th0) cells differentiate into T helper 1 (Th1), T helper 2 (Th2), and T helper 17 (Th17) cells with the same antigenic specificity as their parent cell[68-70]. Th1 cells are a major source of IFN-γ and TNF-β, and promote antibody-independent immune responses[68-70]. These cells activate M1 macrophages

and CD8$^+$ T-cells, and are associated with improved clinical outcomes in cancer[68-70]. Th2 cells produce interleukin 4 (IL-4), interleukin 5 (IL-5), IL-6, interleukin 13 (IL-13), and IL-10 which inhibit Th1 cells and activate M2 macrophages and B-lymphocytes[68-70]. Th2 cells, conventionally associated with pro-tumour activity, have also been linked to improved patient outcomes in cancer[68-70]. Pro-inflammatory Th17 cells produce interleukin 17 (IL-17) which indirectly causes the secretion of IL-8, IL-6, G-CSF, and granulocyte-macrophage colony stimulating factor (GM-CSF)[68-70]. The infiltration of CD4$^+$ and CD8$^+$ T-cells into the TME can be used by clinicians as an indicator of treatment response and prognosis, and an increased TIL percentage in the TNBC TME has been associated with improved prognosis, pathological complete response rate, and overall survival[64, 71]. B-lymphocytes are also critical components of the TME and play an important role in the control of cancer[65].

Upon antigen exposure, B-lymphocytes present an HLA-II-antigen complex to a Th2 CD4$^+$ T-cell which releases cytokines that stimulate B-cell proliferation and differentiation into various subsets including plasma cells (which secrete antibodies), or effector memory B-cells, which provide lasting immunity against a specific antigen[72-75]. In contrast, regulatory B-cells (Bregs) are immunosuppressive and may support tumour development[72-75]. Increased infiltration of B-cells in the TNBC TME is associated with improved patient prognosis[65].

Natural killer cells (CD56$^+$CD16$^\pm$) are important in maintaining homeostasis, as they destroy virus-infected, malignant, and otherwise stressed cells[76, 77]. Unlike T-cells, NK cells can destroy cells that do not express HLA-I molecules[76, 77]. Malignant cells may downregulate HLA-I expression as a mechanism of immune escape, which is important in the context of cancer[76, 77]. Natural killer cells can be divided into two groups: CD56^{high}CD16^{dim} and CD56^{dim}CD16^{high} NK cells[76, 77]. CD56^{high}CD16^{dim} NK cells constitute 10% of circulating NK cells, are major cytokine producers, and are more immature and immunoregulatory than the cytotoxic CD56^{dim}CD16^{high} NK subset[76, 77]. CD16 is closely linked to the antibody-dependent cytotoxic ability of NK cells, while CD56 is constitutively expressed by NK cells and has also been reported to be associated with cytotoxicity and an activated state in other immune cells such as T-cells[78, 79]. HLA-DR expression in NK cells is considered a marker of activation[51].

Monocytes differentiate into macrophages which play a role in either supporting or preventing cancer growth. Three main monocyte subsets are found in the peripheral blood of humans[80-82]. Classical (CD14^{hi}CD16$^-$) monocytes are phagocytic, patrol the endothelium, release pro-

inflammatory factors, and differentiate into anti-tumourigenic M1 macrophages within the tissues[80-82]. Intermediate ($CD14^{+}CD16^{+}$) monocytes are pro-inflammatory and may differentiate into either pro-tumourigenic M2 macrophages or anti-tumourigenic M1 macrophages depending on the signalling molecules to which they are exposed[80-82]. Non-classical ($CD14^{dim}CD16^{+}$) monocytes differentiate into pro-tumourigenic M2 macrophages, patrol the endothelium, and produce inflammatory cytokines[80-82]. M1 macrophages can suppress tumour growth, whereas M2 macrophages promote angiogenesis, treatment resistance and metastasis[80-82]. The CD206 mannose receptor is frequently used by researchers to identify M2 macrophages and immature dendritic cells and plays an important role in the recognition and internalisation of specific ligands[83]. Monocyte subsets found in the blood of TNBC patients may shed light on the macrophage polarisation status within the TME[80-82].

When the immune system fails to prevent tumour formation and growth, other treatment strategies are needed. Chemotherapeutic agents are used to target and destroy rapidly dividing cells[84]. While cancer cells are the primary targets of such therapies, other rapidly dividing cells, such as immune and blood cells, are also affected[84]. As these cell types are vital for successful tumour control, relevant biomarkers must be identified to monitor these cell types in TNBC to improve patient care and disease outcomes.

3.2 Materials and methods

3.2.1 Participant recruitment

Newly diagnosed, treatment-naïve TNBC patients (n=23) and healthy volunteers (n=10) were recruited to participate in this study. All participants were female, over the age of 18 years, and had no prior personal history of breast cancer. Peripheral blood (5 ml) was collected in EDTA tubes via venipuncture prior to the initiation of chemotherapy and again after at least three cycles (first phase) of chemotherapy. The blood was transported to the laboratory at room temperature and processed within 12 hours of collection.

3.2.2 Data collection and management

The following information was collected for each patient: age, body mass index (BMI), tobacco use, histological grading (pre- and post-treatment), percentage of Antigen Kiel 67 (Ki-67) expression, TIL percentage, side (left or right breast) on which the tumour was located, routine

full blood counts (pre- and post-first-phase chemotherapy), and treatment regimen. Tumour histological grade, Ki-67 percentage, and TIL percentage was determined for each patient using biopsied sample and standard histological techniques performed by a diagnostic laboratory. The healthy donor age was recorded, but BMI and tobacco use were not.

Each participant was assigned a depersonalised study number to ensure confidentiality and privacy, and all data were stored on secure devices and encrypted online data storage platforms. Data generated and collected will be stored for 10 years in the secure data repository of the University of Pretoria.

3.2.3 Immunophenotyping of T-cells, B-cells, NK cells, and monocytes using flow cytometry

Circulating $CD4^+$ and $CD8^+$ T-cell, B-cell, NK cell, and monocyte subsets were identified in participant whole blood using a CytoFlex flow cytometer (Beckman Coulter, USA), DURAClone Immunophenotyping Basic kits (Beckman Coulter, USA), and two liquid antibody drop-ins as described in Chapter 2. The FCS files were imported into the Kaluza Analysis software version 2.2.1 (Beckman Coulter, USA) for the exclusion of doublets, as well as the adjustment of scaling and compensation. The FCS files were then imported into FlowJo™ software version 10.9.0 (Beckton Dickenson, USA), where the percentage of the parent cell population and MFI values for each cell subset and their associated markers were determined using a specifically designed gating protocol, as described in Chapter 2. The geometric MFI of different markers was measured as an indication of fluorophore brightness and a relative measure of antigen abundance.

3.2.4 Data and statistical analysis

To detect differences in $CD4^+$ and $CD8^+$ T-cell, B-cell, NK cell, and monocyte subsets between healthy donors and TNBC patients, as well as in patients before and after first-phase chemotherapy, the percentage of the parent cell population and MFI values for each cell subset and their associated markers were determined using FlowJo™ software version 10.9.0 (Beckton Dickenson, USA).

A Shapiro-Wilk test was conducted to determine the distribution of the collected data. The null hypothesis that the data had a normal distribution was rejected for several variables ($p \leq 0.05$).

As data were collected from three participant groups and did not have a normal distribution, a Kruskal-Wallis equality of populations test and Dunn's pairwise comparison test were used to compare the median percentage of population and MFI values between the three groups. A p-value of less than or equal to 0.05 was deemed statistically significant.

Full blood count results for patients before and after first-phase chemotherapy were also collected to complement the flow cytometry data. A Kruskal-Wallis equality of populations test was used to compare median blood cell count values in patients before and after first-phase chemotherapy, and a p-value of less than or equal to 0.05 was deemed statistically significant. The STATA Basic Edition 18.0 statistical software (STATA Corp LLC, USA) was used to conduct all statistical tests. This software was used to calculate the median participant demographic values and generate graphs.

3.3 Results

3.3.1 Participant demographics

The median patient age was 51 years (30-68 years) (Table 3.1), while the healthy donors had a median age of 25.5 years (23-64 years). Patients had a median BMI of 26.2 kg/m^2 (17.6-35.6 kg/m^2) and 17.39 % (n=4) were smokers (Table 3.1). The primary tumour location was divided approximately equally, with 52.17% (n=12) located in the right breast and the remainder (47.83% (n=11) in the left breast (Table 3.1). All patients were diagnosed with TNBC; 91.3% (n=21) were diagnosed with a grade 3 tumour, and the remaining 8.7% (n=2) were diagnosed with a grade 2 tumour (Table 3.1). After the completion of all chemotherapy, the primary tumour site was either biopsied or scanned and of the 18 patients for whom treatment response information was available (follow-up biopsy and scan results after the completion of chemotherapy were not available for 5 individuals), approximately 56% (n=10) demonstrated a PCR, and 44% (n=8) had PIC (Table 3.1).

Table 3.1: Patient demographics and disease characteristics

Variable	Patients
Age; median number of years (range), n=23	51 (30-68)
BMI; median kg/m² (range), n=22	26.2 (17.6-35.6)
Smoker; n (%), n=22	Yes: 4 (17.39)

	No: 18 (78.26) Unknown: 1 (4.35)
Primary tumour location; n (%), n=23	Left breast: 11 (47.83) Right breast:12 (52.17)
Ki-67; median % (range), n=23	73 (15-100)
TIL; median % (range), n=7	15 (2-40)
Tumour subtype; n (%), n=23	TNBC: 23 (100)
Tumour grade; n (%), n=23	Grade 2: 2 (8.7) Grade 3: 21 (91.3)
First-phase treatment regimen: Taxotere-Adriamycin-Cyclophosphamide (TAC)+ Neulasta®; n (%), n=23	23 (100)
Response to treatment at primary tumour site; n (%), n=18	Persistent invasive carcinoma: 8 (44.44%) Pathological complete response: 10 (55.56%)
Response on opposing side; n (%), n=18	Persistent invasive carcinoma:1 (5.56%) Pathological complete response: 1 (5.56%) Benign/Unchanged: 16 (88.89%)
BMI: body mass index. Ki-67: Antigen Kiel-67.TIL: tumour-infiltrating lymphocytes.	

The median Ki-67 expression in biopsied tissue was 73% (15-100%) by immunohistochemistry (Table 3.1). Twenty patients were found to have a high level of Ki-67 expression (≥40%)[85] at the time of diagnosis, and 3 had a low Ki-67 value (<40%)[85]. Immunohistochemical staining for TIL infiltration was only available for 7 patients, and the median TIL% for these patients was 15% (2-40%) (Table 3.1). Approximately 57% (n=4) of these patients had a TIL percentage greater than 10%. Of those with a high TIL percentage (>10%)[86], three were found to have PIC at the primary tumour site, while treatment information was not yet available for the fourth patient. The remaining three patients all had a low TIL percentage (<10%)[86] at the time of diagnosis, and while treatment response information was not available for one of them, the other two achieved a PCR after the completion of chemotherapy.

All patients underwent a first-phase treatment regimen of at least three cycles of TAC chemotherapy with the addition of Neulasta® (granulocyte-colony stimulating factor (G-CSF)). Of the three patients with a low (<40%)[85] percentage of Ki-67, the first had a Ki-67 expression level of 38%, was diagnosed with a grade 2 TNBC tumour, and was found to have PIC at the primary tumour site after the completion of all chemotherapy. The second and third patients had Ki-67 expression levels of 20% and 15% respectively, were both diagnosed with grade 3

TNBC tumours, and achieved a PCR at the primary tumour site after the completion of all chemotherapy. One patient with a Ki-67 expression level of 40% achieved a PCR at the primary tumour site but was found to have PIC in the opposing breast after the completion of all chemotherapy. More detailed demographic information of the participants can be found in Appendix C, Table 1.

3.3.2 Monocyte count and neutrophil-lymphocyte ratio is increased in patients after first-phase chemotherapy

The median lymphocyte and eosinophil cell counts were significantly lower in patients after first-phase chemotherapy (median 2.31 $x10^9$/l vs. 1.14 $x10^9$/l and 0.12 $x10^9$/l vs. 0.01 $x10^9$/l, p=0.0001), although they were still within the normal reference range, while the median monocyte count was increased (median 0.47 $x10^9$/l vs. 0.68 $x10^9$/l, p=0.0005) (Figure 3.1). The median neutrophil-lymphocyte ratio (NLR) also significantly increased after first-phase chemotherapy (median 1.66 vs. 3.69, p=0.0001).

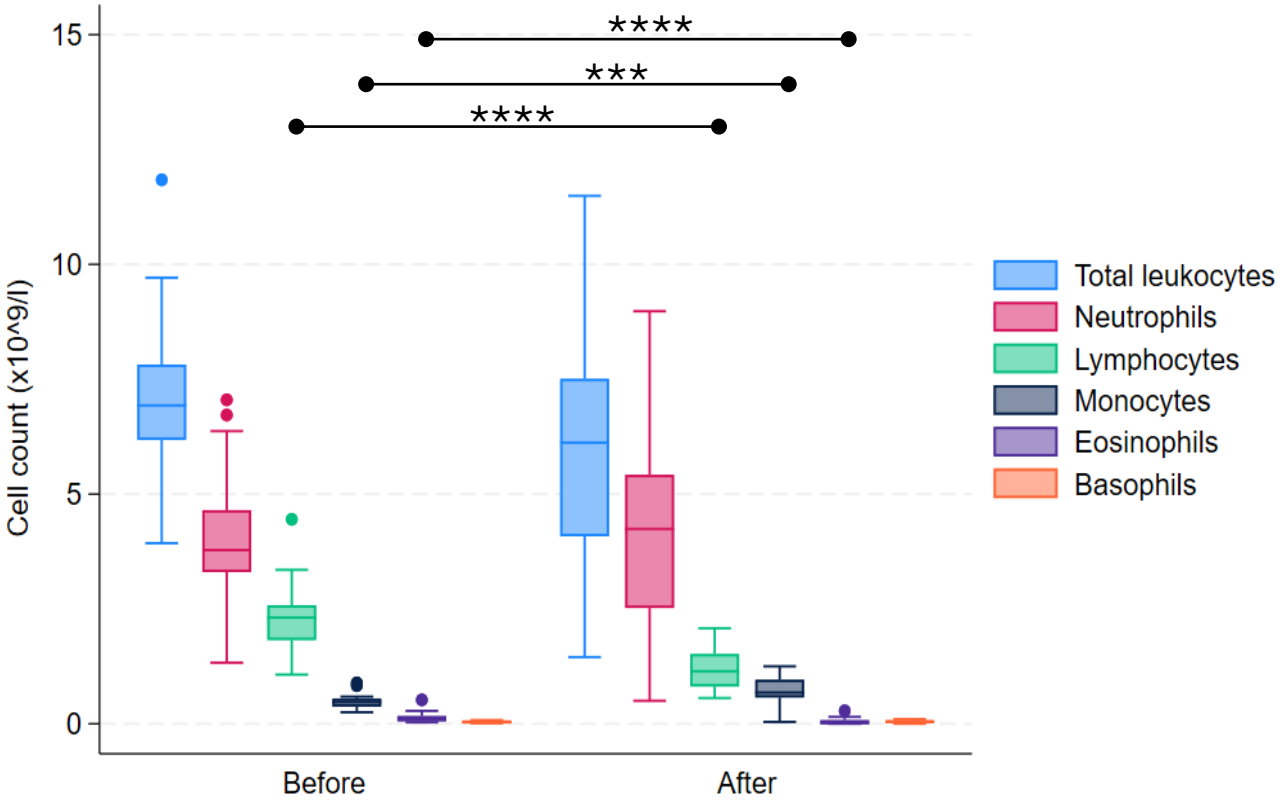

Figure 3.1: Leukocyte subset counts in patients before and after chemotherapy. Eosinophil and lymphocyte counts were reduced while monocyte count and the NLR was increased. **** p≤0.0001, *** p≤0.001. NLR: neutrophil-lymphocyte ratio.

The median erythrocyte count was significantly lower after first-phase chemotherapy (median 4.61 $x10^{12}$/l vs. 3.63 $x10^{12}$/l, p=0.0001) and was below the normal reference range. No significant changes were observed in the total leukocyte, neutrophil, basophil, or platelet counts after the first phase of chemotherapy (Table 3.2). This information was extracted from Full Blood Count (FBC) reports, and the raw data values from these reports can be found in Appendix C, Tables 2 and 3.

Table 3.2: Median full blood count test results and probability values for study patients before and after first-phase chemotherapy

Variable	Normal reference range	Pre-chemotherapy	After first-phase chemotherapy	P-value
Erythrocyte count: median $x10^{12}$/L (range)	3.8-5.5	4.61 (3.97-5.5)	3.63 (2.69-4.81)	0.0001****
Leukocyte count: median $x10^{9}$/L (range)	4.0-12.0	6.93 (3.93-11.84)	6.12 (1.45-11.49)	0.0846
Neutrophil count: median $x10^{9}$/L (range)	2.0-7.5	3.78 (1.33-7.05)	4.24 (0.5-8.98)	0.7500
Lymphocyte count: median $x10^{9}$/L (range)	1.0-4.0	2.31 (1.07-4.45)	1.14 (0.56-2.08)	0.0001****
Monocyte count: median $x10^{9}$/L (range)	0.2-1.0	0.47(0.25-0.89)	0.68 (0.04-1.25)	0.0005***
Eosinophil count: median $x10^{9}$/L (range)	0.0-0.5	0.12 (0.03-0.52)	0.01 (0-0.28)	0.0001****
Basophil count: median $x10^{9}$/L (range)	0.0-0.3	0.04 (0.01-0.08)	0.04 (0-0.1)	0.8505
NLR	-	1.62 (0.61-3.37)	3.69 (0.62-6.3)	0.0001****
Platelet count: median $x10^{9}$/L (range)	150-450	290 (96-369)	324 (61-466)	0.3017
**** p≤0.0001, *** p≤0.001. NLR: neutrophil-lymphocyte ratio.				

3.3.3 The MFI of CD8 on T-cells is increased in patients after first-phase chemotherapy compared to healthy donors

No significant changes in the percentage of circulating $CD3^+$ T-cells, $CD4^+$ T-cells, or $CD8^+$ T-cells was observed among the three participant groups. The MFI of CD8 on $CD3^+$ lymphocytes was significantly higher in patients after first-phase chemotherapy than in healthy donors (median 384 913.5 vs. 339 941, p=0.0074) (Figure 3.2); however, no corresponding changes in the percentage of $CD8^+$ T-cells or the MFI of CD8 on $CD8^+$ T-cells were observed. No significant difference in the MFI of CD4 in $CD3^+$ lymphocytes was found (Figure 3.2). The raw data values are presented in Appendix C, Table 4.

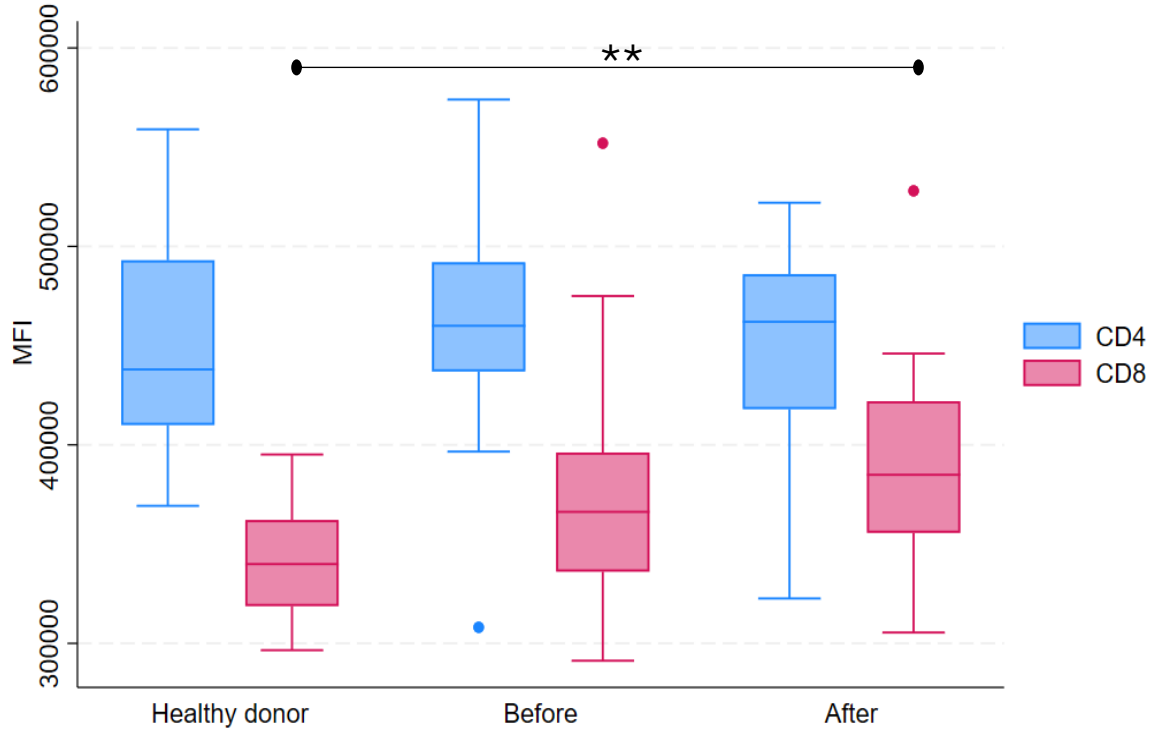

Figure 3.2: The MFI of CD4 and CD8 on T-lymphocytes. A significant increase in the MFI of CD8 on T-lymphocytes was found in patients after first-phase chemotherapy compared to that in healthy donors. ** p≤0.01. MFI: mean fluorescence intensity.

3.3.4 The percentage of B-lymphocytes is reduced in patients after first-phase chemotherapy while the MFI of CD206 is increased

A marked reduction in the overall $CD19^+$ B-cell population percentage was observed when comparing healthy donors to patients following first-phase chemotherapy (median 9.35% vs. 1.105%, p≤0.0001), as well as between treatment-naïve patients and those after first-phase

treatment (median 8.23% vs. 1.105%, p≤0.0001) (Appendix C, Table 5). This difference can be clearly observed in the flow cytometry images of patients 279 and 309 (Figure 3.3).

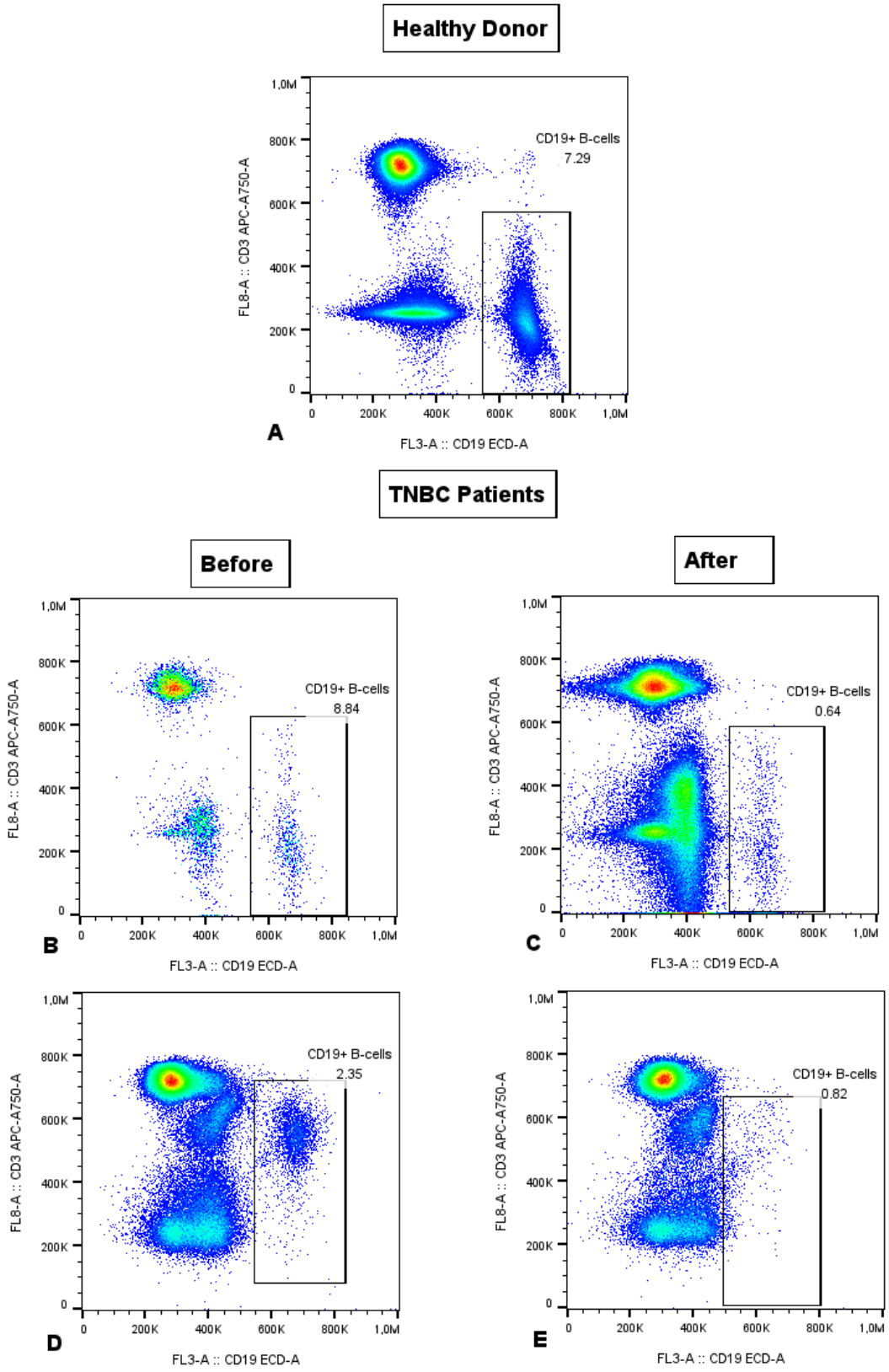

Figure 3.3: A significant decrease in CD19⁺ B-cells was observed in patients after first-phase chemotherapy compared to pre-treatment levels and in healthy donors. The above CD4 vs.CD3 plots showing CD19⁺ B-cell populations were for a healthy donor and two patients before and after first-phase chemotherapy. The percentage of CD19⁺ B-cells in the

healthy donor was 7.29% (A), whereas the percentage of $CD19^+$ B-cells in patient 279 decreased from 8.84% (B) to 0.64% (C) after first-phase chemotherapy. The percentage of $CD19^+$ B-cells in patient 309 decreased from 2.35% (D) to 0.82% (E).

A significant increase in the MFI of CD206 on $CD19^+$ B-cells was observed in patients, both before and after first-phase chemotherapy, compared to healthy donors (median 302 214 vs. 407 500 vs. 179 270.5, p=0.0006 and p≤0.0001, respectively) (Figure 3.4). In addition, a significant increase in the MFI of CD206 on $CD19^+$ B-cells was observed in patients after first-phase chemotherapy compared to pre-first-phase chemotherapy levels (median 407 500 vs. 302 214, p=0.0103) (Figure 3.4) (Appendix C, Table 5).

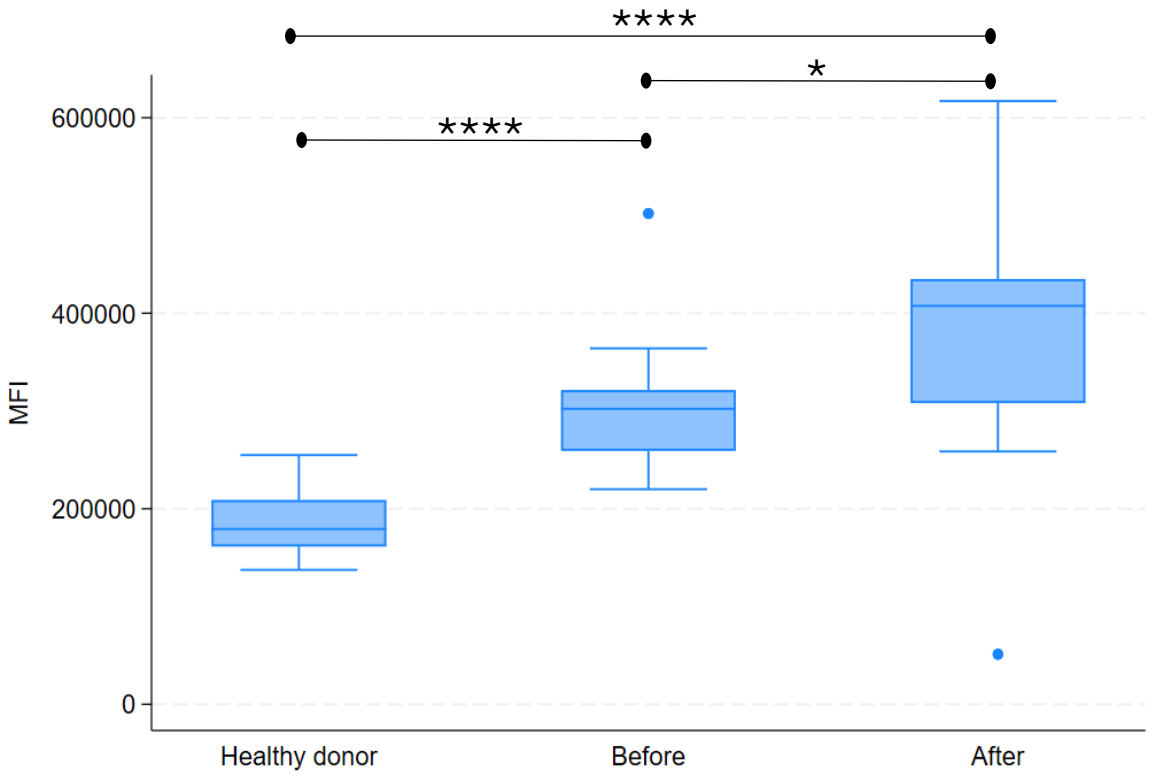

Figure 3.4: The MFI of CD206 on participant B-cells. A significant increase in the MFI of CD206 on $CD19^+$ B-cells was observed in patients compared to that in healthy donors, as well as in patients before and after the first phase of chemotherapy. **** p≤0.0001, * p≤0.05. MFI: mean fluorescence intensity.

3.3.5 The percentage of CD56^{high} NK cells was increased in patients after first-phase chemotherapy

The percentage of CD16^{+}CD56^{+} NK cells did not differ between the healthy donor, pre-treatment, and post-treatment groups. There was, however, an increase in the percentage of CD56^{high} NK cells in patients after receiving first-phase chemotherapy compared to pre-treatment levels (median 4.31% vs. 9.24%, p=0.0014). In addition, there was a non-significant increase in the percentage of CD56^{high} NK cells in patients after the first phase of treatment compared to that in healthy donors (median 9.24% vs. 5.27%, p=0.0665). The largest increase in the percentage of CD56^{high} NK cells after first-phase chemotherapy was observed in patients 270, 276, and 313 (Figure 3.5).

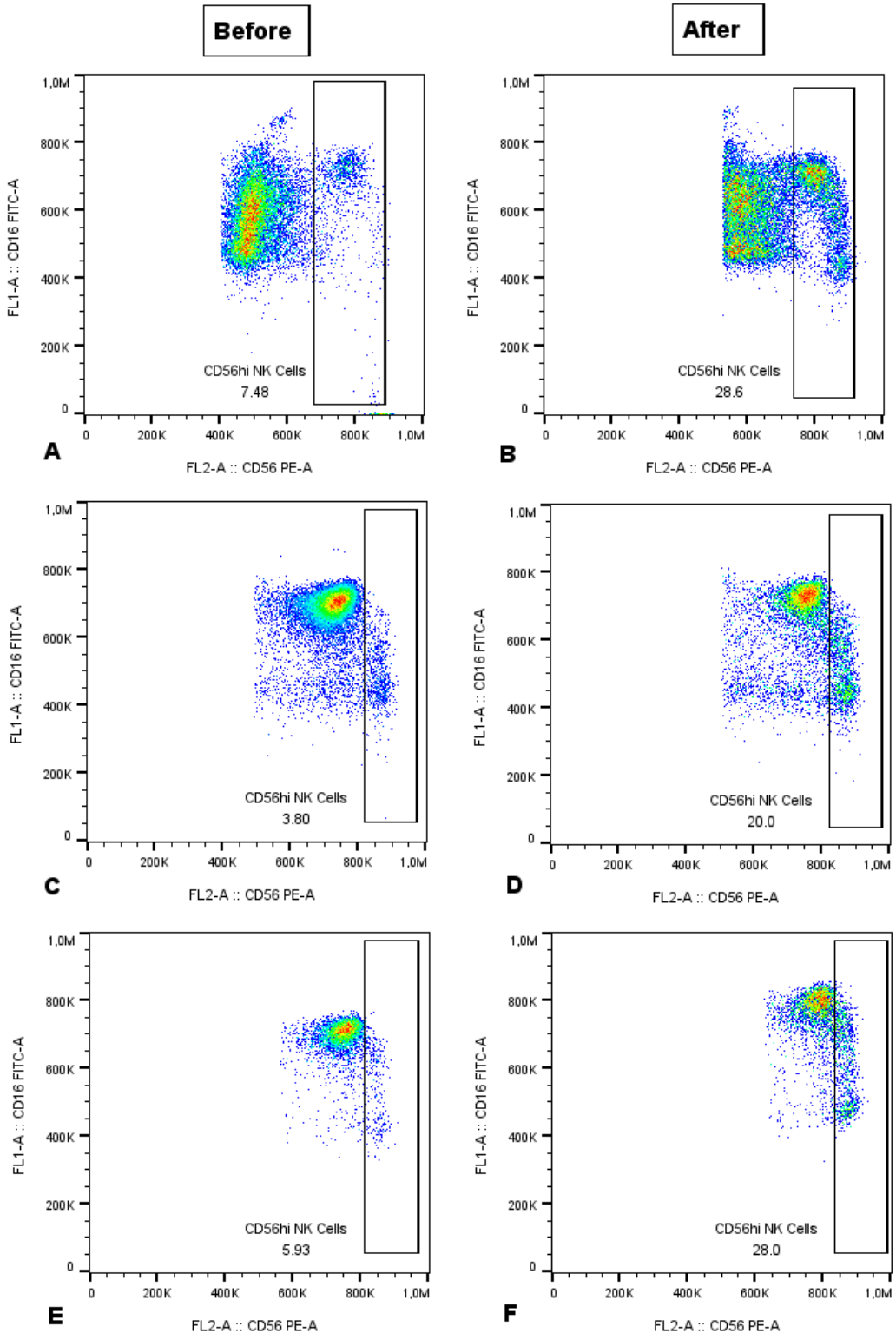

Figure 3.5: An increase in the percentage of CD56^{high} NK cells was observed in patients who received the first phase of chemotherapy. After acquiring the flow cytometry results for each study participant using the method described in Chapter 2, the CD3^{-}CD45^{+} natural killer cell population of each participant was identified. Next, CD56 vs. CD16 plots were used to identify the CD56^{high} NK cells. The CD56 vs. CD16 flow cytometry plots show the CD56^{high}

NK cell populations of the participants before and after the first phase of chemotherapy. The percentage of CD56^{high} NK cells in patient 270 increased from 7.48% (A) to 28.6% (B), the percentage of CD56^{high} NK cells in patient 276 increased from 3.80% (C) to 20.0% (D), and the percentage of CD56^{high} NK cells in patient 313 increased from 5.93% (E) to 28% (F).NK cell: natural killer cell.

The MFI of CD16 in NK cells of patients after first-phase chemotherapy was lower than that of healthy individuals (median 667 000 vs. 692 500, p= 0.0428) (Figure 3.6). An increase in the MFI of CD16 on CD56^{high} NK cells was observed in patients before and after first-phase chemotherapy (median 542 000 vs. 574 000, p=0.0027) (Figure 3.6). A non-significant increase in the MFI of CD16 on CD56^{high} NK cells was observed between healthy donors and patients after first-phase treatment (median 545 000 vs. 574 000, p=0.0678).

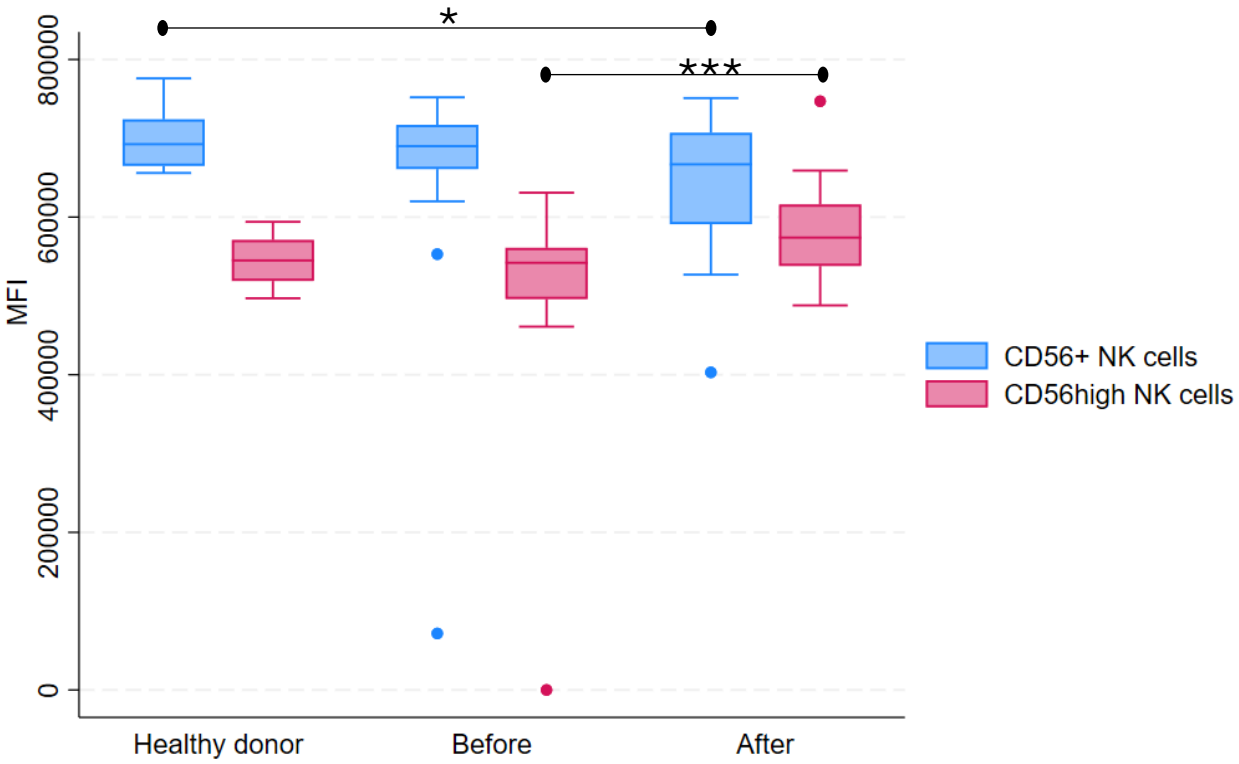

Figure 3.6: The MFI of CD16 on participant NK cells. The MFI of CD16 on CD56^{+} NK cells of patients after first-phase chemotherapy was lower than that of healthy individuals. An increase in the MFI of CD16 on CD56^{high} NK cells was observed in patients after first-phase chemotherapy. *** p≤0.001, * p≤0.05. MFI: mean fluorescence intensity. NK cell: natural killer cell.

The MFI of HLA-DR on NK cells was higher in patients after first-phase chemotherapy than in healthy donors (median 305 042.5 vs. 250 575.5, p=0.0050) and treatment-naïve patients (median 305 042.5 vs. 328 455, p=0.0002) (Figure 3.7). The MFI of HLA-DR on CD56^{high} NK cells was elevated in patients after completing first-phase chemotherapy (median 335 657.5 vs. 312 408, p=0.0023) (Figure 3.7). A non-significant decrease in the MFI of HLA-DR on CD56^{high} NK cells was observed in treatment-naïve patients compared to healthy donors (median 312 408 vs. 329 829, p=0.0514) (Appendix C, Table 6).

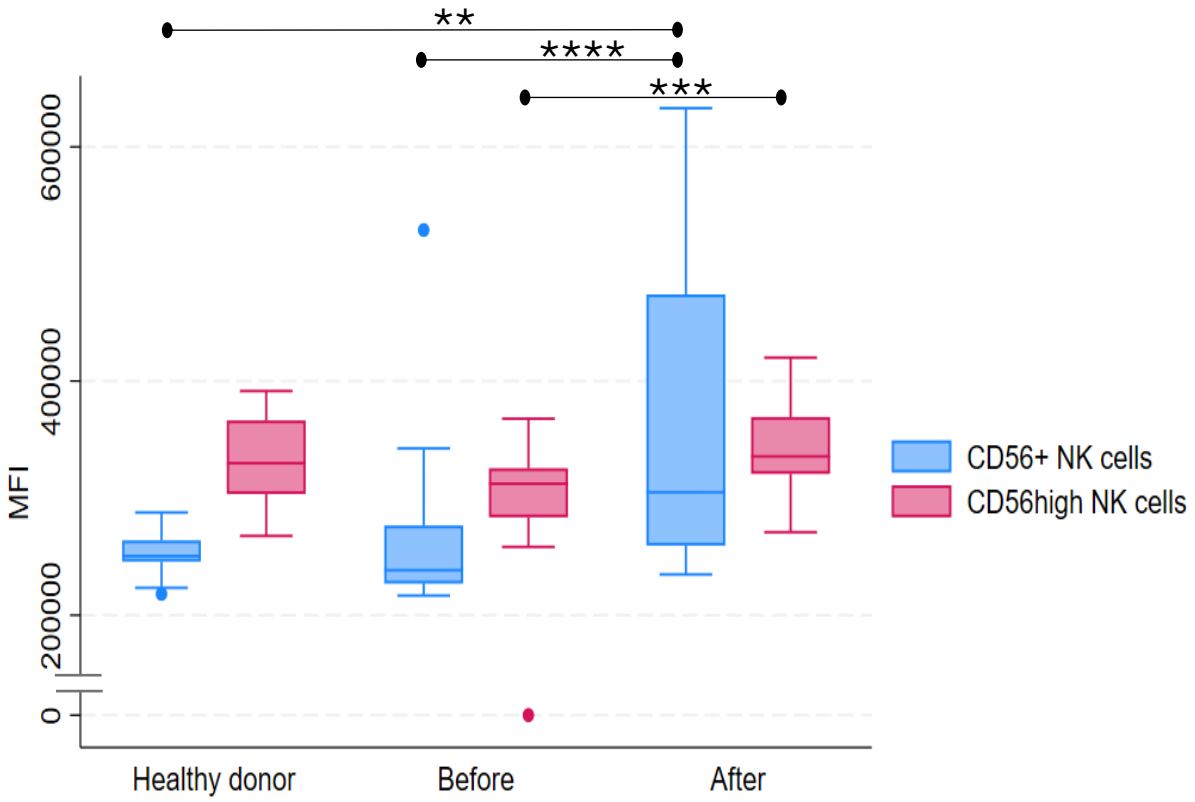

Figure 3.7: The MFI of HLA-DR on participant CD56^{+} and CD56^{high} NK cells. The MFI of HLA-DR in NK cells was notably higher in patients after first-phase chemotherapy than in healthy donors and treatment-naïve patients. The MFI of HLA-DR on CD56^{high} NK cells was elevated in patients after completing first-phase chemotherapy. **** p≤0.0001, *** p≤0.001, ** p≤0.01. MFI: mean fluorescence intensity. NK cell: natural killer cell.

3.3.6 The percentage of CD14^{+} monocytes was increased after first-phase chemotherapy

The total percentage of CD14^{+} monocytes was higher in patients after first-phase chemotherapy than that in healthy donors (median 9.355% vs. 6.55%, p=0.0258) and

treatment-naïve patients (median 9.355% vs. 4.72%, p≤0.0001). An example of this observation can be observed in patients 270, 278, and 279 (Figure 3.8). No differences in the individual monocyte subset percentages were observed.

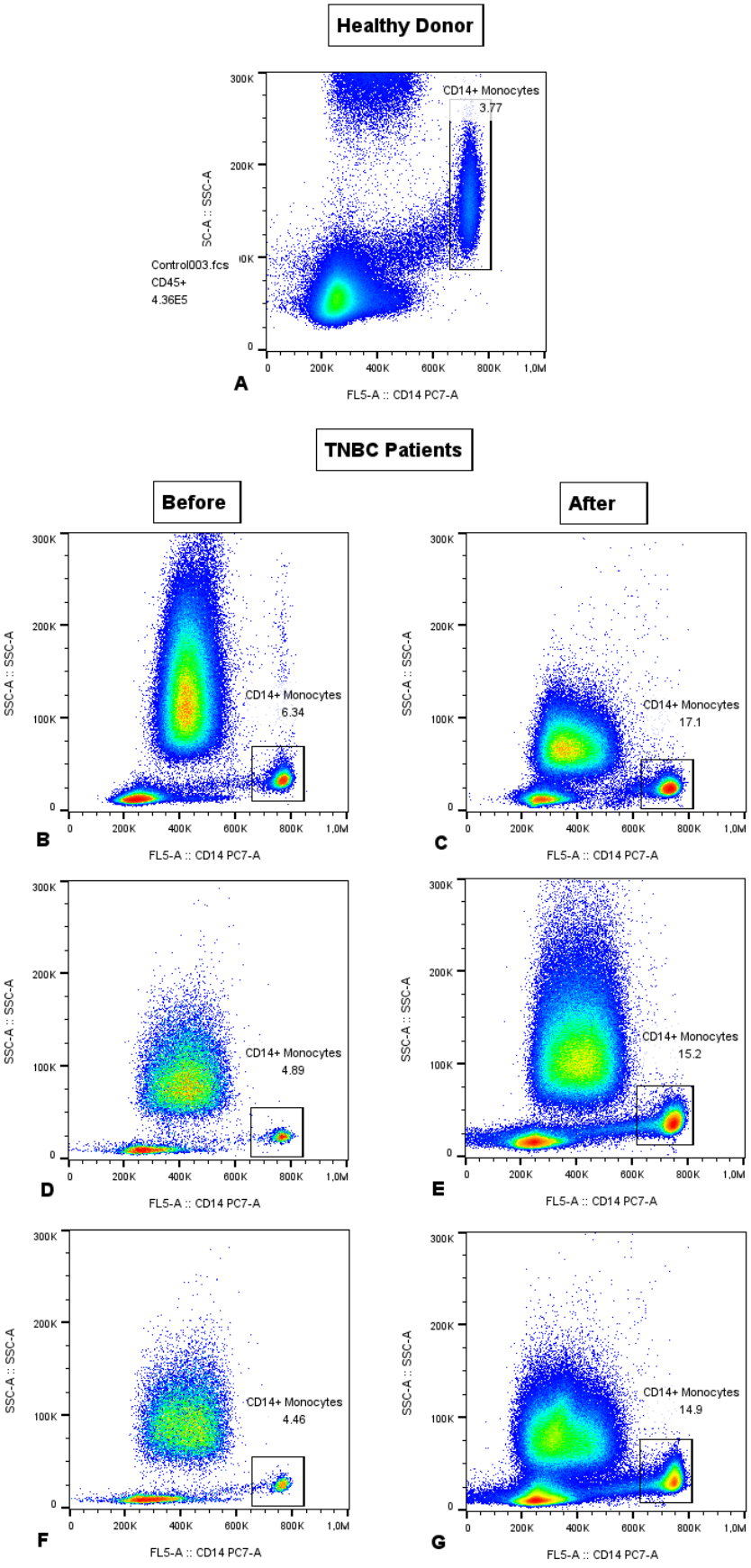

Figure 3.8: An increase in the percentage of CD14$^+$ monocytes was observed in patients after first-phase chemotherapy relative to pre-treatment levels and in healthy donors.

The CD14 vs. SSC-A flow cytometry plots show the total $CD14^+$ monocyte population for a healthy donor and three patients before and after the first-phase chemotherapy. The percentage of total $CD14^+$ monocytes observed in healthy donor 3 was 3.77% (A). The percentage of $CD14^+$ monocytes detected in patient 270 increased from 6.34% (B) to 17.1% (C) after first-phase chemotherapy, while in patient 278 it increased from 4.89% (D) to 15.2% (E). The percentage of $CD14^+$ monocytes detected in the blood of patient 279 increased from 4.46% (F) to 14.9% (G) after the first phase of chemotherapy. SSC-A: side scatter area.

The MFI of CD56 on classical ($CD14^{high}CD16^-$) monocytes was increased in treatment-naïve patients and in patients after first-phase chemotherapy compared to that in healthy donors (median 468 000 vs. 513 500 vs. 386 717, p=0.0247 and p≤0.0001) (Figure 3.9). A significant increase in the MFI of CD56 on classical monocytes was also observed in patients after first-phase chemotherapy compared to pre-treatment levels (median 468 000 vs. 513 500, p=0.0013) (Figure 3.9).

The MFI of CD56 on intermediate ($CD14^+CD16^+$) monocytes was increased in treatment-naïve patients and in patients after first-phase treatment relative to that in healthy donors (median 473 000 vs. 527 500 vs. 408 500, p=0.0247 and p≤0.0001) (Figure 3.9). A significant increase in the MFI of CD56 on intermediate monocytes was also observed after first-phase chemotherapy compared to pre-treatment levels (median 527 500 vs. 473 000, p=0.0027) (Figure 3.9). No significant differences were observed in the MFI of CD56 on non-classical monocytes ($CD14^{dim}CD16^+$).

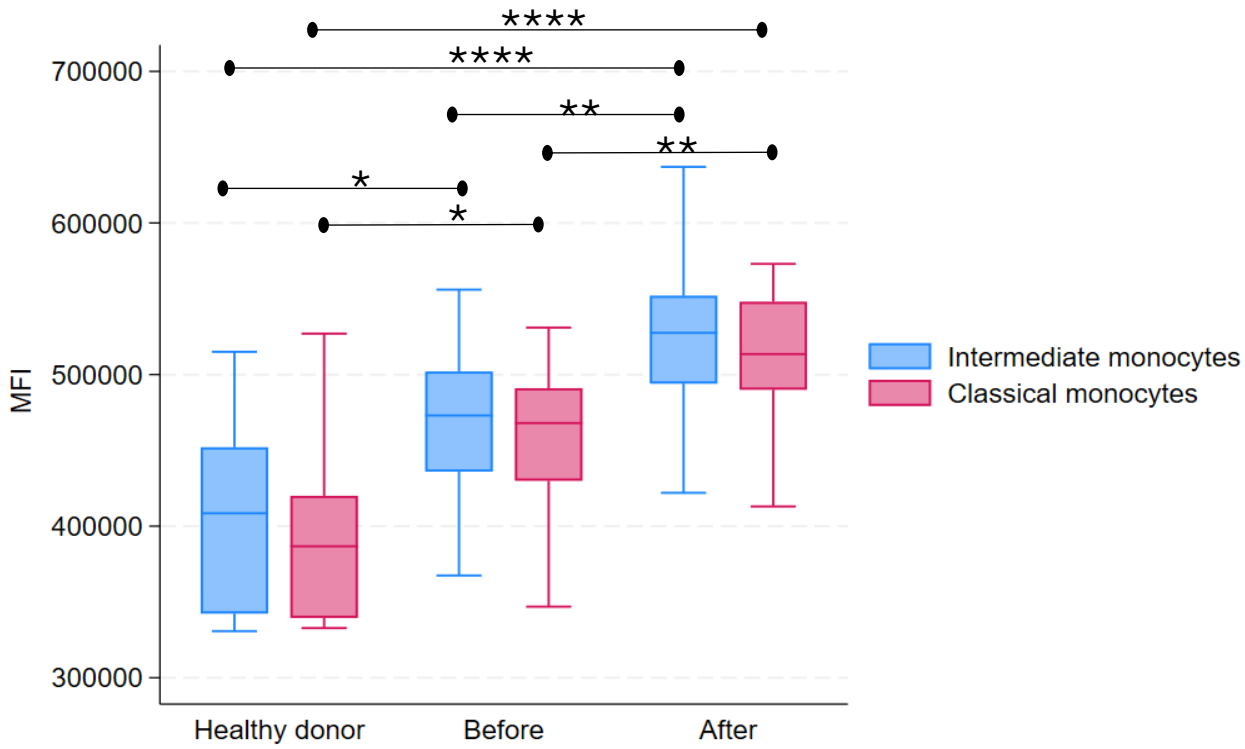

Figure 3.9: The MFI of CD56 on classical and intermediate CD14⁺ monocytes. The MFI of CD56 in classical and intermediate monocytes was higher in patients than in healthy donors. A significant increase in the MFI of CD56 on classical and intermediate monocytes was observed in patients after first-phase chemotherapy. **** p≤0.0001, ** p≤0.01, * p≤0.05. MFI: mean fluorescence intensity.

The MFI of CD206 on classical monocytes ($CD14^{high}CD16^{-}$) was higher in patients before and after first-phase chemotherapy than in healthy donors (median 464 000 vs. 465 000 vs. 449 000, p=0.0268 and p=0.0052, respectively) (Figure 3.10). The MFI of CD206 on intermediate monocytes ($CD14^{+}CD16^{+}$) was also increased in patients before and after first-phase chemotherapy compared to healthy controls (median 481 000 vs. 492 000 vs. 460 000, p=0.0023 and p=0.0003) (Figure 3.10). No significant differences in the MFI of CD206 on non-classical ($CD14^{dim}CD16^{+}$) monocytes were observed among the three participant groups. The median cell percentage and MFI values are presented in Appendix C, Table 7.

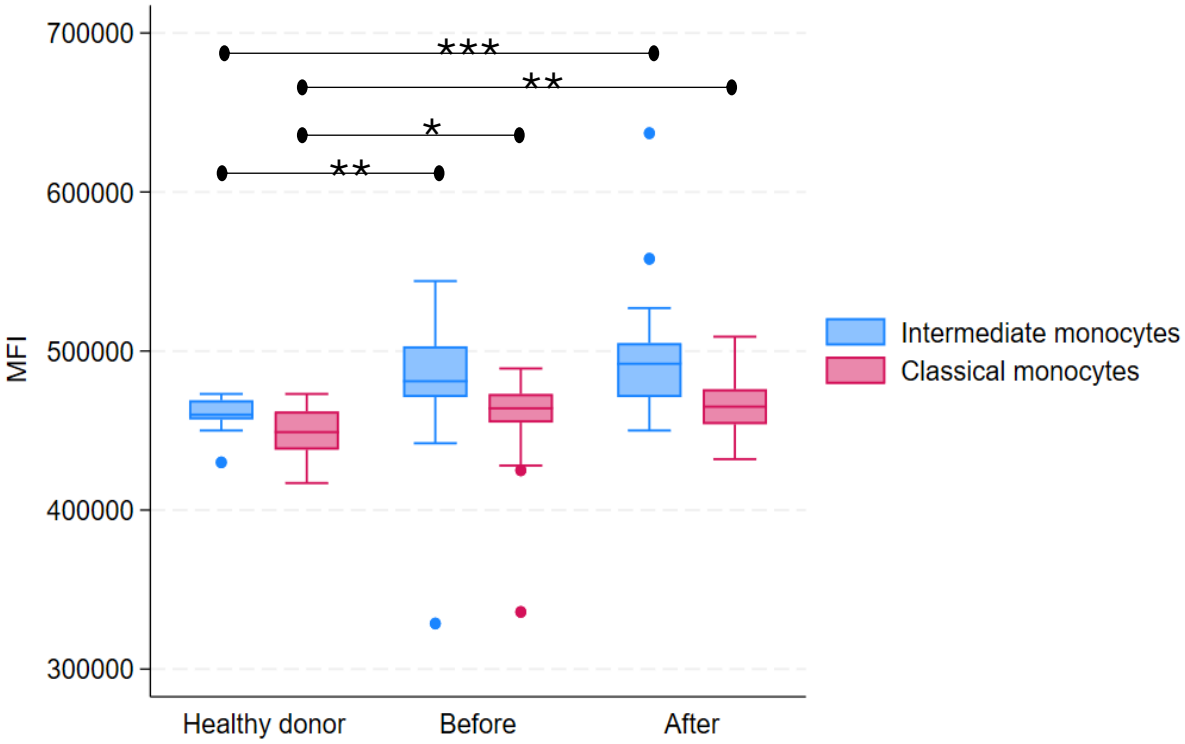

Figure 3.10: The MFI of CD206 in classical and intermediate CD14⁺ monocytes. The MFI of CD206 in intermediate and classical monocytes was higher in patients than in healthy donors. *** p≤0.001, ** p≤0.01, * p≤0.05. MFI: mean fluorescence intensity.

3.4 Discussion

Triple-negative breast cancer is a significant health concern as it is difficult to treat[61]. The immune system plays a critical role in tumourigenesis, tumour progression, and metastasis. Cancer cells actively recruit and stimulate immunosuppressive cells such as Bregs, Th2 and Th17 CD4⁺ T-helper cells, and M2 macrophages in the TME while suppressing anti-tumour immune cells such as CD8⁺ T-cells, Th1 helper T-cells, and M1 macrophages[30, 31, 66-70, 72-77, 80-82]. Evaluating the subsets of these cells found within the peripheral blood of TNBC patients may assist in the identification of surrogate biomarkers and ultimately lead to an improvement in TNBC patient care and survival[62].

A flow cytometric panel and gating strategy was developed to assess the T-cell, B-cell, NK cell, and monocyte immunophenotypic profiles of 23 newly diagnosed TNBC patients before and after first-phase chemotherapy, as well as those of 10 healthy individuals (Chapter 2). The

frequency of the parent cell population and MFI values were noted for each detected population and compared between patients and healthy donors, as well as between patients before and after first-phase chemotherapy. The full blood count results for patients before and after the first phase of chemotherapy were also compared.

3.4.1 Participant demographics correlate with known TNBC characteristics and risk factors

In this investigation, patient demographics and response to treatment correlated with existing literature. The risk of developing cancer peaks at approximately 85 years of age, although this depends on the type of cancer[87]. TNBC is associated with a younger age and higher grade at the time of diagnosis[63, 87, 88]. The median age of the patients in this study was 51 years, and 91.3% of the patients were diagnosed with grade 3 TNBC. Obesity may be a risk factor for the development of higher-grade and higher-stage TNBC tumours, as well as for shorter disease-free and overall survival[89, 90]. In addition, smoking does not appear to increase the risk of developing TNBC[91]. Patients recruited for this study had a median BMI of 26.2 kg/m^2 (considered overweight[89]) and 17.39% were smokers. Anthracycline/taxane-based chemotherapy is frequently used to treat TNBC and approximately 40-50% of patients achieve a PCR after the completion of their chemotherapy regimen[92]. First-phase chemotherapy consisted of at least three cycles of TAC and Neulasta®. Approximately 56% of patients demonstrated a PCR, and 44% had PIC at the primary tumour site after completion of all chemotherapy.

The median percentage of Ki-67 expression identified in the study cohort using immunohistochemistry was 73% and of the 18 patients for whom treatment response information was available, approximately 50% (n=9) of patients which demonstrated a high Ki-67 percentage (≥40%)[85] achieved PCR after the completion of all chemotherapy. Several studies have reported that high levels of Ki-67 (≥ 40%) expressed by TNBC tumours is associated with higher PCR rates but reduced relapse-free survival and overall survival rates in comparison to Ki-67 low TNBC tumours[63, 85, 93-95]. Information on the percentage of TIL infiltration was only available for seven patients, and 57% (n=4) of these patients had a TIL percentage greater than 10%. A high percentage of TIL (>10%) is reported to be associated with improved prognosis and acts as a positive indicator of relapse-free and overall survival in TNBC[86, 96]. Disease-free and overall survival rates were however, not determined in this study.

3.4.2 First-phase chemotherapy affects the levels of various blood cell types

No significant changes in circulating neutrophil, basophil, or platelet levels were observed in patients after first-phase chemotherapy; however, a decrease in lymphocytes and an increase in total monocytes and neutrophil-lymphocyte ratio were observed. Reduced erythrocyte count (below the normal reference range) and eosinophil count were observed in patients after completion of first-phase chemotherapy. Chemotherapy-induced anaemia, thrombocytopenia, and leukopenia's such as lymphopenia or neutropenia, are frequently observed in cancer patients[84, 86, 97, 98]. A significant increase in monocyte count has been observed in breast cancer patients after first-phase chemotherapy in numerous studies; and an elevated eosinophil count is reported to be associated with a positive response to therapy in numerous types of cancer, including metastatic TNBC[99-103]. An increased basophil count is associated with improved progression-free survival in glioblastoma and ovarian cancer patients, but there is a paucity of information on the role of basophils in breast cancer[104, 105]. A high NLR (>1.7) has been reported to be associated with poor outcomes in numerous cancer types, including breast cancer[95].

All patients routinely received G-CSF to alleviate chemotherapy-induced neutropenia. This accounts for the lack of a significant difference in circulating neutrophil levels observed in patients after first-phase chemotherapy compared to healthy donors and pre-treatment levels[106]. There does not appear to be any clear association between the low NLR (<1.7)[95] observed in treatment-naïve patients and their treatment response as 56% of patients achieved a PCR, and 44% demonstrated PIC after the completion of all chemotherapy. The observed decrease in lymphocytes, coupled with no observed change in neutrophil count, may account for the increase in NLR after first-phase chemotherapy. While the reason behind the observed increase in monocyte count after first-phase chemotherapy observed both in this study and in the literature is unclear, the decrease in erythrocyte count in this study's cohort after first-phase chemotherapy correlates with reports of chemotherapy-induced anaemia in the literature[84, 101-103]. The reduction in circulating eosinophils observed in this study's cohort after first-phase chemotherapy may indicate eosinophil homing to the tumour site or may also be a result of the cytotoxic effects of chemotherapy[99, 100]. No significant changes in circulating basophil count were observed in patients after first-phase chemotherapy. Due to the paucity of information on the role of basophils in breast cancer, the significance of this finding is unknown[104, 105]. The lack of a significant change in platelet count in patients after first-phase chemotherapy is unexpected, as thrombocytopenia frequently occurs in patients undergoing chemotherapeutic treatment[98].

3.4.3 First-phase chemotherapy may exert differential effects on lymphocyte subset percentage and MFI values

The proportion of circulating T-cells remained consistent between healthy donors and patients, with no notable variations observed before or after the initial phase of chemotherapy. An increase in the MFI of CD8 on $CD3^+$ T-cells (with no corresponding change in the percentage of $CD8^+$ T-cells or MFI of CD8 on these cells) was observed in patients after first-phase chemotherapy in comparison to healthy donors. No significant difference was observed in the MFI of CD4 on $CD3^+$ lymphocytes.

The scientific literature presents conflicting evidence regarding T-lymphocyte populations in cancer patients undergoing chemotherapy. Whilst some studies have not identified statistically significant alterations in $CD4^+$ and $CD8^+$ T-cell quantities before and after treatment, other investigations have documented an increase in circulating $CD3^+$ and $CD4^+$ T-cells[107-109]. Other studies have reported that $CD4^+$ T-cell quantity decreases and $CD8^+$ T-cell quantity remains the same or increases with each successive cycle of chemotherapy in breast cancer patients[109, 110]. These disparate findings underscore the complexity of immune system responses to chemotherapeutic interventions in oncology patients. The CD8 co-receptor stabilises the T-cell receptor-MHC-I complex during the activation of a cytotoxic T-cell, and CD8 overexpression by $CD8^+$ T-cells has been observed in Severe-Acute Respiratory Syndrome Coronavirus 2 (SARS-CoV-2)-infected patients[111, 112]. There is, however, a paucity of information on increased CD8 in cancer[111, 112].

The absence of a statistically significant difference in the percentage of T-cells between healthy donors and patients prior to initial chemotherapy may suggest an insufficient level of T-cell clonal expansion and infiltration into the tumour in treatment-naïve patients[113]. In addition, an expansion of the Treg subset in treatment-naïve patients in comparison to healthy donors may also be a contributing factor[114] and is investigated in the next chapter. The lack of an observed change in the percentage of circulating T-cells in patients after receiving first-phase chemotherapy compared to pre-treatment levels and healthy donors is unexpected, as lymphopenia is a common side effect of chemotherapy and may indicate that chemotherapy did not cause a change in T-cell infiltration into the TME, that patient T-cells recovered quickly between chemotherapy cycles, or that the TAC chemotherapy regimen may not be as cytotoxic towards T-cells[84, 107].

The decrease in the percentage of circulating $CD19^+$ B-cells in patients after first-phase chemotherapy compared to healthy donors and treatment-naïve patients, aligns with reports of chemotherapy-induced reductions in circulating B-cell levels[84, 97, 108, 109, 115]. While most studies on CD206 has been conducted on dendritic cells and macrophages, the observed increase in the MFI of CD206 on $CD19^+$ B-cells in patients compared to healthy donors, as well as in patients after first-phase chemotherapy may indicate a shift towards a tolerogenic phenotype in TNBC patients both before and after first-phase chemotherapy[112, 115-117].

Approximately 56 of patients achieved a PCR, and 44% demonstrated PIC after the completion of all chemotherapy. No changes in the percentage of T-cells were observed; however, a significant decrease in B-cells was observed in patients after first-phase chemotherapy. An increase in the MFI of CD206 on patient B-cells and CD8 on $CD3^+$ T-cells after first-phase chemotherapy was observed. Wang *et al*.[118] reported an association between poorer patient prognosis, a greater decrease in the percentage of B-cells and $CD4^+$ T-cells, and an increase in the percentage of $CD8^+$ T-cells in breast cancer patients after chemotherapy[111, 112, 118].

3.4.4 An increase in $CD56^{high}$NK cells was observed in patients after first-phase chemotherapy

No statistically significant differences in the percentage of $CD16^+CD56^+$ NK cells were observed between healthy donors and patients, either prior to or following the initial phase of chemotherapy. An increase in the percentage of $CD56^{high}$ NK cells was observed in patients who received first-phase chemotherapy compared with pre-treatment levels. A reduction in the MFI of CD16 in $CD56^+$ NK cells was observed in patients after first-phase chemotherapy compared to that in healthy individuals. An increase in the MFI of CD16 on $CD56^{high}$ NK cells was observed in patients after first-phase chemotherapy compared with pre-treatment levels. An increase in the MFI of HLA-DR in $CD56^+$ NK cells was observed in patients after first-phase chemotherapy compared to that in healthy donors and treatment-naïve patients. The MFI of HLA-DR on $CD56^{high}$ NK cells was elevated in patients after completing first-phase chemotherapy compared to pre-treatment levels.

While numerous studies report no significant changes in circulating $CD56^+$ NK cell quantity in patients after chemotherapy, Mamessier *et al.*[79] observed an increase in the percentage of circulating $CD56^{high}$ NK cells in advanced-stage breast cancer patients[79, 108, 119, 120]. CD16 is closely linked to the antibody-dependent cytotoxic ability of NK cells, and $CD56^{dim}CD16^+$ NK cells have a preferential ability to home to sites of inflammation[79]. HLA-DR expression in NK cells is considered a marker of activation and antigen-presenting ability[51]. Erokhina *et al.*[121] stimulated NK cells with IL-2 *in vitro* and observed that HLA-DR expression was associated with a less differentiated $CD56^{high}$ phenotype[121].

The absence of an observed difference in the percentage of $CD16^+CD56^+$ NK cells between this study's healthy donors and patients, as well as an observed increase in the percentage of $CD56^{high}$ NK cells in patients following initial chemotherapy, aligns with findings reported in the literature[79, 108, 119, 120]. These findings, coupled with the ability of $CD56^{high}$ NK cells to act as precursors to cytotoxic $CD56^{dim}CD16^+$ NK cells, suggest that cytotoxic $CD56^{dim}CD16^+$ NK cell migration into the primary tumour site was increased after first-phase chemotherapy[79, 122]. In the context of this study, the observed decrease in the MFI of CD16 in patient $CD56^+$ NK cells after first-phase chemotherapy in comparison to healthy donors may provide further evidence of increased cytotoxic $CD56^{dim}$ NK cell extravasation and homing after first-phase chemotherapy. In addition, an increase in the MFI of CD16 on $CD56^{high}$ NK cells was observed in patients after first-phase chemotherapy. These $CD56^{high}CD16^{dim}$ NK cells may be intermediaries between the $CD56^{high}$ and $CD56^{dim}$ NK subsets or may represent a weakly cytotoxic subset of $CD56^{high}$ NK cells[79, 122]. The observed increase in the MFI of HLA-DR in $CD56^+$ NK cells and $CD56^{high}$ NK cells in patients following initial-phase chemotherapy, compared to treatment-naïve patients and healthy donors, suggests that initial-phase chemotherapy may have enhanced the function of patient $CD56^+$ and $CD56^{high}$ NK cells[51]. Zhang *et al.*[123] reported an association between high levels of circulating $CD56^+$ NK cells, PCR, and improved overall and relapse free survival in breast cancer patients being treated with neo-adjuvant chemotherapy[123]. In the context of this study, it is unclear how the changes in the percentage of $CD56^+$ and $CD56^{high}$ NK cells and MFI values in patients after first-phase chemotherapy are linked to patient treatment response.

3.4.5 An increase in the MFI of CD56 and CD206 on classical and intermediate monocytes is observed in TNBC patients compared to healthy donors

An increase in the percentage of $CD14^+$ monocytes was observed in patients after first-phase chemotherapy relative to healthy donors and treatment-naïve patients, whereas no change in

individual monocyte subset percentages was observed. The MFI of CD56 on classical and intermediate monocytes was increased in patients relative to that in healthy donors, as well as in patients after first-phase chemotherapy. The MFI of CD206 in intermediate and classical monocytes was increased in patients pre-treatment and after-first phase chemotherapy compared with healthy donors. No change in the MFI of CD56 or CD206 was observed in non-classical monocytes.

Foulds *et al.*[119] immunophenotyped peripheral blood mononuclear cells from breast cancer patients and compared the results with those of healthy donors[119]. They observed an increase in intermediate monocytes and a decrease in classical monocytes, but no change in the percentage of total monocytes[119]. In an investigation into the effect of first-phase Docetaxel and Cyclophosphamide (DOX) chemotherapy (administered in four cycles) on monocyte subsets in breast cancer patients, Valdés-Ferrada *et al.*[103] observed a significant increase in the level of classical monocytes after the first cycle of DOX, and it remained high during successive cycles[103]. In contrast, the level of non-classical monocytes was found to be greatly reduced after one cycle of DOX and gradually increased during subsequent chemotherapy cycles[103]. Although there is limited research on CD56 expression in intermediate, classical, and non-classical monocyte subsets in cancer, Papewalis *et al.*[124] observed a significant increase in $CD16^{+}CD56^{+}$ monocytes in cancer patients compared to healthy controls, as well as an association with tumour spread[124]. The CD206 mannose receptor is associated with the pro-tumourigenic M2 macrophage phenotype and may also play a role in macrophage migration; however, information on CD206 expression in monocytes is lacking[115].

The percentage of $CD14^{+}$ monocytes was higher in patients after first-phase chemotherapy than in healthy donors and treatment-naïve patients, whereas no changes in the percentage of individual monocyte subsets were found. This suggests that a uniform increase in monocyte subsets occurred after the first-phase chemotherapy in response to an increase in cancer cell immunogenicity[125, 126]. Monocytes expressing CD56 are suggested to be precursors to $CD56^{+}$ dendritic cells which may possess lytic effector cell activity against tumour cells as well as superior antigen presentation and stimulatory abilities[78]. However, this conflicts with the observation made by Papewalis *et al.*[124] where an increase in $CD16^{+}CD56^{+}$ monocytes was associated with tumour spread. In the context of this study, the significance of the observed increase in the MFI of CD56 on classical and intermediate monocytes in patients relative to healthy donors, as well as in patients after first-phase chemotherapy is unclear. The favourable differentiation of intermediate and classical monocytes into M2 macrophages may

be reflected by the observed increase in the MFI of CD206 in patients both before and after first-phase chemotherapy, coupled with the observed increase in overall monocyte percentage[115]. Alternatively, an elevated MFI of CD206 in monocytes in the blood may reflect an increase in macrophage migration to the tumour site[127].

An increase in the percentage of $CD14^+$ monocytes was observed in patients after first-phase chemotherapy compared with healthy donors and treatment-naïve patients, whereas no change in the percentage of individual monocyte subsets was observed. In addition, approximately 56% of the patients in this study achieved a PCR after completing all chemotherapy. Axelrod *et al*.[128], after conducting gene expression profiling of peripheral blood immune cells in breast cancer, reported an association between increased classical monocyte-associated genes and PCR[128]. Absolute monocyte count is reported to be an unfavourable prognostic factor in stage II and III TNBC, and that breast cancer patients with an absolute monocyte count >0.48 $x10^9$/L had a shorter overall survival[129]. Another study reported no statistically significant association between the percentage of classical and non-classical monocytes and PCR[103]. In the context of this study, the effect of the increase in the percentage of overall $CD14^+$ monocytes in patients after first-phase chemotherapy on patient treatment response is unclear.

3.5 Conclusion

In this investigation, chemotherapy was found to differentially affect various circulating immune cell subsets. No significant differences in circulating neutrophil, basophil, or platelet counts were observed in the patient cohort after the first phase of chemotherapy. Erythrocyte and eosinophil counts, however, were reduced in patients after first-phase chemotherapy compared with pre-treatment levels. In comparison to healthy donors and treatment-naïve patients, the percentage of $CD19^+$ B-cells was decreased in patients after first-phase chemotherapy, while no significant difference in the percentage of T-cells was observed. No change in the percentage of $CD56^+$ NK cells was observed in patients after first-phase chemotherapy compared to healthy donors and pre-treatment levels; however, an increase in the percentage of $CD56^{high}$ NK cells was observed in patients after receiving first-phase chemotherapy. In addition, an increase in the total $CD14^+$ monocyte count and percentage was observed in patients after first-phase chemotherapy relative to healthy donors and treatment-naïve patients.

Changes in the MFI values of various markers were observed in patients after first-phase chemotherapy compared those in healthy donors and pre-treatment groups. The MFI of CD8 on $CD3^+$ T-cells was higher in patients after first-phase chemotherapy than in healthy donors. The MFI of CD206 on $CD19^+$ B-cells was higher in patients than in healthy donors and in patients after first-phase chemotherapy compared to pre-treatment levels. A decrease in the MFI of CD16 on $CD56^+$ NK cells was observed in patients after first-phase chemotherapy compared with that of healthy individuals and it was also increased on $CD56^{high}$ NK cells in patients after first-phase chemotherapy compared to pre-treatment levels. The MFI of HLA-DR in $CD56^+$ NK cells was higher in patients after first-phase chemotherapy than in healthy donors and treatment-naïve patients. An increase in the MFI of HLA-DR on $CD56^{high}$ NK cells was observed in patients after completing first-phase chemotherapy compared to pre-treatment levels. The MFI of CD56 on classical and intermediate monocytes was increased in patients relative to healthy donors, as well in patients after first-phase chemotherapy. Finally, the MFI of CD206 on intermediate and classical monocytes was increased in patients before and after the first phase of chemotherapy compared to that in healthy donors.

The findings of this study may suggest that chemotherapy did not cause a change in T-cell infiltration into the TME, or that patient T-cells recovered quickly between chemotherapy cycles[84, 107]. An increase in the MFI of CD206 on $CD19^+$ B-cells in patients after receiving first-phase chemotherapy may indicate that first-phase chemotherapy not only decreases the percentage of $CD19^+$ B-cells, but also induces a shift towards a tolerogenic phenotype[115-117]. The findings of this study may suggest that there was an increase in activated cytotoxic $CD56^{dim}CD16^+$ NK cell homing to the primary tumour site after first-phase chemotherapy[51, 79, 122]. In addition, an increase in the MFI of CD16 and HLA-DR on $CD56^{high}$ NK cells in patients after first-phase chemotherapy suggests the presence of activated $CD56^{high}CD16^{dim}$ NK cells, which may be intermediaries between $CD56^{high}$ and $CD56^{dim}$ NK subsets or represent a weakly-cytotoxic subset of $CD56^{high}$ NK cells[51, 79, 122]. The favouring of intermediate and classical monocyte differentiation into pro-tumourigenic M2 macrophages may be reflected by the observed increase in the MFI of CD206 in patients, coupled with the observed increase in overall monocyte percentage in patients both before and after first-phase chemotherapy. Alternatively, an elevated MFI of CD206 on monocytes in the blood may reflect an increase in macrophage migration to the tumour site[127]. Chemotherapy may exert long-term effects on immune cell subset proportions and marker expression[97, 102, 130, 131]. In the context of this study, it is unclear how long the aforementioned changes in immune cell subset percentage or

marker MFI values may last, and whether an association with patient overall and disease-free survival exists.

Manipulation of immune cells by cancer to favour a pro-tumourigenic TME has been well documented in numerous cancer types[132]. Immunosuppressive $CD4^+$ Tregs are essential for the control of immune responses and prevention of autoimmunity, although their exact role in the TME of breast cancer is controversial[132, 133]. To obtain insights into the circulating $CD4^+$ Treg subsets of TNBC patients, the flow cytometric method described in Chapter 2 was used to identify and characterise these cells.

Chapter 4: Comparative analysis of CD4$^+$ Treg immunophenotype in healthy donors and TNBC patients before and after first-phase chemotherapy

4.1 Introduction

CD4$^+$ T-cell subsets play a crucial yet dual role in malignancy[68-70]. Th1 helper T-cells promote antibody-independent immune responses and activate anti-tumourigenic immune cells, whereas Th2 helper T-cells are conventionally associated with pro-tumourigenic activity, such as the activation of M2 macrophages[68-70]. Th17 helper T-cells are pro-inflammatory and stimulate the secretion of IL-6, IL-8, and colony-stimulating factors[68-70]. CD4$^+$ Tregs are another helper T-cell subset with major involvement in malignancy, and increased Treg infiltration into the TME has been observed in numerous cancer types[68-70, 134].

CD4$^+$ regulatory T-cells or Tregs are specialised immunosuppressive cells and are critical to the regulation of innate and adaptive immune responses, as well as the prevention of autoimmunity[135]. They are derived from the same precursors as helper T-cells and can exert their inhibitory function by secreting immunosuppressive cytokines, inducing target cell death, manipulating APC formation and function, and disrupting ATP metabolism[135-137]. Tregs can inhibit co-stimulatory molecule expression on APCs thereby limiting their ability to mount an adaptive immune response[135-137]. They can release Granzymes A, B and perforin to induce effector T-cell apoptosis, and they can secrete immunosuppressive cytokines such as IL-10, TGF-β, IFN-γ, and interleukin 9 (IL-9)[135-137]. In addition, CD39-expressing Tregs can convert ATP into adenosine diphosphate (ADP) and adenosine monophosphate (AMP) which ultimately inhibit effector T-cell activation and proliferation and promote Treg formation[135-137]. The potent immunosuppressive function of Tregs makes them critically important in the context of cancer, as they can suppress anti-tumourigenic immune responses and contribute towards the formation of a pro-tumourigenic TME[137]. Tregs may accumulate in the TME in response to cytokines produced by tumour cells, after expanding *in situ* within the tumour, or through the conversion of conventional T-cells into Tregs[138]. Tregs have a paradoxical role in cancer[139].

Tregs can be classified by their expression of various intracellular and membrane-bound proteins. They are often identified by the expression of CD3, CD4, CD25, CD127, and FoxP3[140]. Helper T-lymphocytes constitutively express CD3 and CD4 and as Tregs express

much higher levels of CD25 on their cell surface than conventional T-cells, CD25 positivity can be used as a Treg-identifying marker[140]. CD127 is inversely correlated with suppressive ability and is either absent or expressed in very small quantities in Tregs[140, 141]. The transcription factor FoxP3 is essential for Treg function, although it may also be expressed by activated conventional T-cells[142].

Treg activation and function can be assessed using markers such as CD39, Helios, and CD45RA[140]. CD45RA expression is associated with a naïve T-cell phenotype and $FoxP3^{+/high}CD45RA^{-}$ Tregs have been defined as activated effector or memory Tregs and $FoxP3^{+}CD45RA^{+}$ Tregs as naïve resting Tregs[136, 138, 143]. Helios positivity can be used to distinguish between Tregs ($FoxP3^{+}Helios^{+}$) and $FoxP3^{+}$ conventional T-cells ($FoxP3^{+}Helios^{-}$)[140]. CD39, while expressed on some conventional T-cells, is a functional marker of enhanced suppressive activity in Tregs and can also be used as a marker for activated ($FoxP3^{+/high}CD45RA^{-}$) Tregs[140]. While numerous novel Treg subsets continue to be identified, the most extensively studied Treg subset is the $CD25^{+/high}$ $FoxP3^{+}$ subset[136]. Changes in the proportion and marker expression of various peripheral blood immune cell subsets, including Tregs, have been reported in cancer patients both before and after receiving chemotherapeutic treatment[84, 101, 144].

An increase in the percentage of $CD25^{+}FoxP3^{+}$ Tregs in metastatic cancers including breast, colorectal, and ovarian cancer is associated with poor treatment response and worse survival rates[140, 145-154]. Tregs can however, serve to mitigate the tumour-promoting effects of inflammation and increased levels of Tregs has been associated with improved patient outcomes in some cancers such as colorectal carcinoma[139]. In ovarian cancer patients undergoing treatment, the Treg percentage fluctuated during the course of chemotherapy before returning to pre-chemotherapy levels after the completion of treatment[147]. Changes in the immunophenotypic profile of Tregs and a decrease in Treg quantity in cancer patients both before and after chemotherapy have also been reported in various studies[155-159]. While the exact role of Tregs in cancer is controversial, they are clearly major role players, and obtaining further insight into changes in their proportion and marker expression in TNBC both before and after treatment exposure is essential due to the limited range of treatments that exist for TNBC as well as the aggressive nature of this breast cancer subtype[61, 63, 160-162].

4.2 Materials and Methods

4.2.1 Immunophenotyping of $CD4^+CD25^+FoxP3^+$ Tregs using flow cytometry

Circulating $CD4^+CD25^+FoxP3^+$ Tregs were identified and characterised in participant whole blood using a CytoFlex flow cytometer (Beckman Coulter, USA), DURAClone IM Treg kits (Beckman Coulter, USA) and a CD127 liquid antibody drop-in as described in Chapter 2. Following data acquisition, the FCS files were imported into the Kaluza Analysis software version 2.2.1 (Beckman Coulter, USA) to exclude doublets and adjust scaling and compensation. These files were then imported into FlowJo™ software version 10.9.0 (Beckton Dickenson, USA), where the percentage of the parent cell population and MFI values of the markers of interest were determined, as described in Chapter 2. The geometric MFI of the different markers was measured as an indication of fluorophore brightness and as a relative measure of antigen abundance. Patients 278, 277, 282, and 283 were excluded from the analysis due to a low number of cells having been acquired.

4.2.2 Data and statistical analysis

To detect differences in the percentage of $CD4^+CD25^+FoxP3^+$ Tregs and their marker expression between healthy donors and TNBC patients, as well as between patients before and after first-phase chemotherapy, the percentage of the parent cell population and MFI values of the markers of interest (CD45RA, CD39, CD127, and Helios) were determined using FlowJo™ software version 10.9.0 (Beckton Dickenson, USA).

A Shapiro-Wilk test was conducted to determine the distribution of the collected data. The null hypothesis that the data had a normal distribution was rejected as $p \leq 0.05$ for several variables. As data were collected from three participant groups and did not have a normal distribution, a Kruskal-Wallis equality of populations test and Dunn's pairwise comparison test were used to compare the median percentage of population and MFI values between healthy donors and patients, and patients before and after first-phase chemotherapy. A p-value of less than or equal to 0.05 was deemed statistically significant. The STATA Basic Edition 18.0 statistical software (STATA Corp LLC, USA) was used to conduct all statistical tests and generate graphs.

4.3 Results

Flow cytometric analysis of circulating $CD4^+CD25^+FoxP3^+$ Tregs was performed in 19 TNBC patients before and after first-phase chemotherapy and in 10 healthy donors. No significant change in the median percentage of $CD25^+FoxP3^+$ Tregs was observed between patients before and after first-phase chemotherapy (median 17.3% vs. 19.3%, p=0.4539) or between patients before and after first-phase chemotherapy and healthy donors (median 17.3% vs. 19.3% vs. 18.65%, p=0.3901 and 0.4275). Between individual patients however, changes in the percentage of $CD25^+FoxP3^+$ Tregs was evident. The largest change in the percentage of $CD25^+FoxP3^+$ Tregs was detected in patient 272 where it decreased from 99.9% to 21.6% after first-phase chemotherapy (Figure 4.1 A and B) and in patient 309, it increased from 6.88% to 98.6% after first-phase chemotherapy (Figure 4.1 C and D). The median frequency of the parent cell populations and MFI values can be found in Appendix D, Table 1.

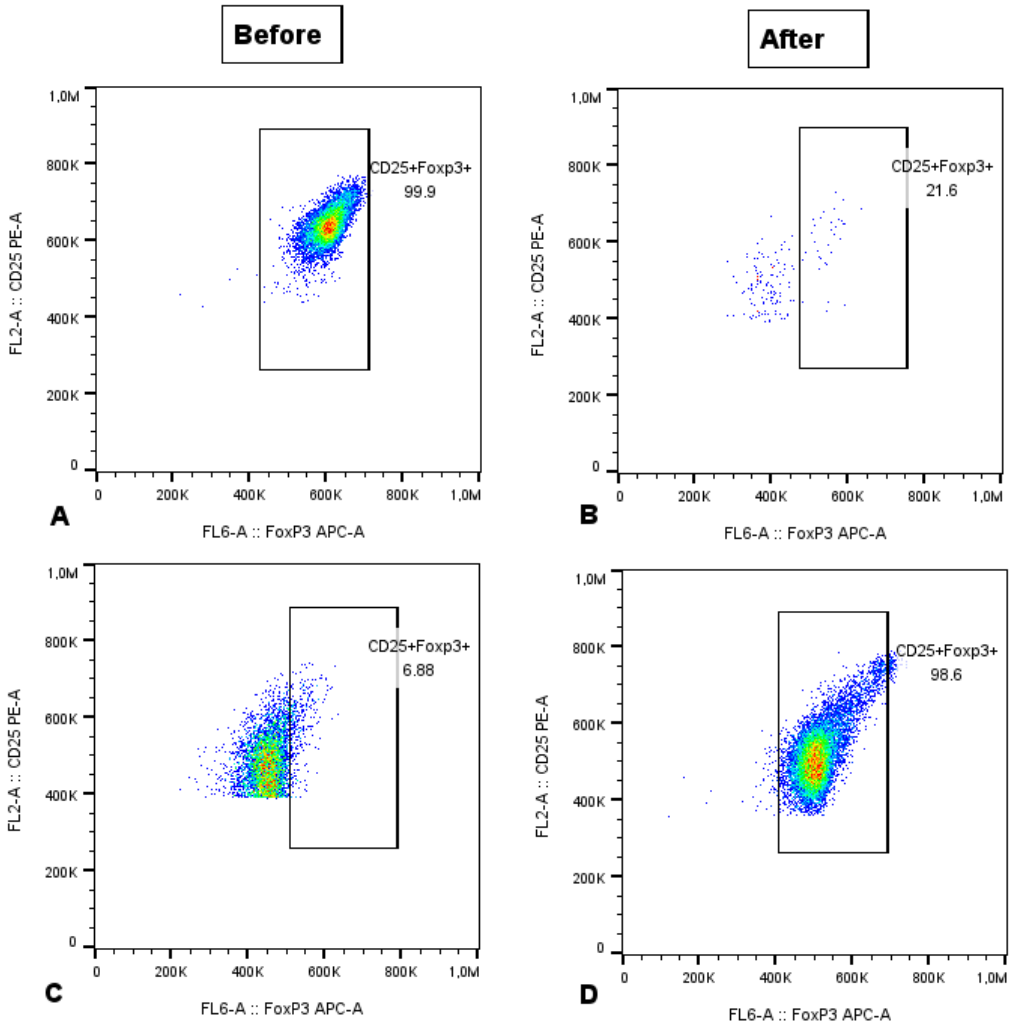

Figure 4.1: The CD25⁺FoxP3⁺ Treg populations detected in patients 272 and 309 before and after first-phase chemotherapy. The above FoxP3 vs. CD25 plots showing CD25⁺FoxP3⁺ Treg populations are for patients 272 and 309 before and after first-phase chemotherapy. The percentage of CD25⁺FoxP3⁺ Tregs detected in patient 272 decreased from 99.9% (A) to 21.6% (B) after first-phase chemotherapy, while the percentage of CD25⁺FoxP3⁺ Tregs detected in patient 309 increased from 6.88% (C) to 98.6% (D) after first-phase chemotherapy. FoxP3: Forkhead Box Protein 3. Treg: regulatory T-cell.

A significant decrease in the MFI of CD45RA on CD25⁺FoxP3⁺ Tregs was observed in patients after first-phase chemotherapy compared with that in treatment-naïve patients (median 285 334 vs. 296 673, p=0.0443) (Figure 4.2 A). A significant increase in the MFI of CD39 on CD25⁺FoxP3⁺ Tregs was observed in treatment-naïve patients compared to healthy donors (median 452 000 vs. 413 500, p=0.0046) and in patients after first-phase chemotherapy compared to healthy donors (median 465 000 vs. 413 500, p=0.0003) (Figure 4.2 B). The

median frequency of the parent cell populations and MFI values can be found in Appendix D Table 1.

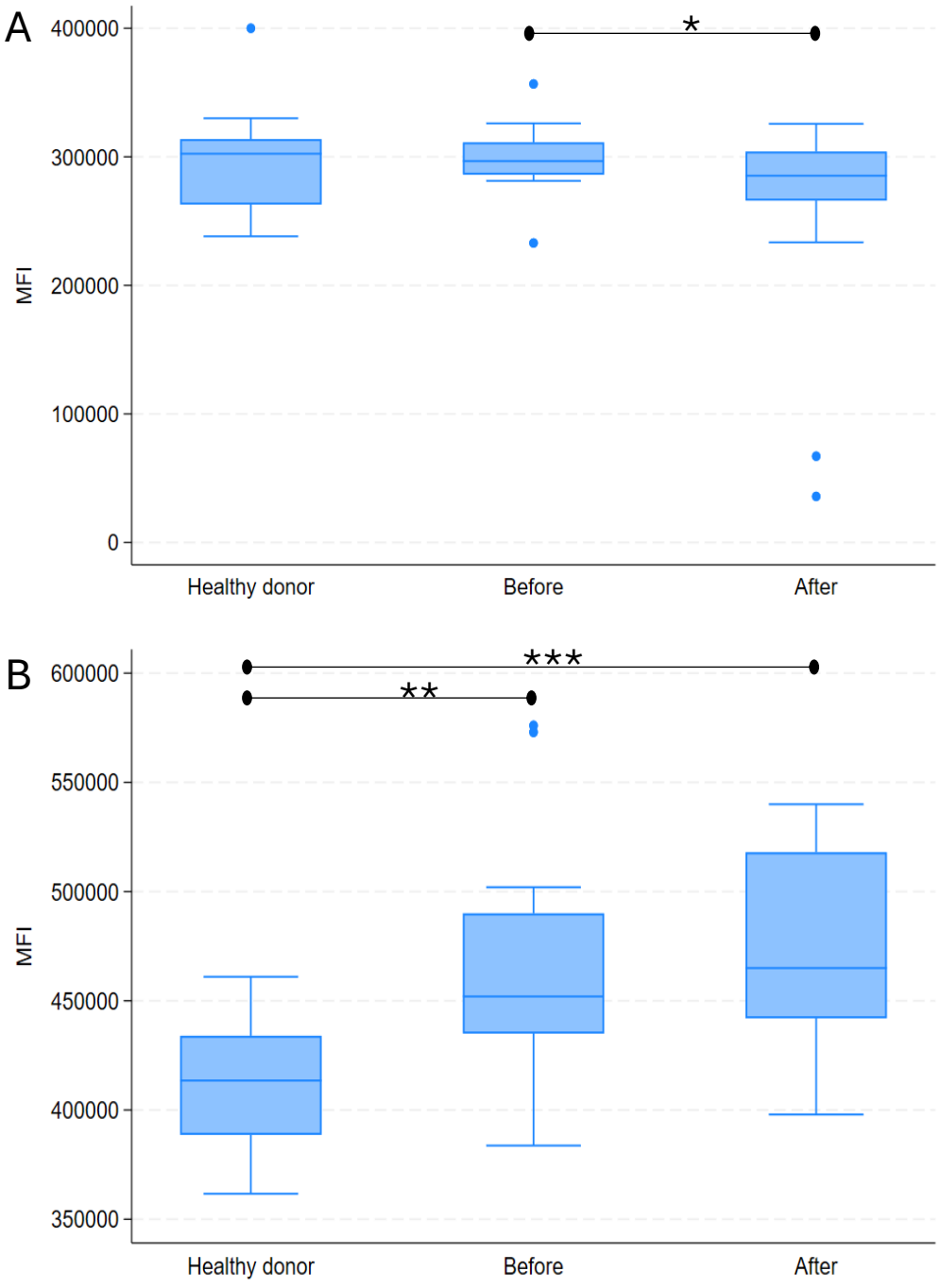

Figure 4.2: The MFI of CD45RA and CD39 on participant CD25⁺FoxP3⁺ Tregs. The median MFI of CD45RA in patient CD25⁺FoxP3⁺ Tregs after first-phase chemotherapy was significantly lower than that in treatment-naïve patients (A), while the median MFI of CD39 on these cells was significantly higher in patients both before and after first-phase chemotherapy

than in healthy donors (B). *** p≤0.001, ** p≤0.01, * p≤0.05. MFI: mean fluorescence intensity. FoxP3: Forkhead Box Protein 3. Treg: regulatory T-cell.

A significant increase in the MFI of CD127 on $CD25^{+}FoxP3^{+}$ Tregs was observed in patients after first-phase chemotherapy compared to that in healthy donors (median 289 945 vs. 258 720.5, p=0.0237) (Figure 4.3 A). A non-significant increase in the MFI of CD127 on $CD25^{+}FoxP3^{+}$ Tregs was observed in treatment-naïve patients compared to that in healthy donors (median 281 161 vs. 258 720.5, p=0.0692).

No significant change in the MFI of Helios on $CD25^{+}FoxP3^{+}$ Tregs was observed between patients before and after first-phase chemotherapy and healthy donors (median 470 000 vs. 484 000 vs. 476 500, p=0.4598 and 0.1046, respectively) (Figure 4.3 B). A non-significant increase in the MFI of Helios on the $CD25^{+}FoxP3^{+}$ Tregs of patients after first-phase chemotherapy compared with pre-treatment levels was observed (median 484 000 vs. 470 000, p=0.0511). The median frequency of parent cell populations and MFI values can be found in Appendix D Table 1.

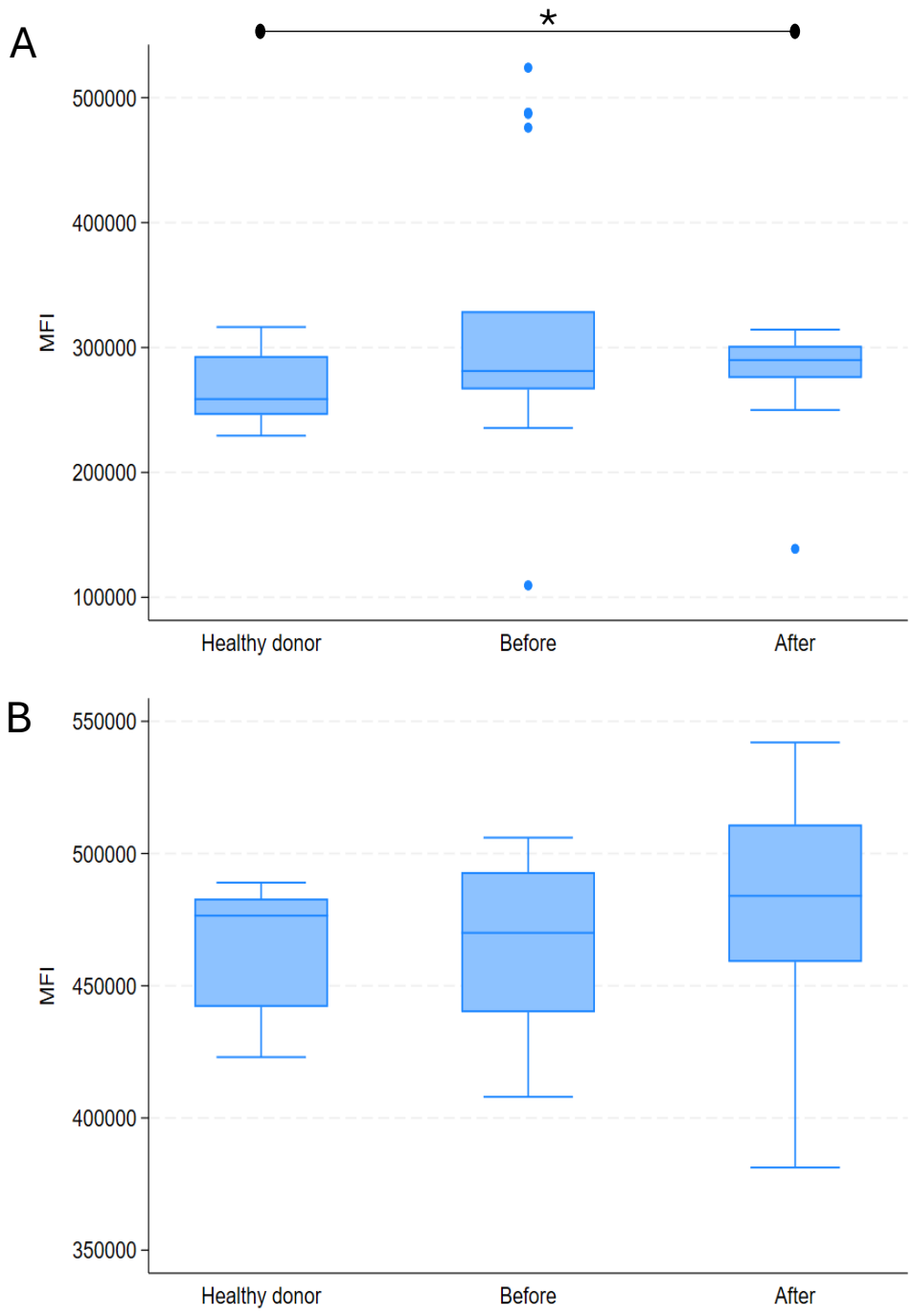

Figure 4.3: The MFI of CD127 and Helios on participant CD25^{+}FoxP3^{+} Tregs. The median MFI of CD127 on patient CD25^{+}FoxP3^{+} Tregs was significantly increased after first-phase chemotherapy in comparison to healthy donors (A), whereas no significant difference in the median MFI of Helios in these cells was observed between healthy donors and patients (B). * p≤0.05. MFI: mean fluorescence intensity. FoxP3: Forehead Box Protein 3. Treg: regulatory T-cell.

4.4 Discussion

$CD4^+$ Tregs are potent immunosuppressors yet while their increased infiltration into the TME has been observed in numerous cancer types, their exact role in the breast cancer TME is controversial[68-70, 132-134, 137]. A flow cytometric panel and gating strategy was developed to assess the $CD4^+CD25^+FoxP3^+$ Treg immunophenotypic profiles of 19 newly diagnosed TNBC patients before and after first-phase chemotherapy, as well as those of 10 healthy individuals (Chapter 2). The frequency of the parent cell population and MFI values were noted for each detected population and compared between patients and healthy donors, as well as between patients before and after first-phase chemotherapy.

No significant change in the median percentage of $CD25^+FoxP3^+$ Tregs was observed between the patient and healthy donor groups, which correlates with the findings of another study[162]. In contrast, other studies have reported an increase in the proportion of $CD25^+FoxP3^+$ Tregs in the peripheral blood of patients with metastatic breast, colorectal, and ovarian cancers compared to that of healthy donors[148-154]. The median percentage of $CD25^+FoxP3^+$ Tregs was similar between patients before and after first-phase chemotherapy, which correlates with the findings of another study[163]. Other studies, however, have reported chemotherapy-induced $CD25^+FoxP3^+$ Treg apoptosis in patients with breast and non-small cell lung cancer[154, 164]. The median percentage of $CD25^+FoxP3^+$ Tregs in the peripheral blood of TNBC patients (both before and after first-phase chemotherapy) and healthy donors was similar, indicating that neither the presence of a TNBC primary tumour nor first-phase chemotherapy caused a change in the percentage of circulating $CD25^+FoxP3^+$ Tregs in the groups as a whole[162, 163].

Some changes were, however, noted in individual patients. The percentage of $CD25^+FoxP3^+$ Tregs increased in patient 309 from 6.88% to 98.6% after first-phase chemotherapy, and this may have influenced patient treatment outcomes as, after the completion of all chemotherapy, this patient presented with PIC at the primary tumour site. There is a paucity of literature describing an increase in $CD25^+FoxP3^+$ Tregs after chemotherapy; however, one study reported that while both the absolute and relative number of $CD25^+$ Tregs decreased during chemotherapy, the proliferative capacity of these cells increased, which may be due to a chemotherapy-induced increase in effector T cells displaying this phenotype[165]. Other studies have reported an initial decrease in the proportion of $FoxP3^+$ Tregs at the start of chemotherapy, with no further decrease observed during subsequent cycles[166]. This suggests

that Tregs can resist chemotherapy-induced destruction or recover quickly between chemotherapy cycles[166]. The observed increase in $CD25^+FoxP3^+$ Tregs in patient 309 after first-phase chemotherapy may be due to an increase in the ability of this patient's $CD25^+FoxP3^+$ Tregs to recover from chemotherapy exposure and resist chemotherapy-induced destruction, or it may indicate a shift in the $CD4^+$ T-cell subset phenotype after first-phase chemotherapy[165, 166].

No correlation or a positive association between circulating $CD25^+FoxP3^+$ Tregs and breast cancer stage and clinical outcomes has been reported[151, 167]. Similarly, no association between the proportion of circulating $CD25^+FoxP3^+$ Tregs and the PCR rate after neoadjuvant chemotherapy was observed in a study on TNBC[167]. In the context of the data presented here however, it is unclear how the percentage of $CD25^+FoxP3^+$ Tregs and treatment response are linked.

A significant decrease in the MFI of CD45RA on $CD25^+FoxP3^+$ Tregs was observed in patients after first-phase chemotherapy compared with that in treatment-naïve patients and, while there is a paucity of reports on changes in the MFI of CD45RA on Tregs in TNBC, this observation may be indicative of a chemotherapy-induced destruction of naïve $CD25^+FoxP3^+$ Tregs and/or an increase in effector $CD25^+FoxP3^+$ Tregs[140, 151, 168]. The lack of a significant difference in the total percentage of $CD25^+FoxP3^+$ Tregs in patients after first-phase chemotherapy, coupled with the observed decrease in the MFI of CD45RA on these cells, may indicate a shift towards an effector Treg phenotype in TNBC patients after first-phase chemotherapy[140, 151]. Approximately 56% of the patients in this study achieved PCR after the completion of chemotherapy. There is a paucity of information on the association between the MFI of CD45RA on $CD25^+FoxP3^+$ Tregs and treatment response in breast cancer patients; however, an association between increased $CD45RA^-FoxP3^{high}$ Treg frequency and poorer patient prognosis has been reported in colorectal and head and neck squamous cell carcinoma patients[169, 170]. An investigation utilising a larger sample size may yield more significant insights into the relationship between CD45RA expression on $CD25^+FoxP3^+$ Tregs and treatment response in TNBC patients.

The MFI of CD39 on $CD25^+FoxP3^+$ Tregs was significantly higher in patients before and after first-phase chemotherapy than in healthy donors. The CD39 molecule is critical for the immunosuppressive function of Tregs, and increased expression of CD39 on Tregs has been

reported in numerous cancer types[155, 156]. The findings of this study may be indicative of an increase in highly suppressive $CD25^{+}FoxP3^{+}$ Tregs in TNBC patients[155, 156]. Chemotherapy-damaged cells release ATP into the extracellular environment therefore, the observed increase in the MFI of CD39 on $CD25^{+}FoxP3^{+}$ Tregs in patients after first-phase chemotherapy in comparison to healthy donors may indicate an increase in CD39-mediated ATP breakdown by $CD25^{+}FoxP3^{+}$ Tregs in TNBC patients after first-phase chemotherapy[155, 157-159]. There is a paucity of information on whether an association exists between the MFI of CD39 on $CD25^{+}FoxP3^{+}$ Tregs and patient treatment response however, an increase in CD39 expression on intratumoural $CD25^{high}FoxP3^{+}$ Tregs is associated with poorer outcomes in colon and gastric cancer patients[171, 172]. Increased circulating $CD39^{+}CD25^{+}CD127^{-}$ Tregs are associated with poorer survival in sepsis patients[173]. It is unclear whether an association exists between the MFI of CD39 on $CD25^{+}$ $FoxP3^{+}$ Tregs and TNBC patient treatment response. A larger study may yield more significant results and provide more insight into the relationship between CD39 on $CD25^{+}FoxP3^{+}$ Tregs and treatment response in TNBC patients.

An increase in the MFI of CD127 on patient $CD25^{+}FoxP3^{+}$ Tregs after first-phase chemotherapy compared to healthy donors was observed. The findings of this study do not correlate with what is reported in the literature as low CD127 expression has conventionally been used as an identifying feature of Tregs, and a decrease in Treg levels after chemotherapy has been reported in a variety of cancer types, including breast cancer[140, 141, 174-176]. Simonetta *et al.*[177] observed an increase in CD127 expression in activated $CD25^{+}FoxP3^{+}$ Tregs and found that these cells demonstrated an increased survival capacity[177]. The lack of a significant difference in the total percentage of $CD25^{+}FoxP3^{+}$ Tregs in patients after first-phase chemotherapy, coupled with the observed increase in the MFI of CD127 on these cells, may indicate a shift towards an activated and treatment-resistant Treg phenotype in TNBC patients after first-phase chemotherapy[177]. The role of intratumoural and circulating Tregs in breast cancer patient treatment response and prognosis is controversial[160-162]. It is unclear whether an association exists between treatment outcome and the MFI of CD127 on $CD25^{+}FoxP3^{+}$ Tregs in this study's patient cohort. Larger studies may yield more significant insights.

The MFI of Helios in $CD25^{+}FoxP3^{+}$ Tregs was similar between patients before and after first-phase chemotherapy, as well as between patients and healthy donors. No significant change in the percentage of circulating $FoxP3^{+}Helios^{+}$ Tregs was observed in non-small cell lung cancer patients compared to healthy donors, whereas an increase in the percentage of circulating $FoxP3^{+}Helios^{+}$ Tregs was observed in renal cell carcinoma and pancreatic cancer

patients compared to healthy donors[178-180]. Helios is essential for Treg stability and a decrease in Helios expression is associated with a decrease in the suppressive activity of Tregs[181-183]. The lack of an observed change in the MFI of Helios in $CD25^+FoxP3^+$ Tregs between patients before and after first-phase chemotherapy, as well as between patients and healthy donors, may indicate that neither the presence of a TNBC tumour nor first-phase chemotherapy affects $CD25^+FoxP3^+$ Treg stability[181-183]. There is a paucity of information on whether an association exists between the MFI of Helios on $CD25^+FoxP3^+$ Tregs and breast cancer patient treatment response; however, in non-small cell lung cancer patients, no significant association was observed between $FoxP3^+Helios^+$ Tregs and cancer progression[178]. A larger study may yield more significant insights into the relationship between Helios expression, $CD25^+FoxP3^+$ Tregs, and treatment response in TNBC patients.

4.5 Conclusion

While changes in the Treg percentage were observed in some patients before and after first-phase chemotherapy, no change in the median percentage of $CD25^+FoxP3^+$ Tregs was observed between patient groups and healthy donors, as well as between all patients before and after first-phase chemotherapy. This may indicate that neither the primary tumour nor the first-phase chemotherapy caused a change in the percentage of circulating $CD25^+FoxP3^+$ Tregs in the majority of TNBC patients in this study. The findings of this study may provide evidence of a shift in the $CD25^+FoxP3^+$ Treg profile towards an activated and highly immunosuppressive effector phenotype after first-phase chemotherapy, although the effect of these findings on patient treatment response is not entirely clear.

Manipulation of immune cells by cancer to favour a pro-tumourigenic TME has been reported in numerous cancer types, and long-term changes to both circulating and intratumoural immune cell subset proportions and marker expression after chemotherapy has also been reported[97, 102, 130-132]. Complex signalling networks exist between cells in the body and are fundamental to the regulation of proper cell growth, differentiation, metabolism, and survival[184]. In cancer, signalling molecule secretion and intercellular signalling are frequently dysregulated, which contributes to uncontrolled cellular proliferation, evasion of apoptosis and immune destruction, stimulation of angiogenesis, and invasion and metastasis[184]. Understanding the effect of cancer and first-phase chemotherapy on cellular communication

and its impact on tumour progression and treatment response is essential for the identification of new therapeutic targets and improvement of existing treatment strategies for TNBC[184].

Chapter 5: Dynamic changes in cytokine and growth factor levels in TNBC patients before and after first-phase chemotherapy

5.1 Introduction

The complex signalling networks that exist between cells in the body are fundamental in regulating cell growth, differentiation, metabolism, and survival[184]. These networks rely on signalling molecules such as cytokines, chemokines, growth factors, and hormones[184]. Dysregulated secretion of these signalling molecules leads to aberrant intercellular communication and may promote the development of various diseases[184]. In cancer, signalling molecule secretion and intercellular signalling are frequently dysregulated, which contributes to uncontrolled cellular proliferation, evasion of apoptosis and immune destruction, stimulation of angiogenesis, and invasion and metastasis[184]. Understanding the interplay between these signalling molecules and tumour growth and progression may provide further insights into tumour biology and allow for the identification of potential therapeutic targets[184].

Cytokines serve as chemical messengers between immune and non-immune cells[185, 186]. They are pleiotropic, may be secreted by multiple cell types, and can exert functions similar to each other[187]. They act in an autocrine or paracrine manner, exert their function at very low doses, and have short half-lives, allowing cells to communicate quickly while minimising signal residue and excessive activation or inhibition of the target cell[185, 186]. Cytokines can be classified into numerous categories based on their function, location, and cell-of-origin[186, 187]. Pro-inflammatory cytokines, such as IL-6, IL-8, IL-12, TNF-α, and interferons stimulate immunocompetent cells[186, 187]. Anti-inflammatory cytokines, such as IL-4, IL-6, IL-10, IL-11, IL-13, and TGF-β suppress immune activity and function[186, 187]. Some cytokines, such as IL-6, may demonstrate both pro- and anti-inflammatory effects depending on the context, and can generate multiple immune responses[186, 187]. Alterations in cytokine levels can occur due to physical trauma, such as surgery and radiation, infection, autoimmunity, and cancer[185].

The cytokine IL-6 is manufactured at sites of inflammation by monocytes and macrophages and can act in either anti- or pro-inflammatory capacities[188-191]. In cancer, IL-6 may also be secreted by tumour cells and aids in promoting angiogenesis, tumour cell growth, macrophage polarisation, and metastasis, or it may serve to mobilise $CD8^+$ cytotoxic T-cells and promote

leukocyte survival, proliferation, and recruitment in certain contexts[192]. Increased IL-6 levels have been detected in the serum of patients with breast cancer and is associated with an increased risk of metastatic disease, treatment resistance, and poorer patient prognosis[189]. IL-8 is a pro-inflammatory cytokine, chemoattractant, and angiogenic factor[192-194]. In the TME, IL-8 promotes preferential recruitment of pro-tumourigenic immune cells and enhances the activity of TAMs, CAFs, and cancer cells[192, 193]. The secretion of IL-8 by breast cancer cells promotes tumour progression, invasion, and metastasis[192]. Increased IL-8 levels in the serum of breast cancer patients have been associated with increased tumour invasiveness and stage as well as poorer patient prognosis[192]. Concurrent IL-6 and IL-8 signalling is critical in TNBC resistance to apoptosis and anchorage-independent growth[195]. The potent anti-inflammatory properties of IL-10 make it one of the most significant cytokines in cancer progression and metastasis, although its exact role in breast cancer is unclear[192]. IL-10 inhibits $CD4^+$ T-cell activation, production of pro-inflammatory cytokines, and dendritic cell differentiation and maturation[192]. It can promote both the differentiation of naïve $CD4^+$ T-cells into Tregs and $CD8^+$ T-cell proliferation and activity[196]. Increased IL-10 levels in the serum of breast cancer patients have been reported, as well as an association between the production of IL-10 by TAMS in the breast cancer TME and therapeutic resistance[196].

Many key characteristics of cancer are regulated by cytokines, and the manipulation of cytokine levels within the TME is one of the ways in which malignant cells modulate their environment to promote an immunosuppressive, pro-tumourigenic TME and enhance their metastatic potential[197]. Several have also been linked to resistance to therapy[192]. The detection of circulating cytokines may provide insight into tumour dynamics[185, 198, 199].

Growth factors also play a pivotal role in key tumourigenic processes by binding to specific cell surface receptors and triggering intracellular signalling pathways[200, 201]. They are involved in promoting cancer cell proliferation (e.g., epidermal growth factor (EGF), platelet-derived growth factor (PDGF), and insulin-like growth factor (IGF)), inhibiting apoptosis (e.g., IGF, hepatocyte growth factor (HGF)), and enhancing invasion and metastasis (EGF, TGF-β)[200, 201]. Several growth factors have been implicated in the growth and development of breast cancer. The VEGF family drives blood vessel formation and homeostasis and can be secreted by cancer cells to promote angiogenesis in and around the TME[202]. Additionally, VEGF may promote the activity of immunosuppressive cells, inhibit cancer cell apoptosis and T-cell recruitment into the TME, and promote an exhausted T-cell phenotype[202, 203]. A correlation between VEGF expression in breast tumours and increased tumour size, histological grade,

and risk of metastasis has been reported[204]. Growth differentiation factor 15 (GDF-15) is a member of the TGF-β family and is released in response to cellular stress signals, such as those observed in inflammation, hypoxia, tissue injury, and malignancy[205]. Circulating GDF-15 levels have been used as a surrogate biomarker for tumour load and progression in breast cancer and have been associated with TNBC treatment resistance and metastasis[206-208].

Secreted growth factors also influence immune responses. For instance, GM-CSF is pro-inflammatory and promotes the survival and activity of myeloid cells (monocytes, macrophages, dendritic cells, and polymorphonuclear neutrophils)[209, 210]. It can drive both tumour progression and suppression[209, 210]. Elevated levels are associated with an aggressive cancer phenotype in some instances, and breast tumour cell-derived GM-CSF has been reported to promote an immunosuppressive TME by stimulating M2 macrophage differentiation and Th2 immune cell responses[209, 211]. Conversely, GM-CSF activates M1 macrophages and dendritic cells and inhibits angiogenesis[209]. Interferon gamma-induced protein 10 (IP-10 or CXCL10) serves as a ligand for the C-X-C motif receptor 3 (CXCR3) molecule and is involved in chemotaxis, cell growth regulation, and the stimulation of apoptosis[212]. It can promote Th1 immune responses, act as a chemoattractant, inhibit angiogenesis, and induce granzyme B production by cytotoxic T-cells[213, 214]. IP-10 can also exert pro-tumourigenic effects, and numerous studies have found that it is overexpressed in cancer and is associated with poor prognosis[215]. Overexpression of IP-10 in breast cancer patients compared to that in healthy controls has been reported and may be correlated with favourable prognostic outcomes in TNBC patients[213, 215].

Chemotherapy affects the levels of cytokines and growth factors present in the TME by causing the death of the tumour cells secreting them[84, 97, 108, 109 101-103]. Numerous reports describing changes in the concentration of cytokines and growth factors such as IL-8, IL-10 and GDF-15 in breast cancer patient plasma in comparison to healthy donors as well as in patient plasma before and after chemotherapy exist[190, 216-219]. These changes may be chemotherapy-induced and form part of an inflammatory response or reflect an upregulation by tumour cells as a means of conferring treatment resistance[196, 205, 220, 221]. The importance of identifying surrogate biomarkers to improve TNBC patient care and disease outcome is highlighted by the pivotal role each cytokine plays in normal physiological functioning, as well as cancer development and progression. They may also provide insight into the mechanisms of therapeutic failure.

5.2 Materials and Methods

5.2.1 Detection of cytokines and growth factors in participant plasma

Seven sandwich ELISA kits were purchased from Elabscience® Bionovation Inc. (Texas, USA) and were used to detect and quantify circulating VEGF, IP-10, GDF-15, IL-10, IL-6, IL-8, and GM-CSF in participant plasma. The wells of each 96-well microplate were pre-coated with capture antibodies specific to the analyte of interest. The sample was incubated in each well to allow the analyte of interest to bind to the capture antibody. Detection antibodies tagged with an enzyme were allowed to bind to the analyte of interest before the enzyme substrate solution was added. A stop solution was added and the optical density was measured using a spectrophotometer. Finally, the concentration of the analyte in each well was calculated using the optical density readings and a standard curve. The following steps were followed for each kit.

5.2.2 Reagent preparation

The standard working solution, biotinylated detection antibody working solution, and the horseradish peroxidase (HRP) conjugate working solutions were prepared shortly before use. To prepare the wash buffer, 30 ml of the wash buffer concentrate was added to 720 ml deionised water. To prepare the standard working solution for each kit, the standard was centrifuged at 10 000 RCF for 1 min using an Allegra® X-12R centrifuge (Beckman Coulter, USA) (brake off) before 1 ml of the reference standard and sample diluent was added, and the tube was allowed to stand for 10 min. After inverting the tube several times, the contents were mixed using a pipette and the tube was allowed to stand for 2 min before being vortexed for 10 seconds (s). The standard working solution concentration for the VEGF ELISA kit (Elabscience® Bionovation Inc., USA) was 2000 picograms per millilitre (pg/ml), the IL-6 and -10 kits (Elabscience® Bionovation Inc., USA) was 100 pg/ml, the GDF-15 kit (Elabscience® Bionovation Inc., USA) was 1500 pg/ml, and the IL-8, GM-CSF, and IP-10 kits (Elabscience® Bionovation Inc., USA) was 500 pg/ml. To create serial dilutions of the standard working solution for each kit, 500 µl of reference standard and sample diluent were added to seven clean, labelled 1.5 ml tubes. A standard working solution (500 µl) (prepared for each kit) was then pipetted into the first tube, the contents were mixed using a pipette, and 500 µl of the resulting solution was pipetted into the second tube. This step was repeated until tube 6. The final tube served as a blank and contained no standard working solution. To prepare the biotinylated detection antibody and HRP working solutions, the biotinylated detection antibody and HRP conjugate concentrates were centrifuged for 1 minute at 800 RCF using an Allegra®

X-12R centrifuge (Beckman Coulter, USA) (brake off) before 73 µl of concentrate was added to 7.23 ml of the correct diluent to create a 1-in-99 dilution.

5.2.3 Sample preparation

Plasma (1.5 ml) that was stored at -80 °C for each healthy donor and patient, both before and after first-phase chemotherapy, was thawed at RT before being diluted in the sample diluent provided in each ELISA kit. A 1-in-4 dilution of participant plasma in the sample diluent was prepared for the GDF-15 ELISA kit (Elabscience® Bionovation Inc., USA), while a 1-in-2 dilution of participant plasma in the sample diluent was prepared for the remaining ELISA kits.

5.2.4 Cytokine and growth factor detection

Serially diluted standard working solution and blank (100 µl) were added in duplicate to the first two columns of the 96-well plate. Diluted participant plasma (100 µl) was added to the remaining wells before the plate was sealed and incubated in the dark for 90 minutes at 37 °C. The liquid in each well was discarded and 100 µl of biotinylated antibody working solution was added to each well before the plate was sealed and incubated in the dark for 60 minutes at 37 °C. The liquid in each well was discarded, and the plate was washed three times (with a 1-minute soak in between) using a BioTek ELx50 (Agilent Technologies, USA) plate washer and the prepared wash buffer. HRP conjugate working solution (100 µl) was added to each well, the plate sealed, and incubated in the dark for 30 minutes at 37 °C. The liquid in each well was discarded, and the plate was washed five times (with a 1-minute soak in between) using a BioTek ELx50 instrument (Agilent Technologies, USA). A volume of 90 µl of substrate reagent was added to each well and the plate was sealed and incubated in the dark at 37 °C for 15 minutes. Stop solution (50 µl) was added to each well and the optical density (OD) value of each well was determined using a BioTek PowerwaveX instrument (Agilent Technologies, USA) set to 450 nm.

5.2.5 Data and statistical analysis

Following the acquisition of the OD values for each sample and standard using 7 ELISA kits and a BioTek PowerwaveX spectrophotometer (Agilent Technologies, USA), the average blank OD value was subtracted from the sample and averaged standard OD values. A four-parameter logistic curve was plotted using Microsoft® Excel® Software version 2410 (Washington, USA) with standard concentration on the x-axis and OD values on the y-axis.

The sample concentration (pg/ml) was determined using the standard curve. The raw data and standard curves are presented in Appendix E, Tables 1 and 2 and Figures 1-7.

A Shapiro-Wilk test was conducted to determine the distribution of the collected data. The null hypothesis that the data had a normal distribution was rejected ($p < 0.05$) for all the variables. As data were collected from three participant groups and did not have a normal distribution, a Kruskal-Wallis equality of populations test and Dunn's pairwise comparison test were used to compare the median concentration of each cytokine between healthy donors and patients, and between patients before and after first-phase chemotherapy. A p-value of less than or equal to 0.05 was deemed statistically significant. To determine whether there was any significant association between the median cytokine concentration (both before and after first-phase chemotherapy) and patient treatment response, a Wilcoxon rank-sum test was used. A p-value of less than or equal to 0.05 was deemed statistically significant. STATA Basic Edition 18.0 statistical software (STATA Corp LLC, USA) was used to conduct all statistical tests and generate graphs.

5.3 Results

5.3.1 The median concentrations of IL-10, IL-6, IL-8, and IP-10 were significantly increased in patients after first-phase chemotherapy compared with pre-treatment levels

The median concentration of IL-10 was significantly increased in patients after receiving first-phase chemotherapy in comparison to treatment-naïve patients (median 0.87 pg/ml vs. 0.30 pg/ml, p=0.0038) (Figure 5.1 A). There was a significant increase in the median concentration of IL-6 in patients after first-phase chemotherapy compared to healthy donors (median 1.21 pg/ml vs. 0.64 pg/ml, p=0.0151) and treatment-naïve patients (1.21 pg/ml vs. 0.64 pg/ml, p=0.0039) (Figure 5.1 B).

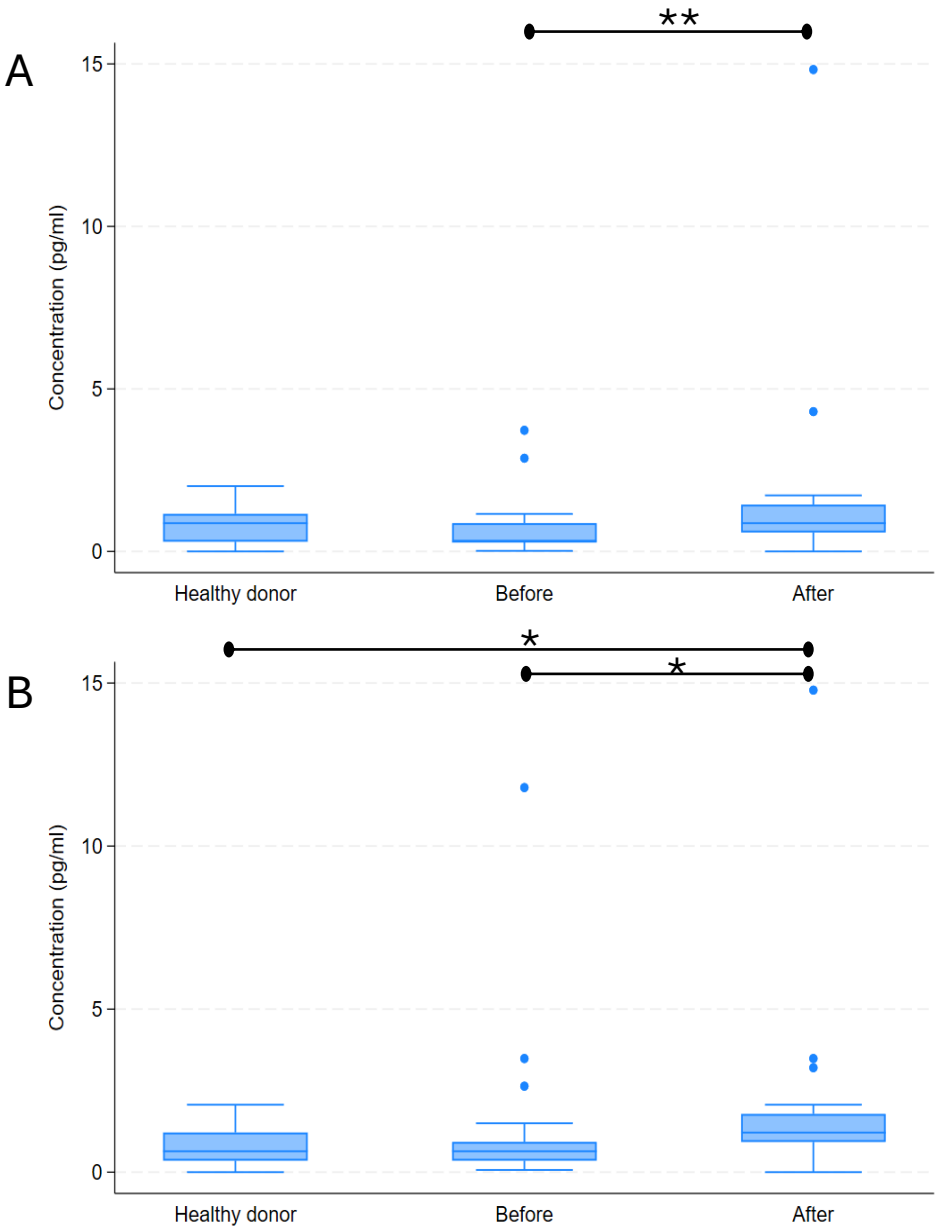

Figure 5.1: The concentration of IL-10 and IL-6 were significantly increased in the plasma of patients after first-phase chemotherapy compared to pre-treatment levels. The median concentration of IL-10 (A) was significantly increased in patients after receiving first-phase chemotherapy compared to treatment-naïve patients, and there was a significant increase in the median concentration of IL-6 (B) in patients after first-phase chemotherapy compared to that in healthy donors and treatment-naïve patients. ** p≤0.01, * p≤0.05. IL-10: interleukin-10. IL-6: interleukin-6.

The median concentration of IP-10 was markedly increased in patients after receiving first-phase chemotherapy compared to healthy donors (311.47 pg/ml vs. 154.91 pg/ml, p=0.0047) and pre-first-phase chemotherapy levels (311.47 pg/ml vs. 204.51 pg/ml, p=0.0231) (Figure

5.2 A). A higher median concentration of IL-8 was observed in patients after receiving first-phase chemotherapy compared to healthy donors (81.56 pg/ml vs. 68.47 pg/ml, p≤0.0001) and treatment-naïve patients (81.56 pg/ml vs. 70.12 pg/ml, p=0.0001) (Figure 5.2 B). The median concentration values and p-values are presented in Appendix E, Table 3.

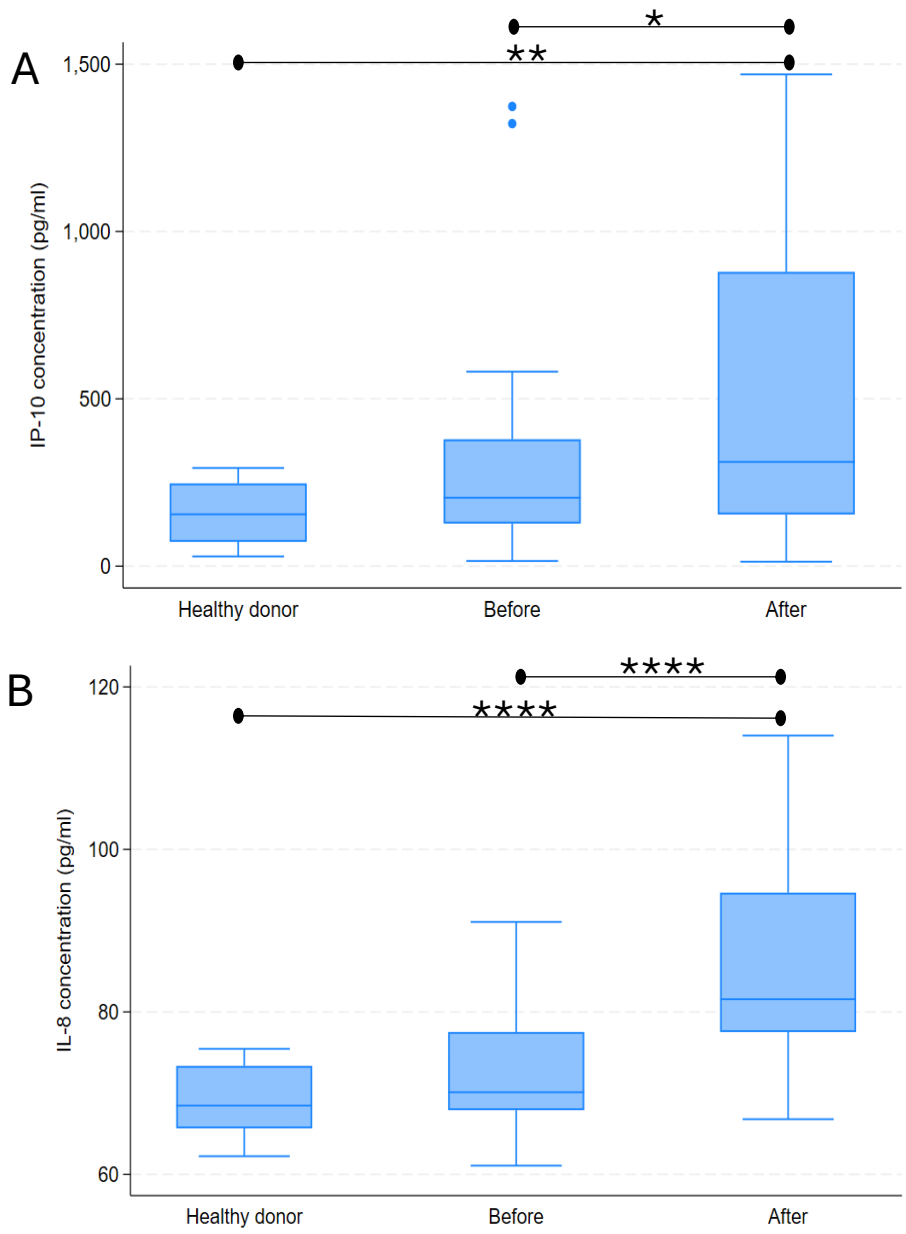

Figure 5.2: The concentrations of IP-10 and IL-8 in patients and healthy donors. An increase in the median concentrations of IP-10 (A) and IL-8 (B) was observed in patient plasma after receiving first-phase chemotherapy compared to healthy donor and treatment-naïve patient plasma. ****p≤0.0001, **p≤0.01, *p≤0.05. IP-10: interferon gamma-induced protein. IL-8: interleukin-8.

5.3.2 The median GDF-15 concentration was significantly higher in patients after first-phase chemotherapy than in healthy donors and treatment-naïve patients

No statistically significant change in the median concentration of VEGF or GM-CSF was observed between healthy donors and patients, both before and after first-phase chemotherapy (Figure 5.3 A and B).

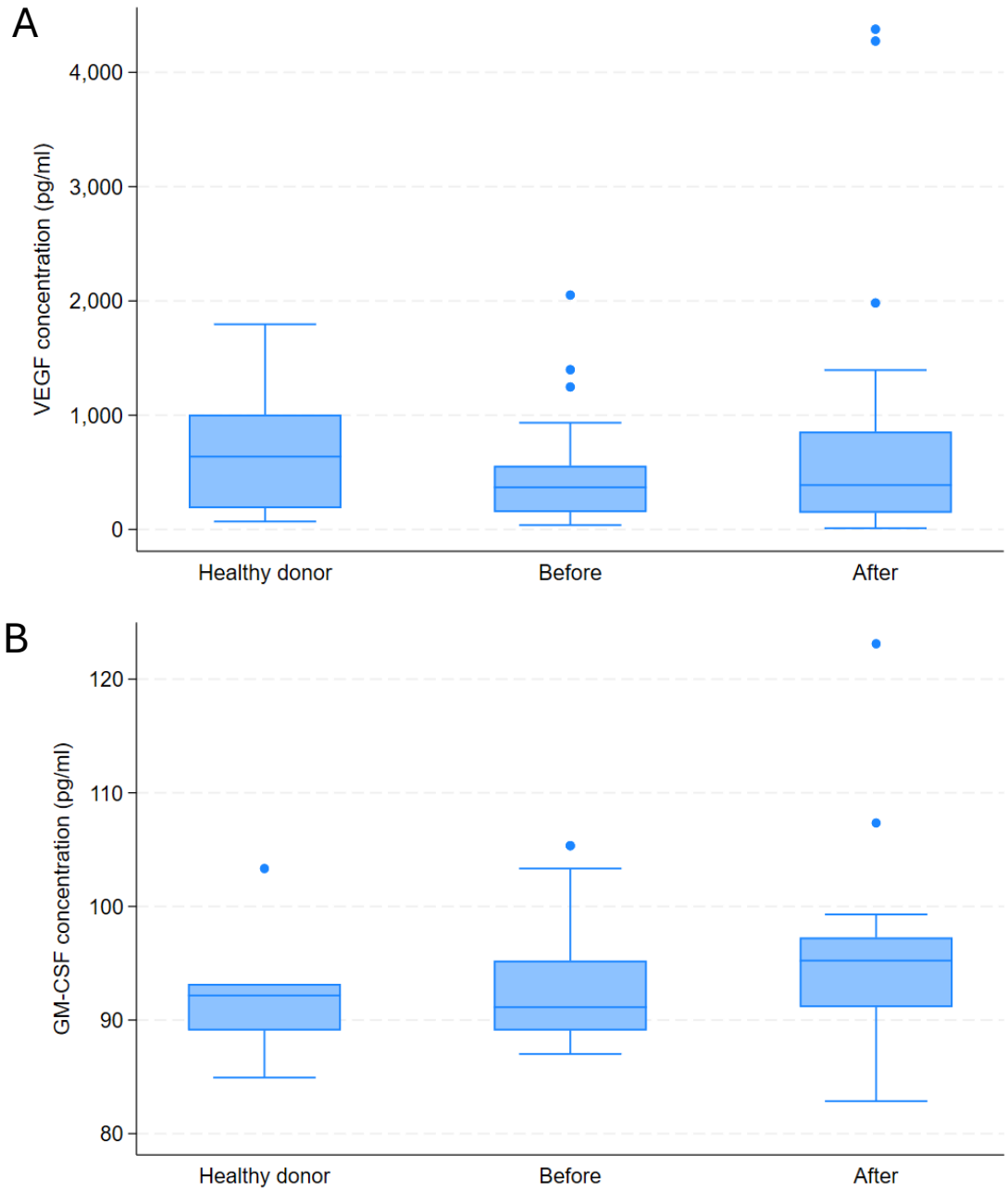

Figure 5.3: The concentration of VEGF and GM-CSF in patients and healthy donors. No statistically significant change in the median concentrations of VEGF (A) or GM-CSF (B) was

observed between healthy donors and patients. VEGF: vascular endothelial growth factor. GM-CSF: granulocyte-macrophage colony stimulating factor.

There was a significant increase in the median concentration of GDF-15 in patients after first-phase chemotherapy compared to healthy donors (median 2 611.36 pg/ml vs. 741.30 pg/ml, p≤0.0001) and pre-treatment levels (median 2 611.36 pg/ml vs. 1 190.9 pg/ml, p≤0.0001) (Figure 5.4). A non-significant increase in the median concentration of GDF-15 was observed in treatment-naïve patients in comparison to healthy donors (median 1 190.9 pg/ml vs. 741.30 pg/ml, p=0.0822). The median concentration values and p-values are presented in Appendix E, Table 3.

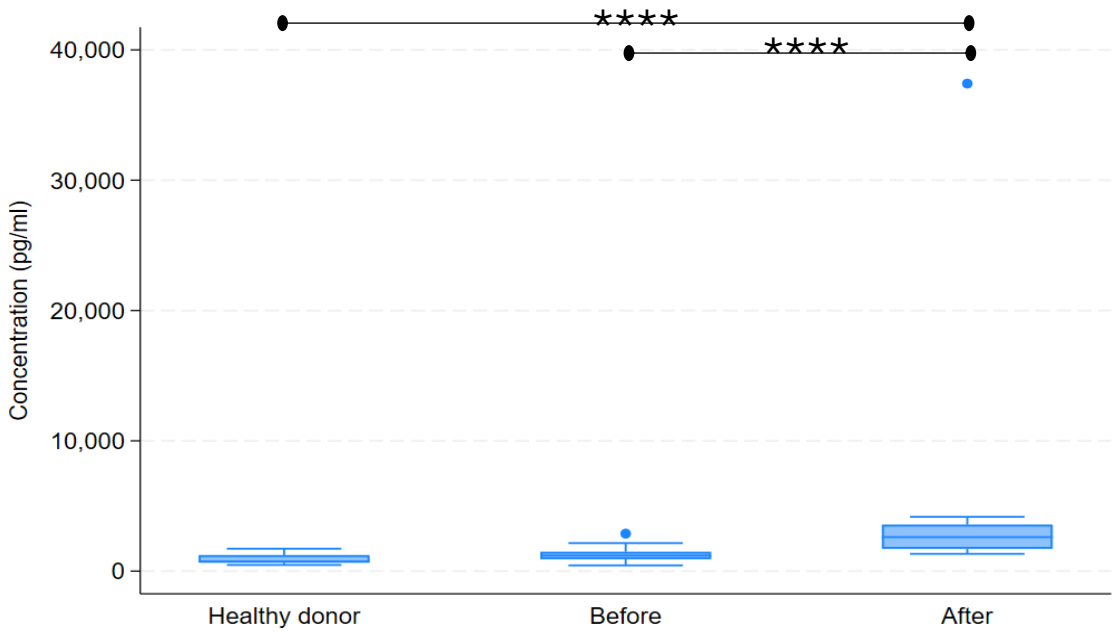

Figure 5.4: The concentration of GDF-15 in patients and healthy donors. There was a significant increase in the median concentration of GDF-15 in patients after first-phase chemotherapy compared to the healthy donor and pre-treatment levels. ****p≤0.0001.GDF-15: growth and differentiation factor-15.

5.3.3 No significant difference in median cytokine concentration was observed after-first phase chemotherapy between those who achieved a pathological complete response and those who did not after the completion of all chemotherapy

No significant difference in the median concentration of circulating VEGF, IP-10, GDF-15, GM-CSF, IL-6, IL-8, or IL-10, both before and after first-phase chemotherapy, was observed between those who achieved a PCR and those who presented with PIC after the completion of all chemotherapy (Table 5.1).

Table 5.1: Median circulating VEGF, IP-10, IL-6, IL-8, IL-10, GDF-15, and GM-CSF concentrations before and after first-phase chemotherapy in those who achieved PCR and those with PIC after the completion of all chemotherapy

	Patients with a PCR (n=10); median pg/ml (range)	**Patients with PIC (n=8); median pg/ml (range)**	**P-value**
Before first-phase chemotherapy			
VEGF	327.23 (58.77-1247.12)	554.69 (39.01-2051.24)	0.1011
IP-10	213.58 (15.34-1373.66)	304.87 (51.70-1322.33)	0.6334
IL-6	0.93 (0.07-2.64)	0.35 (0.07-11.79)	0.2187
IL-8	69.57 (66.80-80.57)	74.93 (67.92-87.37)	0.1243
IL-10	0.44 (0.30-3.73)	0.16 (0.02-2.87)	0.2318
GDF-15	1135.54 (561.61-2875.50)	1434.28 (699.18-2149.23)	0.2743
GM-CSF	93.19 (87.01-105.34)	91.13 (89.08-105.34)	1.0000
After first-phase chemotherapy			
VEGF	310.3 (115.29-4273.69)	689.65 (10.79-4377.48)	0.2743
IP-10	259.51 (106.57-1469.47)	680.08 (13.33-1468.37)	0.2276
IL-6	1.21 (0.64-3.49)	1.5 (0.35-14.78)	0.8162
IL-8	81.06 (66.80-109.49)	91.01 (74.41-114.01)	0.0868
IL-10	1.01 (0.02-1.44)	0.73 (0.30-4.30)	0.4384
GDF-15	2332.26 (1431.58-37412.89)	2984.12 (1379.89-4157.18)	0.7618
GM-CSF	96.25 (84.94-123.12)	92.16 (87.01-99.3)	0.1803

PCR: pathological complete response. PIC: persistent invasive carcinoma. VEGF: vascular endothelial growth factor. IP-10: interferon gamma-induced protein. IL-6: interleukin-6. IL-8: interleukin-8. IL-10: interleukin-10. GDF-15: growth and differentiation factor-15. GM-CSF: granulocyte-macrophage colony stimulating factor.

5.4 Discussion

Many of the hallmarks of cancer are controlled through cellular signalling pathways, and tumour manipulation of cytokine and growth factor levels promotes an immunosuppressive TME and enhances tumour cell metastasis[197]. The detection and evaluation of pro- and anti-tumourigenic cytokines within patient blood may provide insight into the complex cancer-immune cell dynamics in malignant disease and be used to make better treatment decisions and improve patient outcomes[185, 198, 199]. Seven ELISAs were used to assess the levels of circulating VEGF, GDF-15, GM-CSF, IL-6, IL-8, IL-10, and IP-10 in the plasma of 10 healthy donors and 23 newly diagnosed treatment-naïve TNBC patients both before and after first-phase chemotherapy. The concentration (pg/ml) of each cytokine was determined using standard curves and then compared between patients and healthy donors, as well as between patients before and after first-phase chemotherapy.

5.4.1 An increase in the median concentration of IL-10 in patients may indicate an increase in anti-tumour immune cell responses after first-phase chemotherapy

The increase in IL-10 levels in patients after first-phase chemotherapy in comparison to pre-treatment levels correlates with the findings of other studies where IL-10 levels were increased in early breast cancer patients after receiving adjuvant chemotherapy compared to pre-treatment levels[218]. While other studies report an increase in the median concentration of IL-10 in the blood serum or plasma of breast cancer patients in comparison to healthy donors, this was not observed in this study[190, 216-218]. The increase in the median concentration of IL-10 in this study's patient cohort after first-phase chemotherapy may be due to an upregulation in IL-10 production by cancer cells as a means of conferring chemoresistance or in response to chemotherapy-induced inflammation[196, 222].

An increase in the median concentration of IL-6 in breast cancer patients after chemotherapy in comparison to healthy donors and pre-treatment levels was observed in this investigation and has also been reported in breast cancer patients with advanced and metastatic disease[189, 190, 218, 223]. There is a paucity of published information addressing the potential mechanisms behind these changes however, a possible explanation is a chemotherapy-induced inflammatory response or an increase in IL-6 production by cancer cells as a means of avoiding apoptosis and developing treatment resistance[188, 189, 191, 224]. The significance of this study's findings are however, unclear as the median IL-10 and IL-6 concentration value for

healthy donors (median 0.87 pg/ml and 0.64 pg/ml) and patients both before (median 0.30 pg/ml and 0.64 pg/ml) and after first-phase chemotherapy (median 0.87 pg/ml and 1.21 pg/ml) were below the lower limit of detection range (1.56-100 pg/ml) of the ELISA kits used[225, 226].

No significant association was observed between pre- and post-first-phase chemotherapy IL-10 and IL-6 median concentrations and patient treatment outcomes in this study cohort. Increased levels of IL-10 have been associated with increased tumour growth, drug resistance, disease persistence, and poor prognosis in breast cancer, and a correlation between IL-10 levels and increased tumour stage has been reported[227, 228]. Other studies have reported an association between IL-10, overall survival rate, and anti-tumoural immunity in breast cancer patients[190, 216, 217, 228]. Increased IL-6 signalling is associated with metastasis, treatment resistance, disease recurrence, immune suppression, and poorer prognosis in breast cancer patients[189, 191, 229, 230]. In addition, an association between IL-6 and tumour stage has also been found[190]. A larger study may yield more significant results and provide more insight into the relationship between IL-10, IL-6, and treatment response in patients with TNBC.

The observed increase in median IL-8 concentration in patients after first-phase chemotherapy correlates with the findings of other studies and may be chemotherapy-induced, as various chemotherapeutic agents, including doxorubicin, have been shown to increase IL-8 and IL-8 receptor concentrations in patient plasma[190, 218-220]. No significant association between the median concentration of IL-8 before and after first-phase chemotherapy and patient treatment outcomes was observed in this study. An increase in the concentration of IL-8 has been reported in patients who achieved a PCR, and a decrease in IL-8 concentration has been reported in patients with recurrent disease[227]. Some studies have reported an association between an increase in the serum concentration of IL-8 and breast cancer treatment resistance, and poorer overall and progression-free survival; while other studies have reported an association between decreased IL-8 levels and an increase in the overall survival of metastatic breast cancer patients[193, 220, 231]. An investigation of the relationship between IL-8 and treatment response in a larger group of patients with TNBC may yield more significant findings.

The median concentration of IP-10 was markedly increased in patients after receiving first-phase chemotherapy compared to healthy donors and pre-first-phase chemotherapy levels;

and this has also been reported in the literature[215, 232-236]. A positive association between the expression of IP-10 by tumour cells and TIL density, especially that of NK cells and $CD3^+$ T-cells, has been reported[233, 237]. The observations made in this study may provide evidence of enhanced immune-mediated cancer cell apoptosis, increased anti-tumour Th1 T-cell responses, and increased NK and T-cell cytotoxicity, homing, and infiltration into the TME after first-phase chemotherapy[214, 238].

No significant association was observed between the median concentration of IP-10 in patients before and after first-phase chemotherapy and treatment outcomes in this study. Serum IP-10 concentration has been positively correlated with tumour size and aggressiveness, disease resistance, and poor prognosis in breast cancer patients, while other studies have reported a correlation between increased plasma IP-10 concentration and the development of the TNBC subtype[213, 232, 239, 240 241, 242]. In contrast, an association between IP-10 overexpression in the tumour and recurrence-free survival of patients with TNBC has also been reported[213]. These conflicting reports on IP-10's role in cancer may be due to differences in receptor subtype and cell type-dependent functions[214]. An investigation into whether an association exists between treatment outcome and IP-10 plasma concentration may yield more significant findings if conducted in a larger number of TNBC patients than what was used in this study.

5.4.2 An increase in the median concentration of GDF-15 in patients after first-phase chemotherapy may indicate a chemotherapy-induced cellular stress response

The lack of a significant change in the median concentration of VEGF in patients compared to healthy donors and in patients before and after first-phase chemotherapy correlates with the findings of some studies[243, 244]. In contrast, an increase in the concentration of VEGF in the plasma of breast cancer patients in comparison to healthy donors and those with benign breast tumours has been reported in the literature[203, 243, 245-249]. An increase in the concentration of VEGF in breast cancer patient plasma during chemotherapy compared to pre-treatment levels has also been reported[203, 245, 246, 250].The findings of this investigation may indicate that any additional VEGF secreted in the tumour is being used up before it is able to enter the circulation, and that chemotherapy does not induce any changes in VEGF signalling and tumour vasculature in TNBC patients[251]. The lack of a change in the median concentration of GM-CSF in patients compared to healthy donors, as well as in patients before and after first-phase chemotherapy, correlates with some reports in the literature. Other studies have reported a significant increase in circulating GM-CSF concentration in breast cancer patients

both before and during chemotherapy in comparison to healthy donors and treatment-naïve patients, while other studies have reported a significant decrease in the concentration of GM-CSF in breast cancer patient sera before treatment in comparison to that of healthy donors[252-254]. The findings of this study may indicate that GM-CSF is not a means by which TNBC cancer cells seek to manipulate the immune system and evade destruction; and that chemotherapy does not induce an increase in GM-CSF-mediated myeloid cell activity and homing to the tumour site[210, 255, 256].

No association was observed between patient treatment outcome and the median concentration of VEGF and GM-CSF in patient plasma before and after first-phase chemotherapy. Within the literature, an association between increased plasma VEGF levels, poorer patient prognosis, and increased tumour size and stage has been reported[248, 249, 257]. The concentration of VEGF may also serve as a predictor of breast cancer patient overall survival and the risk of disease recurrence[248, 257]. The upregulation of GM-CSF production has been associated with improved patient prognosis in colorectal cancer; however, increased GM-CSF production has been associated with increased tumour aggressiveness, invasiveness, and poor patient prognosis in bladder cancer, glioblastomas, and cancers of the head and neck[209, 258]. A larger study may yield more significant insights into the relationship between VEGF, GM-CSF, and TNBC patient response to treatment.

There was a significant increase in the median plasma concentration of GDF-15 in patients after first-phase chemotherapy compared to that in healthy donors and pre-treatment levels, which correlates with the findings of numerous other studies[35, 259-265]. An increase in the median concentration of GDF-15 was observed in treatment-naïve patients compared with that in healthy donors. Although this result did not reach statistical significance in this study, it correlates with the findings of other studies that report a significant increase in the plasma concentration of GDF-15 in metastatic breast cancer patients in comparison to healthy donors[262-265]. The increase in the median concentration of GDF-15 in patients after first-phase chemotherapy compared to healthy donors and treatment-naïve patients may be due to malignant and non-malignant cell damage caused by exposure to chemotherapeutic agents since GDF-15 expression and secretion is associated with the cellular stress response, hypoxia, and inflammation[205, 221, 266]. Similarly, the increase in median GDF-15 concentration in treatment-naïve TNBC patients compared to healthy donors, although not statistically significant, may be due to the inflammatory and hypoxic nature of the TME[205, 221].

No significant association between the median concentration of GDF-15 before and after first-phase chemotherapy and patient treatment outcomes was observed in this study. The expression and secretion of GDF-15 has been shown to promote EMT in breast cancer, decrease lymphocyte infiltration into the TME, and impede the activity of M1 macrophages[205, 262, 266]. Other studies have however, reported that GDF-15 inhibits tumour cell invasion, increases anti-tumour immune cell activity, and initiates tumour-cell apoptosis[205, 262, 266]. Increased GDF-15 expression by breast cancer cells has been associated with poorer patient prognosis and recurrence-free survival as well as treatment resistance and metastasis[259, 267-272]. An investigation into whether an association exists between treatment outcome and GDF-15, if conducted on a larger number of TNBC patients than that used in this study, may yield more insight into the relationship between GDF-15 and TNBC patient treatment response.

5.4.3 Conclusion

A significant increase in the median concentration of IL-6, IP-10, and IL-8 was observed in patients after first-phase chemotherapy compared to that in healthy donors and pre-treatment levels. In addition, a significant increase in the median concentration of IL-10 was observed in patients who received first-phase chemotherapy compared to that in treatment-naïve patients. The increase in the median concentration of IL-10 and IL-6 in patient plasma after first-phase chemotherapy may be due to an upregulation in IL-10 and IL-6 production by cancer cells as a means of conferring chemoresistance and avoiding apoptosis, or it may be in response to chemotherapy-induced inflammation[188, 189, 191, 196, 222, 224]. The median IL-10 and IL-6 concentration in patients and healthy controls were however, below the lower limit of their respective ELISA kit's detection range. The observed increase in the median concentration of IP-10 and IL-8 in patients after first-phase treatment may be chemotherapy-induced and, in the case of IP-10, provide evidence of an increase in tumour cell apoptosis, anti-tumour immune cell activity, and anti-tumourigenic immune cell infiltration into the TME after first-phase chemotherapy[214, 220, 238]. Approximately 56% of the patients in this study achieved a pathological complete response, while approximately 44% demonstrated persistent invasive carcinoma after the completion of chemotherapy. No significant association was found between patient response to treatment and the median concentrations of circulating VEGF, IP-10, GDF-15, GM-CSF, IL-6, IL-8, and IL-10 before and after first-phase chemotherapy.

Cytokines serve as chemical messengers to create a signalling network or cascade between immune and non-immune cells, and many hallmarks of cancer are regulated by cytokines[185, 186]. Manipulation of cytokine levels within the TME is one way in which malignant cells

modulate their environment to promote an immunosuppressive, pro-tumourigenic TME[197]. As cytokines found within the circulation are those that have not been used at local sites, they have the potential to act as surrogate biomarkers in cancer[185, 198, 199].

Chapter 6: General discussion and conclusion

Breast cancer is the second most commonly diagnosed cancer globally and has the fourth highest cancer mortality rate, making it a healthcare priority[4]. TNBC accounts for 10-20% of invasive breast cancer cases and is highly heterogeneous in its clinical presentation[61, 63, 64]. Patients with this breast cancer subtype have a 5-year survival rate of 60% owing to its aggressive and highly metastatic nature which limits the range of treatment strategies that can be applied[61, 63, 64]. The immune cell components within the TME in TNBC differ from those in other breast cancer subtypes, and T-cells, B-cells, NK cells, and monocytes may play either pro- or anti-tumourigenic roles[30, 31, 65]. Cytokines form a signalling network or cascade between immune and non-immune cells and regulate many cancer hallmarks[185, 186]. The modulation of cytokines within the TME represents one mechanism by which cancer can promote an immunosuppressive, pro-tumourigenic TME, and cytokines present in the circulation possess the potential to serve as surrogate biomarkers in cancer[185, 197-199].

The aim of this study was to compare immune cell subsets and cytokine levels in the peripheral blood of healthy donors, newly diagnosed TNBC patients, and TNBC patients after first-phase chemotherapy. To accomplish this, immunophenotyping was used to identify circulating T-cell, B-cell, NK cell, monocyte, and Treg subsets present in participant samples (Chapters 2-4), and cytokine and growth factor levels (VEGF, IP-10, GM-CSF, IL-6, IL-8, IL-10, and GDF-15) were measured by ELISA in participant plasma samples (Chapter 5). The ELISA and flow cytometry results were then compared between patients and healthy donors, as well as between patients before and after first-phase chemotherapy (Chapters 3-5).

6.1 Chemotherapy affects the percentage of immune cell subsets present in peripheral blood

Malignancy and exposure to chemotherapeutic agents elicit distinct effects on immune cell subset proportions both within the tumour microenvironment and circulation[108]. In the context of this study, the median lymphocyte count decreased after first-phase chemotherapy compared to pre-treatment levels. This was largely due to a marked reduction in the percentage of $CD19^+$ B-cells, as no significant change in the T-cell percentage was observed after first-phase chemotherapy. Despite conflicting reports on the effect of chemotherapy on $CD4^+$ and $CD8^+$ T-cell viability, a chemotherapy-induced reduction in $CD19^+$ B-cell quantity

after chemotherapy has been consistently reported[84, 97, 107-110, 115]. Inconsistencies in the literature regarding the effects of chemotherapy on T-cell subsets may be attributed to variations in participant demographics, breast cancer subtype, chemotherapy regimen, or the utilisation of surgery and radiation[126, 273].

A similar percentage of T-cells was observed in treatment-naïve patients and healthy donors. This may indicate a poor level of T-cell clonal expansion and tumour infiltration in treatment-naïve TNBC patients[113]. A comparable observation was reported in a study which demonstrated that first-phase chemotherapy did not influence T-cell infiltration into the tumour, with T-cells exhibiting resistance to the cytotoxic effects of TAC chemotherapy[84, 107]. A significant increase in the expression of CD8 was observed in patient T-lymphocytes after first-phase chemotherapy compared to healthy donors, but no corresponding increase in the percentage of $CD8^+$ T-cells was detected. The CD8 molecule stabilises the T-cell-receptor-MHC-I complex during T-cell activation and while CD8 overexpression has been reported in SARS-CoV-2-infected individuals, the significance of increased CD8 expression in cancer patients undergoing chemotherapy is not known[111, 112]. A decrease in the percentage of $CD19^+$ B-cells was observed in patients after first-phase chemotherapy, but an increase in the expression of CD206 on these cells in patients both before and after first-phase chemotherapy in comparison to healthy donors was also observed. There is a paucity of information on CD206 expression by $CD19^+$ B-cells in cancer however, based on findings in autoimmune conditions, it may indicate a shift in function towards a more tolerogenic B-cell phenotype possibly influencing antibody production, immune regulation, and antigen presentation[115-117, 274].

The percentage of $CD16^+CD56^+$ NK cells was similar in healthy donors and patients both pre-treatment and after first-phase chemotherapy, and this has been previously reported in numerous other studies[108, 119, 120]. An increase in the percentage of $CD56^{high}$ NK cells in patients after receiving first-phase chemotherapy compared to pre-treatment levels was observed in this study and was also observed by Mamessier *et al.*[79] in advanced-stage breast cancer patients after chemotherapy[79]. This increase may be due to the increase in circulating tumour antigens caused by chemotherapy-induced cell death which drives the expansion of cytotoxic subsets[51, 275]. This is supported by observations of increased CD16 expression in $CD56^{high}$ NK cells in patients after the first phase of chemotherapy. $CD16^{dim}CD56^{high}$ NK cells may be intermediaries between $CD56^{high}$ and $CD56^{dim}$ NK subsets[79, 122]. An increase in the expression of HLA-DR in both $CD16^+CD56^+$ and $CD56^{high}$ NK cells was observed in patients after first-

phase chemotherapy compared with treatment-naïve patients. This may provide evidence of an increase in NK cell activation after first-phase chemotherapy due to a chemotherapy-induced increase in tumour cell immunogenicity[51, 275].

6.2 First-phase chemotherapy has little impact on monocyte and Treg populations

Monocytes play a pleiotropic role in cancer development depending on their differentiation towards either an anti-tumourigenic M1 or pro-tumourigenic M2 phenotype[80-82]. An increase in the total $CD14^+$ monocyte count and percentage was observed in patients after first-phase chemotherapy relative to healthy donors and treatment-naïve patients; however, the relative percentages of classical, intermediate, and non-classical subtypes were not substantially affected. In other studies however, the percentage of classical monocytes increased after first-phase chemotherapy[103].This may be because the samples in this study were taken after the first of phase chemotherapy, whereas other studies monitored these cells after completion of therapy. The findings of this study suggest that, in response to an increase in cancer cell immunogenicity, a uniform increase in monocyte subsets occurs after first-phase chemotherapy[276].

The expression of CD56 in classical monocytes was increased in patients after first-phase chemotherapy compared to pre-treatment levels. In addition, the expression of CD206 in classical monocytes was elevated in patients before and after first-phase chemotherapy compared to that in healthy donors. The expression of CD56 and CD206 on intermediate monocytes was higher in patients than in healthy donors and, in the case of CD56, in patients after first-phase chemotherapy than in treatment-naïve patients. While there is a paucity of information on CD56 expression in monocyte subsets in cancer, $CD56^+$ monocytes are suggested to be precursors to $CD56^+$ dendritic cells which may demonstrate effector cell activity against tumour cells and enhanced antigen presentation and stimulatory abilities[78]. A favouring of intermediate and classical monocyte differentiation into M2 macrophages may be reflected by the observed increase in the MFI of CD206 in patients both before and after first-phase chemotherapy coupled with the observed increase in overall monocyte percentage[78, 115, 127]. Alternatively, an increase in the expression of CD206 on circulating monocytes may reflect an increase in macrophage migration to the tumour site[78, 115, 127].

The specialised immunosuppressive capabilities of $CD4^+$ Tregs and their dual function in malignancy have rendered them a subject of significant interest to cancer researchers and clinicians[68-70, 139]. The median percentage of $CD25^+FoxP3^+$ Tregs was similar between patients and healthy donors, and between patients before and after first-phase chemotherapy, which correlates with two reports in the literature[162, 163]. In contrast, other studies have reported an increase in the proportion of circulating $CD25^+FoxP3^+$ Tregs in metastatic breast, colorectal, and ovarian cancer patients compared to that in healthy donors [148-154, 163-166]. A chemotherapy-induced increase in $CD25^+FoxP3^+$ Treg apoptosis has been reported in patients with breast and non-small cell lung cancer[154, 164].The median percentage of $CD25^+FoxP3^+$ Tregs in the peripheral blood of TNBC patients before and after first-phase chemotherapy remained consistent, suggesting that neither the presence of a TNBC primary tumour nor first-phase chemotherapy resulted in a significant alteration in the percentage of circulating $CD25^+FoxP3^+$ Tregs[162, 163]. It is plausible that the results may have differed if the Treg percentage had been measured upon completion of the treatment regimen.

A decrease in the expression of CD45RA and a concomitant increase in the expression of CD39 and CD127 on patient $CD25^+FoxP3^+$ Tregs after first-phase chemotherapy may be indicative of a shift towards an activated, treatment-resistant, and highly immunosuppressive Treg phenotype in TNBC patients after first-phase chemotherapy[140, 151, 155, 156, 177]. Alternatively, the observed increase in the expression of CD39 on patient $CD25^+FoxP3^+$ Tregs after first-phase chemotherapy may be due to an increase in CD39-mediated ATP breakdown[155, 157-159]. Similarly, the equivalent expression of Helios in patient $CD25^+FoxP3^+$ Tregs after first-phase chemotherapy compared to treatment-naïve patients and healthy donors suggests that first-phase chemotherapy does not affect $CD25^+FoxP3^+$ Treg stability[181-183].

6.3 An increase in inflammation-associated cytokines and growth factors was observed in TNBC patients after first-phase chemotherapy

Intercellular signalling pathways, which rely on signalling molecules such as cytokines and growth factors, are often dysregulated in cancer and chemotherapy may cause changes in the secretory profile of both tumour and immune cells[84, 126, 184]. A significant increase in the median concentrations of IL-6 and IL-10 was observed in patients who received first-phase chemotherapy compared with treatment-naïve patients. While this correlates with other reports in the literature which suggest that this may prevent cancer cell apoptosis by creating an immunosuppressive TME[187, 189, 190, 196, 218, 222, 223, 277], as the actual concentrations were very

low, this is difficult to conclude from this study. This aligns with the percentages of monocytes and Tregs before and after first-phase chemotherapy, which are some of the cell types that secrete these cytokines[187].

An elevation in the plasma concentrations of IL-8 and IP-10 was observed in patients following initial-phase chemotherapy compared to healthy donors and treatment-naïve patients, and this observation is consistent with the findings of other studies[190, 215, 218, 219, 232-236]. The increase in IL-8 may be due to the observed increase in total $CD14^+$ monocytes in participant whole blood after first-phase chemotherapy or due to an increased secretion by T-cells and NK cells[187, 190, 214, 215, 218-220, 232-236, 238, 278]. Alternatively, IL-8 may be released by apoptosing tumour cells and could assist in conferring protection to neighbouring tumour cells[187, 190, 215, 218, 219, 232-236, 278]. In contrast, the release of IP-10 from apoptosing tumour cells may attract T-cells and NK cells to the tumour site and promote their cytotoxic activity[214, 220, 238].

Growth factors also play a role in breast cancer tumour progression in that they promote cancer cell proliferation, invasion, and metastasis, as well as prevent cancer cell apoptosis[200, 201]. A significant increase in the plasma concentration of GDF-15 in patients after exposure to chemotherapy compared to that in healthy donors and pre-treatment levels has been reported in numerous studies and was also observed in this investigation[35, 259-265]. This observation may be a response to chemotherapy-induced cell damage and inflammation, as GDF-15 is released in response to cellular stress signals[205, 221, 266]. Alternatively, this may be linked to the observed increase in $CD14^+$ monocytes in patients after first-phase chemotherapy, as these cells can produce GDF-15[206].

While there was no significant change in the concentrations of VEGF and GM-CSF in this study, it has been reported previously[203, 244-246, 250, 252-254]. The modulation of VEGF by tumour cells to promote tumour growth and progression, as well as the increase in VEGF levels within the TME following chemotherapy, has been observed in numerous cancer types, including breast cancer[203, 250, 279]. The absence of a significant alteration in the concentration of VEGF in treatment-naïve patients compared to healthy donors may suggest that the presence of a TNBC tumour does not induce changes in VEGF signalling, or alternatively, that any excess VEGF produced is being utilised within the TME prior to entering the circulation[245, 246, 279]. The similarity between the median concentrations of VEGF in patients before and after first-phase chemotherapy may indicate that TAC chemotherapy does not induce any changes in VEGF

signalling and tumour vasculature in TNBC patients[210, 251, 255, 256]. No change in the concentration of GM-CSF was observed between the participants of this study, which may indicate that increased production of GM-CSF by tumour cells, lymphocytes, and macrophages is not a mechanism by which TNBC cells promote tumour progression and survival[210, 251, 255, 256]. In addition, this may indicate that chemotherapy does not induce an increase in GM-CSF-mediated myeloid cell activity and homing to the tumour site[210, 251, 255, 256].

6.4 First-phase chemotherapy-induced changes in circulating immune cells and cytokines may affect patient treatment response and prognosis

A pathological complete response was observed in approximately 56% of the patients after the completion of all chemotherapy. An association between poorer patient prognosis, a greater decrease in the percentage of B-cells and $CD4^+$ T-cells, and an increase in the percentage of $CD8^+$ T-cells in breast cancer patients after chemotherapy has been previously reported[111, 112, 118]. An association between high levels of circulating $CD56^+$ NK cells, pathological complete response, and improved overall and relapse-free survival has been observed in breast cancer patients treated with neoadjuvant chemotherapy[123]. Increased absolute monocyte counts are associated with poor prognosis in stage II and III TNBC, with counts >0.48 $x10^9$/l linked to shorter overall survival[129]. This may be due to an increase in monocyte differentiation into TAMs which promotes tumour survival[280]. Previous studies have reported either a positive or no association between the percentage of classical and non-classical monocytes and pathological complete response[103, 128]. In the context of this study, it is unclear how the percentage of $CD4^+$ and $CD8^+$ T-cells, $CD19^+$ B-cells, $CD56^+$ NK cells, $CD56^{high}$ NK cells, and $CD14^+$ monocytes, as well as marker MFI values in patients after first-phase chemotherapy compared to healthy donors and treatment-naïve patients, may be associated with treatment response.

The role of intratumoural and circulating Tregs in breast cancer patient treatment response and prognosis is controversial[160-162]. A positive association between circulating $CD25^+FoxP3^+$ Tregs, breast cancer stage, and clinical outcomes has been reported[151, 167]. In contrast, no association between the proportion of circulating $CD25^+FoxP3^+$ Tregs and treatment response was found in a study of TNBC[167]. An association between increased $CD45RA^-FoxP3^{high}$ Treg frequency and poorer patient prognosis has been reported in colorectal and head and neck squamous cell carcinoma patients, and an increase in CD39 expression on intratumoural $CD25^{high}FoxP3^+$ Tregs is associated with poorer outcomes in colon and gastric cancer

patients[169-172]. Similarly, an increase in circulating $CD39^{+}CD25^{+}CD127^{-}$ Tregs in sepsis patients was associated with poorer survival[173], and may also be true in cancer cases. In non-small cell lung cancer patients, no association between $FoxP3^{+}Helios^{+}$ Tregs and cancer progression has been observed; however, there is a paucity of information on whether an association exists between the expression of Helios and $CD25^{+}FoxP3^{+}$ Tregs and treatment response in breast cancer patients[178]. In the context of the data presented here, it is unclear how the percentage of $CD25^{+}FoxP3^{+}$ Tregs and the expression of CD45RA, CD39, CD127, and Helios on these cells are linked to treatment response. An investigation using a larger sample size may yield more significant insights.

The crucial role of cytokines and growth factors in tumour development, progression, and metastasis means that they may serve as both diagnostic and prognostic biomarkers in cancer[281]. No statistically significant association between treatment response and the concentrations of circulating VEGF, IP-10, GDF-15, GM-CSF, IL-6, IL-8, and IL-10 was found in this study's patient cohort, which contrasts with other reports in the literature. Elevated IL-10, IL-6, IL-8, IP-10, and VEGF levels and signalling have been associated with an increase in tumour growth, drug resistance, disease persistence, metastasis, and poorer overall patient survival and prognosis in breast cancer[189, 191, 193, 220, 227-231, 248, 249, 257]. The literature has reported conflicting associations between elevated GM-CSF and GDF-15 concentrations and patient outcomes in various malignancies, including breast cancer[205-209, 258, 262, 266]. These studies have demonstrated both favourable and unfavourable correlations with prognosis and survival rates.

The findings of this study elucidate the necessity for immunotherapeutic interventions that can augment T- and B-cell anti-tumourigenic activities and suppress Treg pro-tumourigenic activity. Immunotherapies utilising naturally-occurring or engineered T-cells, B-cells, and NK cells represent an emerging area of research and have demonstrated potential; however, certain challenges must be surmounted before they can be implemented in a clinical setting[282, 283]. The use of monoclonal antibodies to block Treg chemokine and inhibitory receptors, as well as the selective depletion of Tregs both within the TME and the circulation using certain chemotherapeutic agents, have all demonstrated great promise; however, the effects of such treatments on overall patient survival and treatment response are controversial and are still being investigated[284].

IL-6, IL-8, IL-10, IP-10, VEGF, GM-CSF, and GDF-15 are potentially valuable therapeutic targets. The blocking of IL-6 and IL-8 signalling using antibodies was found to significantly enhance the sensitivity of drug-resistant breast cancer cells and to reduce $HER2^+$ breast cancer tumour growth and metastasis[281]. In a TNBC cell line, inhibition of IL-6 and IL-8 signalling reduced colony formation and survival *in vitro,* as well as tumour engraftment and enlargement *in vivo*[285]. Lim *et al.*[286] introduced intratumoural vaccination of CXCL9- and IP-10-engineered dendritic cells into a murine non-small cell lung cancer model and observed an increase in T-cell infiltration and activation in the TME[286]. Administration of intratumoural recombinant IP-10 in a severe combined immunodeficiency disease (SCID) mouse model of non-small cell lung cancer induced cancer cell apoptosis and prevented metastasis through angiostatic mechanisms; however, these effects were dependent on continued treatment[287].

6.5 Study limitations

The exploratory nature of this study means that it has some challenges and limitations. The limited amount of time available for patient recruitment and the specific inclusion and exclusion criteria meant that this study was conducted using a small sample size. In addition, blood was collected only at two time points (before and after first-phase chemotherapy), and analysis at other intervals, especially after treatment completion, may have yielded different results. Age matching may improve comparability between healthy donor and patient groups. The number of events detected via flow cytometric analysis may have been reduced because of chemotherapy-induced cytotoxicity. In addition, the median concentration of IL-6 and IL-10 in patients and healthy donors measuring below the detection limit of the ELISA kits used may have implications on the validity of this study's findings. The use of additional phenotypic markers and cytokines in the analysis, as well as the inclusion of assays to assess cell function, may have provided more detailed insights into the effect of first-phase chemotherapy on the activity and secretory profile of these cells.

6.6 Future directions

Evaluating immune cell subsets and cytokine levels in a larger group of TNBC patients before and after first-phase chemotherapy and comparing these data to those of age-matched healthy donors may generate findings that are more generalisable to other populations. In addition, collection of whole blood not only before and after first-phase chemotherapy but also

after the completion of all chemotherapy may allow for the detection and analysis of both transient and long-term chemotherapy-induced changes in immune cell subsets and cytokine levels in patients with TNBC. The evaluation of immune cell subsets and cytokine expression in tumour samples before and after first-phase chemotherapy, and after the completion of all chemotherapy, may also prove to be beneficial, as immune cell subsets and cytokines within the circulation may not be identical to that of the TME. A longer follow-up period would allow more insight into the effect of chemotherapy-induced changes in circulating immune cell subsets and cytokine levels on overall and disease-free survival rates.

To better understand the effect of a TNBC tumour and chemotherapy on the activity and secretory profile of circulating immune cells, functional assays should be performed. Enzyme-linked immunospot (ELISPOT) assays, which allow for the characterisation of signalling molecule secretion and immune responses at a single-cell level, could be used to assess the secretion of pro- and anti-tumourigenic cytokines by T-cells, B-cells, NK cells, monocytes, and Tregs[288, 289]. NK cell cytotoxicity or degranulation assays could also be included to obtain greater insight into the effect of first-phase chemotherapy on NK cell cytolytic activity[290]. The expansion of the basic and Treg flow cytometry antibody panel to facilitate the detection of additional T-cell, B-cell, NK cell, monocyte, and Treg subsets would enable more comprehensive analysis of the effect of TNBC and chemotherapy on pro- and anti-tumourigenic immune cell subsets within the circulation and, by extension, the TME. Similarly, the assessment of additional cytokines and growth factors, such as IFN-γ and TNF-α, in TNBC patients before and after initial chemotherapy, and the potential impact on patient treatment response and prognosis, would be highly advantageous.

6.7 Conclusion

Breast cancer, especially TNBC, is a major healthcare concern, and immune cell subsets and cytokines within the TME may affect tumour growth, progression, and metastasis. Circulating immune cell subsets and cytokines have the potential to act as surrogate biomarkers for TNBC and understanding the effects of first-phase chemotherapy on the immune system, patient treatment response, and prognosis is crucial. This study highlighted the differences in immune cell subsets between treatment-naïve TNBC patients and healthy donors and showed an increase in $CD56^{high}$ NK cells and $CD14^{+}$ monocytes after first-phase chemotherapy. Little to no change was observed in T-cells and Tregs, with a decrease in B-cell numbers. Increases in soluble factors, such as IP-10, GDF-15, and cytokines, after first-phase chemotherapy may

promote the recruitment of cytotoxic immune cells to the TME and may stimulate further immune-mediated tumour destruction. These findings may have significant implications for the treatment response and prognosis of patients with TNBC and may assist in the identification of novel treatment strategies.

References

1. NCI [Internet]. What is Cancer? Internet: National Cancer Institute 2021 [updated 2021; cited 2023 19/01]. Available from: https://www.cancer.gov/about-cancer/understanding/what-is-cancer.
2. WHO [Internet]. Cancer. Internet: World Health Organisation; 2022 [cited 2023 19/01/2023]. Available from: https://www.who.int/news-room/fact-sheets/detail/cancer.
3. UK Cr [Internet]. Rare cancers. Internet: Cancer Research UK; 2022 [cited 2023 19/01]. Available from: https://www.cancerresearchuk.org/about-cancer/rare-cancers.
4. Bray F, Laversanne M, Sung H, Ferlay J, Siegel RL, Soerjomataram I, et al. Global cancer statistics 2022: GLOBOCAN estimates of incidence and mortality worldwide for 36 cancers in 185 countries. CA Cancer J. Clin. 2024; doi:10.3322/caac.21834
5. Cancer WIAfRo [Internet]. South Africa Fact Sheet 2022. Internet: Global Cancer Observatory; 2022 [cited 2024 18/04/2024]. Available from: https://gco.iarc.who.int/media/globocan/factsheets/populations/710-south-africa-fact-sheet.pdf.
6. Finestone E, Wishnia J. Estimating the burden of cancer in South Africa. 2022. 2022; 6 doi:10.4102/sajo.v6i0.220
7. Black E, Richmond R. Improving early detection of breast cancer in sub-Saharan Africa: why mammography may not be the way forward. Global Health. 2019; 15(1):3. doi:10.1186/s12992-018-0446-6
8. CANSA [Internet]. Early Detection of Breast Cancer is Vital. Internet: CANSA; 2021 [cited 2023 01/02]. Available from: https://cansa.org.za/early-detection-of-breast-cancer-is-vital/.
9. WHO [Internet]. Breast Cancer. Internet: WHO; 2021 [cited 2023 01/02]. Available from: https://www.who.int/news-room/fact-sheets/detail/breast-cancer.
10. Anyigba CA, Awandare GA, Paemka L. Breast cancer in sub-Saharan Africa: The current state and uncertain future. Exp. Biol. Med. (Maywood). 2021; 246(12):1377-87. doi:10.1177/15353702211006047
11. Katsura C, Ogunmwonyi I, Kankam HK, Saha S. Breast cancer: presentation, investigation and management. Br. J. Hosp. Med. (Lond.). 2022; 83(2):1-7. doi:10.12968/hmed.2021.0459
12. Watkins EJ. Overview of breast cancer. Jaapa. 2019; 32(10):13-7. doi:10.1097/01.JAA.0000580524.95733.3d
13. da Luz FAC, Araújo BJ, de Araújo RA. The current staging and classification systems of breast cancer and their pitfalls: Is it possible to integrate the complexity of this neoplasm into a unified staging system? Crit. Rev. Oncol. Hematol. 2022; 178:103781. doi:10.1016/j.critrevonc.2022.103781
14. Cooper G. The Cell: A Molecular Approach. 2 ed. Sutherland, editor. Internet: Sinauer Associates; 2000.
15. Hanahan D, Weinberg RA. The hallmarks of cancer. Cell. 2000; 100(1):57-70. doi:10.1016/s0092-8674(00)81683-9
16. Gutschner T, Diederichs S. The hallmarks of cancer: a long non-coding RNA point of view. RNA Biol. 2012; 9(6):703-19. doi:10.4161/rna.20481
17. Hanahan D, Weinberg RA. Hallmarks of cancer: the next generation. Cell. 2011; 144(5):646-74. doi:10.1016/j.cell.2011.02.013

18. de Vries NL, Mahfouz A, Koning F, de Miranda N. Unraveling the Complexity of the Cancer Microenvironment With Multidimensional Genomic and Cytometric Technologies. Front. Oncol. 2020; 10:1254. doi:10.3389/fonc.2020.01254
19. Mittal S, Brown NJ, Holen I. The breast tumor microenvironment: role in cancer development, progression and response to therapy. Expert Rev. Mol. Diagn. 2018; 18(3):227-43. doi:10.1080/14737159.2018.1439382
20. Xing Y, Ruan G, Ni H, Qin H, Chen S, Gu X, et al. Tumor Immune Microenvironment and Its Related miRNAs in Tumor Progression. Front. Immunol. 2021; 12:624725. doi:10.3389/fimmu.2021.624725
21. Asif PJ, Longobardi C, Hahne M, Medema JP. The Role of Cancer-Associated Fibroblasts in Cancer Invasion and Metastasis. Cancers (Basel). 2021; 13(18) doi:10.3390/cancers13184720
22. Ghiabi P, Jiang J, Pasquier J, Maleki M, Abu-Kaoud N, Rafii S, et al. Endothelial cells provide a notch-dependent pro-tumoral niche for enhancing breast cancer survival, stemness and pro-metastatic properties. PLoS One. 2014; 9(11):e112424. doi:10.1371/journal.pone.0112424
23. Wu Q, Li B, Li Z, Li J, Sun S, Sun S. Cancer-associated adipocytes: key players in breast cancer progression. J. Hematol. Oncol. 2019; 12(1):95. doi:10.1186/s13045-019-0778-6
24. Tan K, Naylor MJ. Tumour Microenvironment-Immune Cell Interactions Influencing Breast Cancer Heterogeneity and Disease Progression. Front. Oncol. 2022; 12:876451. doi:10.3389/fonc.2022.876451
25. Vinay Kumar AA, Jon Aster. Neoplasia. [Internet] Robbin's and Cotran Pathologic Basis of Disease. 10 ed. Internet: Elsevier 2021.[Available from: https://www.clinicalkey.com/#!/content/book/3-s2.0-B9780323531139000078.
26. Estrella V, Chen T, Lloyd M, Wojtkowiak J, Cornnell HH, Ibrahim-Hashim A, et al. Acidity generated by the tumor microenvironment drives local invasion. Cancer Res. 2013; 73(5):1524-35. doi:10.1158/0008-5472.Can-12-2796
27. Holl EK, Frazier VN, Landa K, Beasley GM, Hwang ES, Nair SK. Examining Peripheral and Tumor Cellular Immunome in Patients With Cancer. Front. Immunol. 2019; 10:1767. doi:10.3389/fimmu.2019.01767
28. Abbott M, Ustoyev Y. Cancer and the Immune System: The History and Background of Immunotherapy. Semin. Oncol. Nurs. 2019; 35(5):150923. doi:10.1016/j.soncn.2019.08.002
29. Gonzalez H, Hagerling C, Werb Z. Roles of the immune system in cancer: from tumor initiation to metastatic progression. Genes Dev. 2018; 32(19-20):1267-84. doi:10.1101/gad.314617.118
30. Li MO, Wan YY, Sanjabi S, Robertson AK, Flavell RA. Transforming growth factor-beta regulation of immune responses. Annu. Rev. Immunol. 2006; 24:99-146. doi:10.1146/annurev.immunol.24.021605.090737
31. Rabinovich GA, Gabrilovich D, Sotomayor EM. Immunosuppressive strategies that are mediated by tumor cells. Annu. Rev. Immunol. 2007; 25:267-96. doi:10.1146/annurev.immunol.25.022106.141609
32. King J, Mir H, Singh S. Association of Cytokines and Chemokines in Pathogenesis of Breast Cancer. Prog. Mol. Biol. Transl. Sci. 2017; 151:113-36. doi:10.1016/bs.pmbts.2017.07.003
33. Balta E, Wabnitz GH, Samstag Y. Hijacked Immune Cells in the Tumor Microenvironment: Molecular Mechanisms of Immunosuppression and Cues to Improve T Cell-Based Immunotherapy of Solid Tumors. Int. J. Mol. Sci. 2021; 22(11) doi:10.3390/ijms22115736

34. Hornyák L, Dobos N, Koncz G, Karányi Z, Páll D, Szabó Z, et al. The Role of Indoleamine-2,3-Dioxygenase in Cancer Development, Diagnostics, and Therapy. Front. Immunol. 2018; 9:151. doi:10.3389/fimmu.2018.00151
35. Rapoport BL, Steel HC, Hlatshwayo N, Theron AJ, Meyer PWA, Nayler S, et al. Systemic Immune Dysregulation in Early Breast Cancer Is Associated With Decreased Plasma Levels of Both Soluble Co-Inhibitory and Co-Stimulatory Immune Checkpoint Molecules. Front. Immunol. 2022; 13:823842. doi:10.3389/fimmu.2022.823842
36. team ACSmaec [Internet]. Types of stem cell and bone marrow transplants Internet: American Cancer Society; 2020 [updated 2020; cited 2023 26/01]. Available from: https://www.cancer.org/treatment/treatments-and-side-effects/treatment-types/stem-cell-transplant/types-of-transplants.html.
37. team TACSmaec [Internet]. How surgery is used for cancer. Internet: American Cancer Society; 2019 [cited 2023 26/01]. Available from: https://www.cancer.org/treatment/treatments-and-side-effects/treatment-types/surgery/how-surgery-is-used-for-cancer.html.
38. team ACSmaec [Internet]. How radiation therapy is used to treat cancer. Internet: American Cancer Society; 2019 [cited 2023 26/01]. Available from: https://www.cancer.org/treatment/treatments-and-side-effects/treatment-types/radiation/basics.html.
39. team TACSmaec [Internet]. Hormone Therapy. Internet: American Cancer Society; 2020 [cited 2023 26/01]. Available from: https://www.cancer.org/treatment/treatments-and-side-effects/treatment-types/hormone-therapy.html.
40. team TAcsmaec [Internet]. Chemotherapy. Internet: American Cancer Society; 2019 [updated 2019; cited 2023 26/01/2023]. Available from: https://www.cancer.org/treatment/treatments-and-side-effects/treatment-types/chemotherapy.html.
41. Barzaman K, Moradi-Kalbolandi S, Hosseinzadeh A, Kazemi MH, Khorramdelazad H, Safari E, et al. Breast cancer immunotherapy: Current and novel approaches. Int. Immunopharmacol. 2021; 98:107886. doi:10.1016/j.intimp.2021.107886
42. Lustberg MB. Management of neutropenia in cancer patients. Clin. Adv. Hematol. Oncol. 2012; 10(12):825-6.
43. Picot J, Guerin CL, Le Van Kim C, Boulanger CM. Flow cytometry: retrospective, fundamentals and recent instrumentation. Cytotechnology. 2012; 64(2):109-30. doi:10.1007/s10616-011-9415-0
44. Bonilla DL, Reinin G, Chua E. Full Spectrum Flow Cytometry as a Powerful Technology for Cancer Immunotherapy Research. Front Mol Biosci. 2020; 7:612801. doi:10.3389/fmolb.2020.612801
45. Coulter B [Internet]. History of Flow Cytometry. Internet: Beckman Coulter; [cited 2023 04/09/2023]. Available from: https://www.beckman.co.za/resources/technologies/flow-cytometry/history.
46. Cluster of Differentiation (CD) antigens [Internet]In: Julius Cruse RL, Huan Wang editor. Immunology Guidebook. Internet: Elsevier; 2007. p. 47-124.[Available from: https://www.ncbi.nlm.nih.gov/pmc/articles/PMC7158181/#!po=70.0000.
47. Lu L, Barbi J, Pan F. The regulation of immune tolerance by FOXP3. Nat. Rev. Immunol. 2017; 17(11):703-17. doi:10.1038/nri.2017.75
48. Saraiva DP, Jacinto A, Borralho P, Braga S, Cabral MG. HLA-DR in Cytotoxic T Lymphocytes Predicts Breast Cancer Patients' Response to Neoadjuvant Chemotherapy. Front. Immunol. 2018; 9:2605. doi:10.3389/fimmu.2018.02605

49. Mousset CM, Hobo W, Woestenenk R, Preijers F, Dolstra H, van der Waart AB. Comprehensive Phenotyping of T Cells Using Flow Cytometry. Cytometry Part A. 2019; 95(6):647-54. doi:https://doi.org/10.1002/cyto.a.23724
50. Marimuthu R, Francis H, Dervish S, Li SCH, Medbury H, Williams H. Characterization of Human Monocyte Subsets by Whole Blood Flow Cytometry Analysis. J Vis Exp. 2018; (140) doi:10.3791/57941
51. Erokhina SA, Streltsova MA, Kanevskiy LM, Grechikhina MV, Sapozhnikov AM, Kovalenko EI. HLA-DR-expressing NK cells: Effective killers suspected for antigen presentation. J. Leukoc. Biol. 2020; 109(2):327-37. doi:10.1002/jlb.3ru0420-668rr
52. Kust SA, Ustiuzhanina MO, Streltsova MA, Shelyakin PV, Kryukov MA, Lutsenko GV, et al. HLA-DR Expression in Natural Killer Cells Marks Distinct Functional States, Depending on Cell Differentiation Stage. Int. J. Mol. Sci. 2024; 25(9):4609.
53. Velounias RL, Tull TJ. Human B-cell subset identification and changes in inflammatory diseases. Clin. Exp. Immunol. 2022; 210(3):201-16. doi:10.1093/cei/uxac104
54. Terrén I, Orrantia A, Vitallé J, Zenarruzabeitia O, Borrego F. NK Cell Metabolism and Tumor Microenvironment. Front. Immunol. 2019; 10:2278. doi:10.3389/fimmu.2019.02278
55. Wang S, Liu R, Yu Q, Dong L, Bi Y, Liu G. Metabolic reprogramming of macrophages during infections and cancer. Cancer Lett. 2019; 452:14-22. doi:10.1016/j.canlet.2019.03.015
56. Xiong S, Dong L, Cheng L. Neutrophils in cancer carcinogenesis and metastasis. J. Hematol. Oncol. 2021; 14(1):173. doi:10.1186/s13045-021-01187-y
57. Lee YS, Radford KJ. The role of dendritic cells in cancer. Int. Rev. Cell Mol. Biol. 2019; 348:123-78. doi:10.1016/bs.ircmb.2019.07.006
58. Parkin J, Cohen B. An overview of the immune system. Lancet. 2001; 357(9270):1777-89. doi:10.1016/s0140-6736(00)04904-7
59. Charles Janeway PT. T cell-mediated cytotoxicity. [Internet] Immunobiology: The immune system in health and disease. 5 ed. Internet: Garland Science; 2001.[Available from: https://www.ncbi.nlm.nih.gov/books/NBK27101/#:~:text=Cytotoxic%20CD8%20T%20cells%20carry,which%20the%20granzymes%20can%20enter.
60. Coulter B. CytoFLEX Ready to Use Daily QC Fluorospheres. Internet: Beckman Coulter; 2023.
61. Baranova A, Krasnoselskyi M, Starikov V, Kartashov S, Zhulkevych I, Vlasenko V, et al. Triple-negative breast cancer: current treatment strategies and factors of negative prognosis. J. Med. Life. 2022; 15(2):153-61. doi:10.25122/jml-2021-0108
62. Goodale D, Phay C, Brown W, Gray-Statchuk L, Furlong P, Lock M, et al. Flow cytometric assessment of monocyte activation markers and circulating endothelial cells in patients with localized or metastatic breast cancer. Cytometry B Clin. Cytom. 2009; 76(2):107-17. doi:10.1002/cyto.b.20449
63. Kumar P, Aggarwal R. An overview of triple-negative breast cancer. Arch. Gynecol. Obstet. 2016; 293(2):247-69. doi:10.1007/s00404-015-3859-y
64. Gao G, Wang Z, Qu X, Zhang Z. Prognostic value of tumor-infiltrating lymphocytes in patients with triple-negative breast cancer: a systematic review and meta-analysis. BMC Cancer. 2020; 20(1):179. doi:10.1186/s12885-020-6668-z
65. Furukawa N, Stearns V, Santa-Maria CA, Popel AS. The tumor microenvironment and triple-negative breast cancer aggressiveness: shedding light on mechanisms and targeting. Expert Opin. Ther. Targets. 2022; 26(12):1041-56. doi:10.1080/14728222.2022.2170779
66. Zhang N, Bevan MJ. CD8(+) T cells: foot soldiers of the immune system. Immunity. 2011; 35(2):161-8. doi:10.1016/j.immuni.2011.07.010

67. Raskov H, Orhan A, Christensen JP, Gögenur I. Cytotoxic CD8+ T cells in cancer and cancer immunotherapy. Br. J. Cancer. 2021; 124(2):359-67. doi:10.1038/s41416-020-01048-4
68. Luckheeram RV, Zhou R, Verma AD, Xia B. CD4$^+$T cells: differentiation and functions. Clin. Dev. Immunol. 2012; 2012:925135. doi:10.1155/2012/925135
69. Zhu X, Zhu J. CD4 T Helper Cell Subsets and Related Human Immunological Disorders. Int. J. Mol. Sci. 2020; 21(21) doi:10.3390/ijms21218011
70. Richardson JR, Schöllhorn A, Gouttefangeas C, Schuhmacher J. CD4+ T Cells: Multitasking Cells in the Duty of Cancer Immunotherapy. Cancers (Basel). 2021; 13(4) doi:10.3390/cancers13040596
71. Zhu Y, Zhu X, Tang C, Guan X, Zhang W. Progress and challenges of immunotherapy in triple-negative breast cancer. Biochimica et Biophysica Acta (BBA) - Reviews on Cancer. 2021; 1876(2):188593. doi:https://doi.org/10.1016/j.bbcan.2021.188593
72. Fremd C, Schuetz F, Sohn C, Beckhove P, Domschke C. B cell-regulated immune responses in tumor models and cancer patients. Oncoimmunology. 2013; 2(7):e25443. doi:10.4161/onci.25443
73. Rastogi I, Jeon D, Moseman JE, Muralidhar A, Potluri HK, McNeel DG. Role of B cells as antigen presenting cells. Front. Immunol. 2022; 13:954936. doi:10.3389/fimmu.2022.954936
74. Vazquez MI, Catalan-Dibene J, Zlotnik A. B cells responses and cytokine production are regulated by their immune microenvironment. Cytokine. 2015; 74(2):318-26. doi:10.1016/j.cyto.2015.02.007
75. de Gruijter NM, Jebson B, Rosser EC. Cytokine production by human B cells: role in health and autoimmune disease. Clin. Exp. Immunol. 2022; 210(3):253-62. doi:10.1093/cei/uxac090
76. Paul S, Lal G. The Molecular Mechanism of Natural Killer Cells Function and Its Importance in Cancer Immunotherapy. Front. Immunol. 2017; 8 doi:10.3389/fimmu.2017.01124
77. Rodriguez-Mogeda C, van Ansenwoude CMJ, van der Molen L, Strijbis EMM, Mebius RE, de Vries HE. The role of CD56bright NK cells in neurodegenerative disorders. J. Neuroinflammation. 2024; 21(1):48. doi:10.1186/s12974-024-03040-8
78. Van Acker HH, Capsomidis A, Smits EL, Van Tendeloo VF. CD56 in the Immune System: More Than a Marker for Cytotoxicity? Front. Immunol. 2017; 8:892. doi:10.3389/fimmu.2017.00892
79. Mamessier E, Pradel LC, Thibult ML, Drevet C, Zouine A, Jacquemier J, et al. Peripheral blood NK cells from breast cancer patients are tumor-induced composite subsets. J. Immunol. 2013; 190(5):2424-36. doi:10.4049/jimmunol.1200140
80. Olingy CE, Dinh HQ, Hedrick CC. Monocyte heterogeneity and functions in cancer. J. Leukoc. Biol. 2019; 106(2):309-22. doi:10.1002/jlb.4ri0818-311r
81. Yang J, Zhang L, Yu C, Yang X-F, Wang H. Monocyte and macrophage differentiation: circulation inflammatory monocyte as biomarker for inflammatory diseases. Biomarker Research. 2014; 2(1):1. doi:10.1186/2050-7771-2-1
82. Zhang Q, Sioud M. Tumor-Associated Macrophage Subsets: Shaping Polarization and Targeting. Int. J. Mol. Sci. 2023; 24(8) doi:10.3390/ijms24087493
83. Azad AK, Rajaram MV, Schlesinger LS. Exploitation of the Macrophage Mannose Receptor (CD206) in Infectious Disease Diagnostics and Therapeutics. J Cytol Mol Biol. 2014; 1(1) doi:10.13188/2325-4653.1000003
84. Sharma A, Jasrotia S, Kumar A. Effects of Chemotherapy on the Immune System: Implications for Cancer Treatment and Patient Outcomes. Naunyn Schmiedebergs Arch. Pharmacol. 2024; 397(5):2551-66. doi:10.1007/s00210-023-02781-2

85. Wang W, Wu J, Zhang P, Fei X, Zong Y, Chen X, et al. Prognostic and predictive value of Ki-67 in triple-negative breast cancer. Oncotarget. 2016; 7(21):31079-87. doi:10.18632/oncotarget.9075
86. Salgado R, Denkert C, Demaria S, Sirtaine N, Klauschen F, Pruneri G, et al. The evaluation of tumor-infiltrating lymphocytes (TILs) in breast cancer: recommendations by an International TILs Working Group 2014. Ann. Oncol. 2015; 26(2):259-71. doi:10.1093/annonc/mdu450
87. Montégut L, López-Otín C, Kroemer G. Aging and cancer. Mol. Cancer. 2024; 23(1):106. doi:10.1186/s12943-024-02020-z
88. Bou Zerdan M, Ghorayeb T, Saliba F, Allam S, Bou Zerdan M, Yaghi M, et al. Triple Negative Breast Cancer: Updates on Classification and Treatment in 2021. Cancers (Basel). 2022; 14(5) doi:10.3390/cancers14051253
89. Harborg S, Zachariae R, Olsen J, Johannsen M, Cronin-Fenton D, Bøggild H, et al. Overweight and prognosis in triple-negative breast cancer patients: a systematic review and meta-analysis. npj Breast Cancer. 2021; 7(1):119. doi:10.1038/s41523-021-00325-6
90. Sun H, Zou J, Chen L, Zu X, Wen G, Zhong J. Triple-negative breast cancer and its association with obesity. Mol Clin Oncol. 2017; 7(6):935-42. doi:10.3892/mco.2017.1429
91. Kawai M, Malone KE, Tang MT, Li CI. Active smoking and the risk of estrogen receptor-positive and triple-negative breast cancer among women ages 20 to 44 years. Cancer. 2014; 120(7):1026-34. doi:10.1002/cncr.28402
92. van den Ende NS, Nguyen AH, Jager A, Kok M, Debets R, van Deurzen CHM. Triple-Negative Breast Cancer and Predictive Markers of Response to Neoadjuvant Chemotherapy: A Systematic Review. Int. J. Mol. Sci. 2023; 24(3) doi:10.3390/ijms24032969
93. Keam B, Im SA, Lee KH, Han SW, Oh DY, Kim JH, et al. Ki-67 can be used for further classification of triple negative breast cancer into two subtypes with different response and prognosis. Breast Cancer Res. 2011; 13(2):R22. doi:10.1186/bcr2834
94. Wu Q, Ma G, Deng Y, Luo W, Zhao Y, Li W, et al. Prognostic Value of Ki-67 in Patients With Resected Triple-Negative Breast Cancer: A Meta-Analysis. Front. Oncol. 2019; 9 doi:10.3389/fonc.2019.01068
95. Chae S, Kang KM, Kim HJ, Kang E, Park SY, Kim JH, et al. Neutrophil-lymphocyte ratio predicts response to chemotherapy in triple-negative breast cancer. Curr. Oncol. 2018; 25(2):e113-e9. doi:10.3747/co.25.3888
96. Huertas-Caro CA, Ramírez MA, Rey-Vargas L, Bejarano-Rivera LM, Ballen DF, Nuñez M, et al. Tumor infiltrating lymphocytes (TILs) are a prognosis biomarker in Colombian patients with triple negative breast cancer. Sci. Rep. 2023; 13(1):21324. doi:10.1038/s41598-023-48300-4
97. Verma R, Foster RE, Horgan K, Mounsey K, Nixon H, Smalle N, et al. Lymphocyte depletion and repopulation after chemotherapy for primary breast cancer. Breast Cancer Res. 2016; 18(1):10. doi:10.1186/s13058-015-0669-x
98. Gao A, Zhang L, Zhong D. Chemotherapy-induced thrombocytopenia: literature review. Discov Oncol. 2023; 14(1):10. doi:10.1007/s12672-023-00616-3
99. Ghebeh H, Elshenawy MA, AlSayed AD, Al-Tweigeri T. Peripheral Blood Eosinophil Count is Associated with Response to Chemoimmunotherapy in Metastatic Triple-Negative Breast Cancer. Immunotherapy. 2022; 14(4):189-99. doi:10.2217/imt-2021-0149
100. Varricchi G, Galdiero MR, Loffredo S, Lucarini V, Marone G, Mattei F, et al. Eosinophils: The unsung heroes in cancer? Oncoimmunology. 2018; 7(2):e1393134. doi:10.1080/2162402x.2017.1393134

101. Massa C, Karn T, Denkert C, Schneeweiss A, Hanusch C, Blohmer JU, et al. Differential effect on different immune subsets of neoadjuvant chemotherapy in patients with TNBC. J Immunother Cancer. 2020; 8(2) doi:10.1136/jitc-2020-001261
102. Patysheva M, Frolova A, Larionova I, Afanas'ev S, Tarasova A, Cherdyntseva N, et al. Monocyte programming by cancer therapy. Front. Immunol. 2022; 13 doi:10.3389/fimmu.2022.994319
103. Valdés-Ferrada J, Muñoz-Durango N, Pérez-Sepulveda A, Muñiz S, Coronado-Arrázola I, Acevedo F, et al. Peripheral Blood Classical Monocytes and Plasma Interleukin 10 Are Associated to Neoadjuvant Chemotherapy Response in Breast Cancer Patients. Front. Immunol. 2020; 11 doi:10.3389/fimmu.2020.01413
104. Zheng L, Yu M, Zhang S. Prognostic value of pretreatment circulating basophils in patients with glioblastoma. Neurosurg. Rev. 2021; 44(6):3471-8. doi:10.1007/s10143-021-01524-2
105. Bax HJ, Chauhan J, Stavraka C, Khiabany A, Nakamura M, Pellizzari G, et al. Basophils from Cancer Patients Respond to Immune Stimuli and Predict Clinical Outcome. Cells. 2020; 9(7):1631.
106. Shokane LL, Bezuidenhout S, Lundie M. Use of granulocyte colony-stimulating factor in patients with chemotherapy-induced neutropaenia. Health SA. 2023; 28:2221. doi:10.4102/hsag.v28i0.2221
107. Gao H, Ouyang D, Guan X, Xu J, Chen Q, Zeng L, et al. Immune characteristics and clinical significance of peripheral blood lymphocytes in breast cancer. BMC Cancer. 2024; 24(1):50. doi:10.1186/s12885-024-11815-8
108. Waidhauser J, Schuh A, Trepel M, Schmälter AK, Rank A. Chemotherapy markedly reduces B cells but not T cells and NK cells in patients with cancer. Cancer Immunol. Immunother. 2020; 69(1):147-57. doi:10.1007/s00262-019-02449-y
109. Sánchez-Margalet V, Barco-Sánchez A, Vilariño-García T, Jiménez-Cortegana C, Pérez-Pérez A, Henao-Carrasco F, et al. Circulating regulatory T cells from breast cancer patients in response to neoadjuvant chemotherapy. Transl Cancer Res. 2019; 8(1):59-65. doi:10.21037/tcr.2018.12.30
110. Sewell HF, Halbert CF, Robins RA, Galvin A, Chan S, Blamey RW. Chemotherapy-induced differential changes in lymphocyte subsets and natural-killer-cell function in patients with advanced breast cancer. Int. J. Cancer. 1993; 55(5):735-8. doi:https://doi.org/10.1002/ijc.2910550506
111. Gascoigne NR, Zal T, Yachi PP, Hoerter JA. Co-receptors and recognition of self at the immunological synapse. Curr. Top. Microbiol. Immunol. 2010; 340:171-89. doi:10.1007/978-3-642-03858-7_9
112. Ganji A, Farahani I, Khansarinejad B, Ghazavi A, Mosayebi G. Increased expression of CD8 marker on T-cells in COVID-19 patients. Blood Cells Mol. Dis. 2020; 83:102437. doi:10.1016/j.bcmd.2020.102437
113. Verma R, Hanby AM, Horgan K, Verghese ET, Volpato M, Carter CR, et al. Levels of different subtypes of tumour-infiltrating lymphocytes correlate with each other, with matched circulating lymphocytes, and with survival in breast cancer. Breast Cancer Res. Treat. 2020; 183(1):49-59. doi:10.1007/s10549-020-05757-5
114. Palazón-Carrión N, Jiménez-Cortegana C, Sánchez-León ML, Henao-Carrasco F, Nogales-Fernández E, Chiesa M, et al. Circulating immune biomarkers in peripheral blood correlate with clinical outcomes in advanced breast cancer. Sci. Rep. 2021; 11(1):14426. doi:10.1038/s41598-021-93838-w

115. van der Zande HJP, Nitsche D, Schlautmann L, Guigas B, Burgdorf S. The Mannose Receptor: From Endocytic Receptor and Biomarker to Regulator of (Meta)Inflammation. Front. Immunol. 2021; 12:765034. doi:10.3389/fimmu.2021.765034
116. Schuette V, Embgenbroich M, Ulas T, Welz M, Schulte-Schrepping J, Draffehn AM, et al. Mannose receptor induces T-cell tolerance via inhibition of CD45 and up-regulation of CTLA-4. Proc. Natl. Acad. Sci. U. S. A. 2016; 113(38):10649-54. doi:10.1073/pnas.1605885113
117. Royer P-J, Emara M, Yang C, Al-Ghouleh A, Tighe P, Jones N, et al. The Mannose Receptor Mediates the Uptake of Diverse Native Allergens by Dendritic Cells and Determines Allergen-Induced T Cell Polarization through Modulation of IDO Activity. The Journal of Immunology. 2010; 185(3):1522-31. doi:10.4049/jimmunol.1000774
118. Wang W, Wang Y, Cao Z. Changes of proportions of circulating lymphocyte subsets in cancer patients after chemotherapy. Transl Cancer Res. 2021; 10(9):4169-79. doi:10.21037/tcr-21-1688
119. Foulds GA, Vadakekolathu J, Abdel-Fatah TMA, Nagarajan D, Reeder S, Johnson C, et al. Immune-Phenotyping and Transcriptomic Profiling of Peripheral Blood Mononuclear Cells From Patients With Breast Cancer: Identification of a 3 Gene Signature Which Predicts Relapse of Triple Negative Breast Cancer. Front. Immunol. 2018; 9 doi:10.3389/fimmu.2018.02028
120. Čelešnik H, Potočnik U. Peripheral Blood Transcriptome in Breast Cancer Patients as a Source of Less Invasive Immune Biomarkers for Personalized Medicine, and Implications for Triple Negative Breast Cancer. Cancers (Basel). 2022; 14(3):591.
121. Erokhina SA, Streltsova MA, Kanevskiy LM, Telford WG, Sapozhnikov AM, Kovalenko EI. HLA-DR+ NK cells are mostly characterized by less mature phenotype and high functional activity. Immunol. Cell Biol. 2018; 96(2):212-28. doi:https://doi.org/10.1111/imcb.1032
122. Poli A, Michel T, Thérésine M, Andrès E, Hentges F, Zimmer J. CD56bright natural killer (NK) cells: an important NK cell subset. Immunology. 2009; 126(4):458-65. doi:https://doi.org/10.1111/j.1365-2567.2008.03027.x
123. Zhang C, Wu F, Lu X, Wang S, Wu M, Chen N, et al. Peripheral NK cell count predicts response and prognosis in breast cancer patients underwent neoadjuvant chemotherapy. Front. Immunol. 2024; 15 doi:10.3389/fimmu.2024.1437193
124. Papewalis C, Jacobs B, Baran AM, Ehlers M, Stoecklein NH, Willenberg HS, et al. Increased numbers of tumor-lysing monocytes in cancer patients. Mol. Cell. Endocrinol. 2011; 337(1):52-61. doi:https://doi.org/10.1016/j.mce.2011.01.020
125. Wu J, Waxman DJ. Immunogenic chemotherapy: Dose and schedule dependence and combination with immunotherapy. Cancer Lett. 2018; 419:210-21. doi:10.1016/j.canlet.2018.01.050
126. Galluzzi L, Buqué A, Kepp O, Zitvogel L, Kroemer G. Immunological Effects of Conventional Chemotherapy and Targeted Anticancer Agents. Cancer Cell. 2015; 28(6):690-714. doi:10.1016/j.ccell.2015.10.012
127. Cornwell WD, Kim V, Fan X, Vega ME, Ramsey FV, Criner GJ, et al. Activation and polarization of circulating monocytes in severe chronic obstructive pulmonary disease. BMC Pulm. Med. 2018; 18(1):101. doi:10.1186/s12890-018-0664-y
128. Axelrod ML, Wang Y, Xu Y, Sun X, Bejan CA, Gonzalez-Ericsson PI, et al. Peripheral Blood Monocyte Abundance Predicts Outcomes in Patients with Breast Cancer. Cancer Research Communications. 2022; 2(5):286-92. doi:10.1158/2767-9764.Crc-22-0023
129. Wen J, Ye F, Huang X, Li S, Yang L, Xiao X, et al. Prognostic Significance of Preoperative Circulating Monocyte Count in Patients With Breast Cancer: Based on a Large Cohort Study. Medicine. 2015; 94(49):e2266. doi:10.1097/md.0000000000002266

130. Dixon-Douglas J, Virassamy B, Clarke K, Hun M, Luen SJ, Savas P, et al. Sustained lymphocyte decreases after treatment for early breast cancer. npj Breast Cancer. 2024; 10(1):94. doi:10.1038/s41523-024-00698-4
131. Mackay IR, Goodyear MDE, Riglar C, Penschow J. Effect on natural killer and antibody-dependent cellular cytotoxicity of adjuvant cytotoxic chemotherapy including melphalan in breast cancer. Cancer Immunol. Immunother. 1983; 16(2):98-100. doi:10.1007/BF00199239
132. Ohue Y, Nishikawa H. Regulatory T (Treg) cells in cancer: Can Treg cells be a new therapeutic target? Cancer Sci. 2019; 110(7):2080-9. doi:10.1111/cas.14069
133. Kos K, de Visser KE. The Multifaceted Role of Regulatory T Cells in Breast Cancer. Annu Rev Cancer Biol. 2021; 5:291-310. doi:10.1146/annurev-cancerbio-042920-104912
134. Kim H-J, Cantor H. CD4 T-cell Subsets and Tumor Immunity: The Helpful and the Not-so-Helpful. Cancer Immunology Research. 2014; 2(2):91-8. doi:10.1158/2326-6066.Cir-13-0216
135. Goswami TK, Singh M, Dhawan M, Mitra S, Emran TB, Rabaan AA, et al. Regulatory T cells (Tregs) and their therapeutic potential against autoimmune disorders - Advances and challenges. Hum. Vaccin. Immunother. 2022; 18(1):2035117. doi:10.1080/21645515.2022.2035117
136. Grant CR, Liberal R, Mieli-Vergani G, Vergani D, Longhi MS. Regulatory T-cells in autoimmune diseases: Challenges, controversies and—yet—unanswered questions. Autoimmunity Reviews. 2015; 14(2):105-16. doi:https://doi.org/10.1016/j.autrev.2014.10.012
137. Li C, Jiang P, Wei S, Xu X, Wang J. Regulatory T cells in tumor microenvironment: new mechanisms, potential therapeutic strategies and future prospects. Mol. Cancer. 2020; 19(1):116. doi:10.1186/s12943-020-01234-1
138. Chaudhary B, Elkord E. Regulatory T Cells in the Tumor Microenvironment and Cancer Progression: Role and Therapeutic Targeting. Vaccines (Basel). 2016; 4(3) doi:10.3390/vaccines4030028
139. Frydrychowicz M, Boruczkowski M, Kolecka-Bednarczyk A, Dworacki G. The Dual Role of Treg in Cancer. Scand. J. Immunol. 2017; 86(6):436-43. doi:https://doi.org/10.1111/sji.12615
140. Santegoets SJ, Dijkgraaf EM, Battaglia A, Beckhove P, Britten CM, Gallimore A, et al. Monitoring regulatory T cells in clinical samples: consensus on an essential marker set and gating strategy for regulatory T cell analysis by flow cytometry. Cancer Immunol. Immunother. 2015; 64(10):1271-86. doi:10.1007/s00262-015-1729-x
141. Liu W, Putnam AL, Xu-Yu Z, Szot GL, Lee MR, Zhu S, et al. CD127 expression inversely correlates with FoxP3 and suppressive function of human CD4+ T reg cells. J. Exp. Med. 2006; 203(7):1701-11. doi:10.1084/jem.20060772
142. Duggleby R, Danby RD, Madrigal JA, Saudemont A. Clinical Grade Regulatory CD4+ T Cells (Tregs): Moving Toward Cellular-Based Immunomodulatory Therapies. Front. Immunol. 2018; 9 doi:10.3389/fimmu.2018.00252
143. Tian Y, Babor M, Lane J, Schulten V, Patil VS, Seumois G, et al. Unique phenotypes and clonal expansions of human CD4 effector memory T cells re-expressing CD45RA. Nature Communications. 2017; 8(1):1473. doi:10.1038/s41467-017-01728-5
144. Liu J, Wang X, Deng Y, Yu X, Wang H, Li Z. Research Progress on the Role of Regulatory T Cell in Tumor Microenvironment in the Treatment of Breast Cancer. Front. Oncol. 2021; 11 doi:10.3389/fonc.2021.766248
145. Gobert M, Treilleux I, Bendriss-Vermare N, Bachelot T, Goddard-Leon S, Arfi V, et al. Regulatory T Cells Recruited through CCL22/CCR4 Are Selectively Activated in Lymphoid

Infiltrates Surrounding Primary Breast Tumors and Lead to an Adverse Clinical Outcome. Cancer Res. 2009; 69(5):2000-9. doi:10.1158/0008-5472.Can-08-2360
146. Liyanage UK, Moore TT, Joo H-G, Tanaka Y, Herrmann V, Doherty G, et al. Prevalence of Regulatory T Cells Is Increased in Peripheral Blood and Tumor Microenvironment of Patients with Pancreas or Breast Adenocarcinoma1. The Journal of Immunology. 2002; 169(5):2756-61. doi:10.4049/jimmunol.169.5.2756
147. Park A, Govindaraj C, Xiang SD, Halo J, Quinn M, Scalzo-Inguanti K, et al. Substantially Modified Ratios of Effector to Regulatory T Cells During Chemotherapy in Ovarian Cancer Patients Return to Pre-Treatment Levels at Completion: Implications for Immunotherapy. Cancers (Basel). 2012; 4(2):581-600.
148. Gheybi MK, Farrokhi S, Ravanbod MR, Ostovar A, Mehrzad V, Nematollahi P. The correlation of CD19 + CD24 + CD38 + B cells and other clinicopathological variables with the proportion of circulating Tregs in breast cancer patients. Breast Cancer. 2017; 24(6):756-64. doi:10.1007/s12282-017-0775-y
149. Erfani N, Hamedi-Shahraki M, Rezaeifard S, Haghshenas M, Rasouli M, Samsami Dehaghani A. FoxP3+ Regulatory T Cells in Peripheral Blood of Patients with Epithelial Ovarian Cancer. Iran J. Immunol. 2014; 11(2):105-12.
150. Clarke SL, Betts GJ, Plant A, Wright KL, El-Shanawany TM, Harrop R, et al. CD4+CD25+FOXP3+ Regulatory T Cells Suppress Anti-Tumor Immune Responses in Patients with Colorectal Cancer. PLoS One. 2006; 1(1):e129. doi:10.1371/journal.pone.0000129
151. Ostapchuk YO, Perfilyeva YV, Kustova EA, Urazalieva NT, Omarbaeva NA, Talaeva SG, et al. Functional heterogeneity of circulating T regulatory cell subsets in breast cancer patients. Breast Cancer. 2018; 25(6):687-97. doi:10.1007/s12282-018-0874-4
152. Rech AJ, Mick R, Kaplan DE, Chang K-M, Domchek SM, Vonderheide RH. Homeostasis of peripheral FoxP3+ CD4+ regulatory T cells in patients with early and late stage breast cancer. Cancer Immunol. Immunother. 2010; 59(4):599-607. doi:10.1007/s00262-009-0780-x
153. Zahran AM, El-Badawy O, Kamel LM, Rayan A, Rezk K, Abdel-Rahim MH. Accumulation of Regulatory T Cells in Triple Negative Breast Cancer Can Boost Immune Disruption. Cancer Manag. Res. 2021; 13(null):6019-29. doi:10.2147/CMAR.S285128
154. Horlock C, Stott B, Dyson PJ, Morishita M, Coombes RC, Savage P, et al. The effects of trastuzumab on the CD4+CD25+FoxP3+ and CD4+IL17A+ T-cell axis in patients with breast cancer. Br. J. Cancer. 2009; 100(7):1061-7. doi:10.1038/sj.bjc.6604963
155. Timperi E, Barnaba V. CD39 Regulation and Functions in T Cells. Int. J. Mol. Sci. 2021; 22(15):8068.
156. Mandapathil M, Lang S, Gorelik E, Whiteside TL. Isolation of functional human regulatory T cells (Treg) from the peripheral blood based on the CD39 expression. J. Immunol. Methods. 2009; 346(1):55-63. doi:https://doi.org/10.1016/j.jim.2009.05.004
157. Martins I, Tesniere A, Kepp O, Michaud M, Schlemmer F, Senovilla L, et al. Chemotherapy induces ATP release from tumor cells. Cell Cycle. 2009; 8(22):3723-8. doi:10.4161/cc.8.22.10026
158. Boyd-Tressler A, Penuela S, Laird DW, Dubyak GR. Chemotherapeutic drugs induce ATP release via caspase-gated pannexin-1 channels and a caspase/pannexin-1-independent mechanism. J. Biol. Chem. 2014; 289(39):27246-63. doi:10.1074/jbc.M114.590240
159. Sun X, Wu Y, Gao W, Enjyoji K, Csizmadia E, Müller CE, et al. CD39/ENTPD1 Expression by CD4+Foxp3+ Regulatory T Cells Promotes Hepatic Metastatic Tumor Growth in Mice. Gastroenterology. 2010; 139(3):1030-40. doi:https://doi.org/10.1053/j.gastro.2010.05.007

160. Li M, Xu J, Jiang C, Zhang J, Sun T. Predictive and Prognostic Role of Peripheral Blood T-Cell Subsets in Triple-Negative Breast Cancer. Front. Oncol. 2022; 12:842705. doi:10.3389/fonc.2022.842705
161. Oshi M, Asaoka M, Tokumaru Y, Angarita FA, Yan L, Matsuyama R, et al. Abundance of Regulatory T Cell (Treg) as a Predictive Biomarker for Neoadjuvant Chemotherapy in Triple-Negative Breast Cancer. Cancers (Basel). 2020; 12(10) doi:10.3390/cancers12103038
162. Jørgensen N, Lænkholm A-V, Sækmose SG, Hansen LB, Hviid TVF. Peripheral blood immune markers in breast cancer: Differences in regulatory T cell abundance are related to clinical parameters. Clin. Immunol. 2021; 232:108847. doi:https://doi.org/10.1016/j.clim.2021.108847
163. Audia S, Nicolas A, Cathelin D, Larmonier N, Ferrand C, Foucher P, et al. Increase of CD4+CD25+ regulatory T cells in the peripheral blood of patients with metastatic carcinoma: a Phase I clinical trial using cyclophosphamide and immunotherapy to eliminate CD4+CD25+ T lymphocytes. Clin. Exp. Immunol. 2007; 150(3):523-30. doi:10.1111/j.1365-2249.2007.03521.x
164. Zhang L, Dermawan K, Jin M, Liu R, Zheng H, Xu L, et al. Differential impairment of regulatory T cells rather than effector T cells by paclitaxel-based chemotherapy. Clin. Immunol. 2008; 129(2):219-29. doi:https://doi.org/10.1016/j.clim.2008.07.013
165. Pircher A, Gamerith G, Amann A, Reinold S, Popper H, Gächter A, et al. Neoadjuvant chemo-immunotherapy modifies CD4+CD25+ regulatory T cells (Treg) in non-small cell lung cancer (NSCLC) patients. Lung Cancer. 2014; 85(1):81-7. doi:https://doi.org/10.1016/j.lungcan.2014.04.001
166. McCoy MJ, Lake RA, van der Most RG, Dick IM, Nowak AK. Post-chemotherapy T-cell recovery is a marker of improved survival in patients with advanced thoracic malignancies. Br. J. Cancer. 2012; 107(7):1107-15. doi:10.1038/bjc.2012.362
167. Zhang L, Wang XI, Ding J, Sun Q, Zhang S. The predictive and prognostic value of Foxp3+/CD25+ regulatory T cells and PD-L1 expression in triple negative breast cancer. Ann. Diagn. Pathol. 2019; 40:143-51. doi:https://doi.org/10.1016/j.anndiagpath.2019.04.004
168. Tanaka A, Sakaguchi S. Regulatory T cells in cancer immunotherapy. Cell Res. 2017; 27(1):109-18. doi:10.1038/cr.2016.151
169. Ihara F, Sakurai D, Horinaka A, Makita Y, Fujikawa A, Sakurai T, et al. CD45RA(-)Foxp3(high) regulatory T cells have a negative impact on the clinical outcome of head and neck squamous cell carcinoma. Cancer Immunol. Immunother. 2017; 66(10):1275-85. doi:10.1007/s00262-017-2021-z
170. Ward-Hartstonge KA, Kemp RA. Regulatory T-cell heterogeneity and the cancer immune response. Clin Transl Immunology. 2017; 6(9):e154. doi:10.1038/cti.2017.43
171. Cai XY, Wang XF, Li J, Dong JN, Liu JQ, Li NP, et al. High expression of CD39 in gastric cancer reduces patient outcome following radical resection. Oncol. Lett. 2016; 12(5):4080-6. doi:10.3892/ol.2016.5189
172. Szeponik L, Ahlmanner F, Sundström P, Rodin W, Gustavsson B, Bexe Lindskog E, et al. Intratumoral regulatory T cells from colon cancer patients comprise several activated effector populations. BMC Immunol. 2021; 22(1):58. doi:10.1186/s12865-021-00449-1
173. Huang H, Xu R, Lin F, Bao C, Wang S, Ji C, et al. High circulating CD39+ regulatory T cells predict poor survival for sepsis patients. Int. J. Infect. Dis. 2015; 30:57-63. doi:https://doi.org/10.1016/j.ijid.2014.11.006
174. Maoxi L, Haiyi L. Impact on CD4+ CD25High-CD127low regulatory T (Treg) cells of neoadjuvant therapy for rectal cancer patients. Indian J. Pathol. Microbiol. 2024; 67(1):10-4. doi:10.4103/ijpm.ijpm_433_22

175. MAEDA K, HAZAMA S, TOKUNO K, KAN S, MAEDA Y, WATANABE Y, et al. Impact of Chemotherapy for Colorectal Cancer on Regulatory T-Cells and Tumor Immunity. Anticancer Res. 2011; 31(12):4569-74.
176. Verma C, Eremin JM, Robins A, Bennett AJ, Cowley GP, El-Sheemy MA, et al. Abnormal T regulatory cells (Tregs: FOXP3+, CTLA-4+), myeloid-derived suppressor cells (MDSCs: monocytic, granulocytic) and polarised T helper cell profiles (Th1, Th2, Th17) in women with large and locally advanced breast cancers undergoing neoadjuvant chemotherapy (NAC) and surgery: failure of abolition of abnormal treg profile with treatment and correlation of treg levels with pathological response to NAC. J. Transl. Med. 2013; 11(1):16. doi:10.1186/1479-5876-11-16
177. Simonetta F, Chiali A, Cordier C, Urrutia A, Girault I, Bloquet S, et al. Increased CD127 expression on activated FOXP3+CD4+ regulatory T cells. Eur. J. Immunol. 2010; 40(9):2528-38. doi:10.1002/eji.201040531
178. Muto S, Owada Y, Inoue T, Watanabe Y, Yamaura T, Fukuhara M, et al. Clinical significance of expanded Foxp3+ Helios- regulatory T cells in patients with non-small cell lung cancer. Int. J. Oncol. 2015; 47(6):2082-90. doi:10.3892/ijo.2015.3196
179. Elkord E, Sharma S, Burt DJ, Hawkins RE. Expanded subpopulation of FoxP3+ T regulatory cells in renal cell carcinoma co-express Helios, indicating they could be derived from natural but not induced Tregs. Clin. Immunol. 2011; 140(3):218-22. doi:https://doi.org/10.1016/j.clim.2011.04.014
180. Liu M-F, Jin C, Wu T, Chen E-H, Lu M, Qin H-L. Helios serves as a suppression marker to reduce regulatory T cell function in pancreatic cancer patients. Immunol. Res. 2021; 69(3):275-84. doi:10.1007/s12026-021-09200-9
181. Kim H-J, Barnitz RA, Kreslavsky T, Brown FD, Moffett H, Lemieux ME, et al. Stable inhibitory activity of regulatory T cells requires the transcription factor Helios. Science. 2015; 350(6258):334-9. doi:doi:10.1126/science.aad0616
182. Sebastian M, Lopez-Ocasio M, Metidji A, Rieder SA, Shevach EM, Thornton AM. Helios Controls a Limited Subset of Regulatory T Cell Functions. The Journal of Immunology. 2016; 196(1):144-55. doi:10.4049/jimmunol.1501704
183. Yu W-q, Ji N-f, Gu C-j, Wang Y-l, Huang M, Zhang M-s. Coexpression of Helios in Foxp3+ Regulatory T Cells and Its Role in Human Disease. Dis. Markers. 2021; 2021(1):5574472. doi:https://doi.org/10.1155/2021/5574472
184. Su J, Song Y, Zhu Z, Huang X, Fan J, Qiao J, et al. Cell–cell communication: new insights and clinical implications. Signal Transduction and Targeted Therapy. 2024; 9(1):196. doi:10.1038/s41392-024-01888-z
185. Aziz N. Measurement of Circulating Cytokines and Immune-Activation Markers by Multiplex Technology in the Clinical Setting: What Are We Really Measuring? For. Immunopathol. Dis. Therap. 2015; 6(1-2):19-22. doi:10.1615/ForumImmunDisTher.2015014162
186. Liu G, Jiang C, Lin X, Yang Y. Point-of-care detection of cytokines in cytokine storm management and beyond: Significance and challenges. VIEW. 2021; 2(4):20210003. doi:https://doi.org/10.1002/VIW.20210003
187. Sprague AH, Khalil RA. Inflammatory cytokines in vascular dysfunction and vascular disease. Biochem. Pharmacol. 2009; 78(6):539-52. doi:10.1016/j.bcp.2009.04.029
188. Tanaka T, Narazaki M, Kishimoto T. IL-6 in inflammation, immunity, and disease. Cold Spring Harb. Perspect. Biol. 2014; 6(10):a016295. doi:10.1101/cshperspect.a016295
189. Manore SG, Doheny DL, Wong GL, Lo H-W. IL-6/JAK/STAT3 Signaling in Breast Cancer Metastasis: Biology and Treatment. Front. Oncol. 2022; 12 doi:10.3389/fonc.2022.866014

190. Kozłowski L, Zakrzewska I, Tokajuk P, Wojtukiewicz MZ. Concentration of interleukin-6 (IL-6), interleukin-8 (IL-8) and interleukin-10 (IL-10) in blood serum of breast cancer patients. Rocz. Akad. Med. Bialymst. 2003; 48:82-4.
191. Kumari N, Dwarakanath BS, Das A, Bhatt AN. Role of interleukin-6 in cancer progression and therapeutic resistance. Tumour Biol. 2016; 37(9):11553-72. doi:10.1007/s13277-016-5098-7
192. Habanjar O, Bingula R, Decombat C, Diab-Assaf M, Caldefie-Chezet F, Delort L. Crosstalk of Inflammatory Cytokines within the Breast Tumor Microenvironment. Int. J. Mol. Sci. 2023; 24(4):4002.
193. Fousek K, Horn LA, Palena C. Interleukin-8: A chemokine at the intersection of cancer plasticity, angiogenesis, and immune suppression. Pharmacol. Ther. 2021; 219:107692. doi:10.1016/j.pharmthera.2020.107692
194. Bendre MS, Montague DC, Peery T, Akel NS, Gaddy D, Suva LJ. Interleukin-8 stimulation of osteoclastogenesis and bone resorption is a mechanism for the increased osteolysis of metastatic bone disease. Bone. 2003; 33(1):28-37. doi:10.1016/s8756-3282(03)00086-3
195. Hartman ZC, Poage GM, den Hollander P, Tsimelzon A, Hill J, Panupinthu N, et al. Growth of Triple-Negative Breast Cancer Cells Relies upon Coordinate Autocrine Expression of the Proinflammatory Cytokines IL-6 and IL-8. Cancer Res. 2013; 73(11):3470-80. doi:10.1158/0008-5472.Can-12-4524-t
196. Chang CM, Lam HYP, Hsu HJ, Jiang SJ. Interleukin-10: A double-edged sword in breast cancer. Tzu Chi Med J. 2021; 33(3):203-11. doi:10.4103/tcmj.tcmj_162_20
197. Morris RM, Mortimer TO, O'Neill KL. Cytokines: Can Cancer Get the Message? Cancers (Basel). 2022; 14(9):2178.
198. Kartikasari AER, Huertas CS, Mitchell A, Plebanski M. Tumor-Induced Inflammatory Cytokines and the Emerging Diagnostic Devices for Cancer Detection and Prognosis. Front. Oncol. 2021; 11 doi:10.3389/fonc.2021.692142
199. Stenken JA, Poschenrieder AJ. Bioanalytical chemistry of cytokines – A review. Anal. Chim. Acta. 2015; 853:95-115. doi:https://doi.org/10.1016/j.aca.2014.10.009
200. Stone WL, Leavitt L, Varacallo M. Physiology, Growth Factor. StatPearls. Treasure Island (FL): StatPearls Publishing

201. Mansour MA, Caputo VS, Aleem E. Highlights on selected growth factors and their receptors as promising anticancer drug targets. The International Journal of Biochemistry & Cell Biology. 2021; 140:106087. doi:https://doi.org/10.1016/j.biocel.2021.106087
202. Lapeyre-Prost A, Terme M, Pernot S, Pointet AL, Voron T, Tartour E, et al. Chapter Seven - Immunomodulatory Activity of VEGF in Cancer. In: Galluzzi L, editor. Int. Rev. Cell Mol. Biol.: Academic Press; 2017. p. 295-342.
203. Adams J, Carder PJ, Downey S, Forbes MA, MacLennan K, Allgar V, et al. Vascular endothelial growth factor (VEGF) in breast cancer: comparison of plasma, serum, and tissue VEGF and microvessel density and effects of tamoxifen. Cancer Res. 2000; 60(11):2898-905.
204. Liu Y, Tamimi RM, Collins LC, Schnitt SJ, Gilmore HL, Connolly JL, et al. The association between vascular endothelial growth factor expression in invasive breast cancer and survival varies with intrinsic subtypes and use of adjuvant systemic therapy: results from the Nurses' Health Study. Breast Cancer Res. Treat. 2011; 129(1):175-84. doi:10.1007/s10549-011-1432-3
205. Siddiqui JA, Pothuraju R, Khan P, Sharma G, Muniyan S, Seshacharyulu P, et al. Pathophysiological role of growth differentiation factor 15 (GDF15) in obesity, cancer, and

cachexia. Cytokine Growth Factor Rev. 2022; 64:71-83. doi:https://doi.org/10.1016/j.cytogfr.2021.11.002
206. Wischhusen J, Melero I, Fridman WH. Growth/Differentiation Factor-15 (GDF-15): From Biomarker to Novel Targetable Immune Checkpoint. Front. Immunol. 2020; 11 doi:10.3389/fimmu.2020.00951
207. Spanopoulou A, Gkretsi V. Growth differentiation factor 15 (GDF15) in cancer cell metastasis: from the cells to the patients. Clin. Exp. Metastasis. 2020; 37(4):451-64. doi:10.1007/s10585-020-10041-3
208. He Y, Zhang X, Zhang Y, Luo W, Zhu Z, Song K, et al. Growth differentiation factor 15 is required for triple-negative breast cancer cell growth and chemoresistance. Anticancer Drugs. 2023; 34(3):351-60. doi:10.1097/cad.0000000000001434
209. Kumar A, Taghi Khani A, Sanchez Ortiz A, Swaminathan S. GM-CSF: A Double-Edged Sword in Cancer Immunotherapy. Front. Immunol. 2022; 13 doi:10.3389/fimmu.2022.901277
210. Lee KMC, Achuthan AA, Hamilton JA. GM-CSF: A Promising Target in Inflammation and Autoimmunity. Immunotargets Ther. 2020; 9:225-40. doi:10.2147/itt.S262566
211. Su X, Xu Y, Fox GC, Xiang J, Kwakwa KA, Davis JL, et al. Breast cancer–derived GM-CSF regulates arginase 1 in myeloid cells to promote an immunosuppressive microenvironment. The Journal of Clinical Investigation. 2021; 131(20) doi:10.1172/JCI145296
212. Liu M, Guo S, Stiles JK. The emerging role of CXCL10 in cancer (Review). Oncol. Lett. 2011; 2(4):583-9. doi:10.3892/ol.2011.300
213. Chuan T, Li T, Yi C. Identification of CXCR4 and CXCL10 as Potential Predictive Biomarkers in Triple Negative Breast Cancer (TNBC). Med. Sci. Monit. 2020; 26:e918281. doi:10.12659/msm.918281
214. Liu M, Guo S, Hibbert JM, Jain V, Singh N, Wilson NO, et al. CXCL10/IP-10 in infectious diseases pathogenesis and potential therapeutic implications. Cytokine Growth Factor Rev. 2011; 22(3):121-30. doi:10.1016/j.cytogfr.2011.06.001
215. Ejaeidi AA, Craft BS, Puneky LV, Lewis RE, Cruse JM. Hormone receptor-independent CXCL10 production is associated with the regulation of cellular factors linked to breast cancer progression and metastasis. Exp. Mol. Pathol. 2015; 99(1):163-72. doi:https://doi.org/10.1016/j.yexmp.2015.06.002
216. Merendino RA, Arena A, Capozza AB, Chillemi S, Mesiti M. Serum levels of interleukin-10 in patients affected by breast cancer. Immunol. Lett. 1996; 53(1):59-60. doi:https://doi.org/10.1016/0165-2478(96)02598-9
217. Alves MT, Simões R, Pestana RMC, de Oliveira AN, Oliveira HHM, Soares CE, et al. Interleukin-10 Levels are Associated with Doxorubicin-Related Cardiotoxicity in Breast Cancer Patients in a One-Year Follow-Up Study. Immunol. Invest. 2022; 51(4):883-98. doi:10.1080/08820139.2021.1882486
218. Lindholm A, Abrahamsen M-L, Buch-Larsen K, Marina D, Andersson M, Helge JW, et al. Pro-inflammatory cytokines increase temporarily after adjuvant treatment for breast cancer in postmenopausal women: a longitudinal study. Breast Cancer Res. 2024; 26(1):142. doi:10.1186/s13058-024-01898-3
219. Motyka J, Gacuta E, Kicman A, Kulesza M, Ławicki P, Ławicki S. Plasma Levels of CXC Motif Chemokine 1 (CXCL1) and Chemokine 8 (CXCL8) as Diagnostic Biomarkers in Luminal A and B Breast Cancer. Journal of Clinical Medicine. 2022; 11(22):6694.
220. Tan C, Hu W, He Y, Zhang Y, Zhang G, Xu Y, et al. Cytokine-mediated therapeutic resistance in breast cancer. Cytokine. 2018; 108:151-9. doi:https://doi.org/10.1016/j.cyto.2018.03.020

221. Adela R, Banerjee SK. GDF-15 as a Target and Biomarker for Diabetes and Cardiovascular Diseases: A Translational Prospective. J Diabetes Res. 2015; 2015:490842. doi:10.1155/2015/490842
222. Salkeni MA, Naing A. Interleukin-10 in cancer immunotherapy: from bench to bedside. Trends Cancer. 2023; 9(9):716-25. doi:10.1016/j.trecan.2023.05.003
223. Bower JE, Ganz PA, Irwin MR, Cole SW, Carroll J, Kuhlman KR, et al. Acute and Chronic Effects of Adjuvant Therapy on Inflammatory Markers in Breast Cancer Patients. JNCI Cancer Spectrum. 2022; 6(4) doi:10.1093/jncics/pkac052
224. Vyas D, Laput G, Vyas AK. Chemotherapy-enhanced inflammation may lead to the failure of therapy and metastasis. Onco Targets Ther. 2014; 7:1015-23. doi:10.2147/ott.S60114
225. Inc. EB. Elabscience® Human IL-10 (Interleukin 10) ELISA kit. Product information booklet: 2024.
226. Inc. EB. Elabscience® Human IL-6 (Interleukin-6) ELISA kit.
227. Foldi J, Blenman KRM, Marczyk M, Gunasekharan V, Polanska A, Gee R, et al. Peripheral blood immune parameters, response, and adverse events after neoadjuvant chemotherapy plus durvalumab in early-stage triple-negative breast cancer. Breast Cancer Res. Treat. 2024; 208(2):369-77. doi:10.1007/s10549-024-07426-3
228. Hamidullah, Changkija B, Konwar R. Role of interleukin-10 in breast cancer. Breast Cancer Res. Treat. 2012; 133(1):11-21. doi:10.1007/s10549-011-1855-x
229. Salgado R, Junius S, Benoy I, Van Dam P, Vermeulen P, Van Marck E, et al. Circulating interleukin-6 predicts survival in patients with metastatic breast cancer. Int. J. Cancer. 2003; 103(5):642-6. doi:https://doi.org/10.1002/ijc.10833
230. Dethlefsen C, Højfeldt G, Hojman P. The role of intratumoral and systemic IL-6 in breast cancer. Breast Cancer Res. Treat. 2013; 138(3):657-64. doi:10.1007/s10549-013-2488-z
231. Gunnarsdottir FB, Bendahl P-O, Johansson A, Benfeitas R, Rydén L, Bergenfelz C, et al. Serum immuno-oncology markers carry independent prognostic information in patients with newly diagnosed metastatic breast cancer, from a prospective observational study. Breast Cancer Res. 2023; 25(1):29. doi:10.1186/s13058-023-01631-6
232. Narita D, Seclaman E, Anghel A, Ilina R, Cireap N, Negru S, et al. Altered levels of plasma chemokines in breast cancer and their association with clinical and pathological characteristics. Neoplasma. 2016; 63(1):141-9. doi:10.4149/neo_2016_017
233. Lee MH, Laajala E, Kreutzman A, Järvinen P, Nísen H, Mirtti T, et al. The tumor and plasma cytokine profiles of renal cell carcinoma patients. Sci. Rep. 2022; 12(1):13416. doi:10.1038/s41598-022-17592-3
234. Jafarzadeh A, Fooladseresht H, Nemati M, Assadollahi Z, Sheikhi A, Ghaderi A. Higher circulating levels of chemokine CXCL10 in patients with breast cancer: Evaluation of the influences of tumor stage and chemokine gene polymorphism. Cancer Biomark. 2016; 16:545-54. doi:10.3233/CBM-160596
235. Khalaf AF, Al-naqqash MA, Alawn NA, Ad'hiah AH. Biomarker significance of serum CXCL8, CXCL10 and CXCL16 in breast tumors of Iraqi patients. Baghdad Science Journal. 2020; 17(1 (Suppl.)):0199-.
236. Youssry SA, Hussein AE, El-Sheredy AG, Ramadan R, El-Sheredy HG. Clinical Relevance of LC3B, CXCL10, and Bcl-2 in Breast Cancer. Jordan Journal of Biological Sciences. 2019; 12(4)
237. Kim M, Choi HY, Woo JW, Chung YR, Park SY. Role of CXCL10 in the progression of in situ to invasive carcinoma of the breast. Sci. Rep. 2021; 11(1):18007. doi:10.1038/s41598-021-97390-5

238. Liu H, Yang Z, Lu W, Chen Z, Chen L, Han S, et al. Chemokines and chemokine receptors: A new strategy for breast cancer therapy. Cancer Medicine. 2020; 9(11):3786-99. doi:https://doi.org/10.1002/cam4.3014
239. Clark AM, Heusey HL, Griffith LG, Lauffenburger DA, Wells A. IP-10 (CXCL10) Can Trigger Emergence of Dormant Breast Cancer Cells in a Metastatic Liver Microenvironment. Front. Oncol. 2021; 11 doi:10.3389/fonc.2021.676135
240. Espinoza JA, Jabeen S, Batra R, Papaleo E, Haakensen V, Timmermans Wielenga V, et al. Cytokine profiling of tumor interstitial fluid of the breast and its relationship with lymphocyte infiltration and clinicopathological characteristics. Oncoimmunology. 2016; 5(12):e1248015. doi:10.1080/2162402x.2016.1248015
241. Wu X, Sun A, Yu W, Hong C, Liu Z. CXCL10 mediates breast cancer tamoxifen resistance and promotes estrogen-dependent and independent proliferation. Mol. Cell. Endocrinol. 2020; 512:110866. doi:https://doi.org/10.1016/j.mce.2020.110866
242. Jabeen S, Espinoza JA, Torland LA, Zucknick M, Kumar S, Haakensen VD, et al. Noninvasive profiling of serum cytokines in breast cancer patients and clinicopathological characteristics. Oncoimmunology. 2019; 8(2):e1537691. doi:10.1080/2162402X.2018.1537691
243. Stathopoulos J, Armakolas A, Gomatos IP. Plasma VEGF levels in breast cancer patients with and without metastases. Oncol. Lett. 2010; 1(4):739-41. doi:10.3892/ol_00000129
244. Xin L, Zhiyuan X. Evaluating serum level of granulocyte, macrophage and granulocyte-macrophage colony-stimulating factors in patients with breast tumor: Serum level of G-CSF, M-CSF, and GM-CSF in breast tumor. Cell. Mol. Biol. 2022; 68(5):146-52. doi:10.14715/cmb/2022.68.5.20
245. Belgore FM, Lip GYH, Bareford D, Wadley M, Stonelake P, Blann AD. Plasma levels of vascular endothelial growth factor (VEGF) and its receptor, flt-1, in haematological cancers: A comparison with breast cancer. Am. J. Hematol. 2001; 66(1):59-61. doi:https://doi.org/10.1002/1096-8652(200101)66:1<59::AID-AJH1011>3.0.CO;2-Z
246. Caine GJ, Stonelake PS, Lip GYH, Blann AD. Changes in plasma vascular endothelial growth factor, angiopoietins, and their receptors following surgery for breast cancer. Cancer Lett. 2007; 248(1):131-6. doi:https://doi.org/10.1016/j.canlet.2006.06.011
247. Coşkun U, Günel N, Sancak B, Günel U, Onuk E, Bayram O, et al. Significance of serum vascular endothelial growth factor, insulin-like growth factor-I levels and nitric oxide activity in breast cancer patients. The Breast. 2003; 12(2):104-10. doi:https://doi.org/10.1016/S0960-9776(02)00214-X
248. Wu Y, Saldana L, Chillar R, Vadgama JV. Plasma vascular endothelial growth factor is useful in assessing progression of breast cancer post surgery and during adjuvant treatment. Int. J. Oncol. 2002; 20(3):509-16. doi:10.3892/ijo.20.3.509
249. Nishimura R, Nagao K, Miyayama H, Matsuda M, Baba K-i, Yamashita H, et al. Higher plasma vascular endothelial growth factor levels correlate with menopause, overexpression of p53, and recurrence of breast cancer. Breast Cancer. 2003; 10(2):120-8. doi:10.1007/BF02967636
250. KÜMmel S, Eggemann H, LÜFtner D, Thomas A, Jeschke S, Zerfel N, et al. Changes in the Circulating Plasma Levels of VEGF and VEGF-D after Adjuvant Chemotherapy in Patients with Breast Cancer and 1 to 3 Positive Lymph Nodes. Anticancer Res. 2006; 26(2C):1719.
251. Wild R, Dings RP, Subramanian I, Ramakrishnan S. Carboplatin selectively induces the VEGF stress response in endothelial cells: Potentiation of antitumor activity by combination treatment with antibody to VEGF. Int. J. Cancer. 2004; 110(3):343-51. doi:10.1002/ijc.20100

252. Tsavaris N, Kosmas C, Vadiaka M, Kanelopoulos P, Boulamatsis D. Immune changes in patients with advanced breast cancer undergoing chemotherapy with taxanes. Br. J. Cancer. 2002; 87(1):21-7. doi:10.1038/sj.bjc.6600347
253. Ławicki S, Czygier M, Wojtukiewicz M, Szmitkowski M. [The plasma levels and diagnostic utility of granulocyte-colony stimulating factor (G-CSF) and granulocyte-macrophage - colony stimulating factor (GM-CSF) in patients with I and II stage of breast cancer]. Przegl. Lek. 2009; 66(7):365-9.
254. Czygier M, Lawicki S, Szmitkowski M. [Plasma granulocyte-macrophage colony stimulating factor (GM-CSF) and activity of enzymes in granulocytes of breast cancer patients]. Przegl. Lek. 2006; 63:654-7.
255. Khajah M, Millen B, Cara DC, Waterhouse C, McCafferty DM. Granulocyte-macrophage colony-stimulating factor (GM-CSF): a chemoattractive agent for murine leukocytes in vivo. J. Leukoc. Biol. 2011; 89(6):945-53. doi:10.1189/jlb.0809546
256. Mouchemore KA, Anderson RL. Immunomodulatory effects of G-CSF in cancer: Therapeutic implications. Semin. Immunol. 2021; 54:101512. doi:https://doi.org/10.1016/j.smim.2021.101512
257. Linderholm B, Grankvist K, Wilking N, Johansson M, Tavelin B, Henriksson R. Correlation of Vascular Endothelial Growth Factor Content With Recurrences, Survival, and First Relapse Site in Primary Node-Positive Breast Carcinoma After Adjuvant Treatment. J. Clin. Oncol. 2000; 18(7):1423-31. doi:10.1200/jco.2000.18.7.1423
258. Hong I-S. Stimulatory versus suppressive effects of GM-CSF on tumor progression in multiple cancer types. Exp. Mol. Med. 2016; 48(7):e242-e. doi:10.1038/emm.2016.64
259. Staff AC, Trovik J, Zahl EAG, Wik E, Wollert KC, Kempf T, et al. Elevated Plasma Growth Differentiation Factor-15 Correlates with Lymph Node Metastases and Poor Survival in Endometrial Cancer. Clin. Cancer Res. 2011; 17(14):4825-33. doi:10.1158/1078-0432.Ccr-11-0715
260. Wang X, Li Y, Tian H, Qi J, Li M, Fu C, et al. Macrophage inhibitory cytokine 1 (MIC-1/GDF15) as a novel diagnostic serum biomarker in pancreatic ductal adenocarcinoma. BMC Cancer. 2014; 14(1):578. doi:10.1186/1471-2407-14-578
261. Wischhusen J, Melero I, Fridman WH. Growth/Differentiation Factor-15 (GDF-15): From Biomarker to Novel Targetable Immune Checkpoint. Front. Immunol. 2020; 11:951. doi:10.3389/fimmu.2020.00951
262. Altena R, Fehrmann RS, Boer H, de Vries EG, Meijer C, Gietema JA. Growth differentiation factor 15 (GDF-15) plasma levels increase during bleomycin- and cisplatin-based treatment of testicular cancer patients and relate to endothelial damage. PLoS One. 2015; 10(1):e0115372. doi:10.1371/journal.pone.0115372
263. Rapoport BL, Steel HC, Hlatshwayo N, Theron AJ, Meyer PWA, Nayler S, et al. Systemic Immune Dysregulation in Early Breast Cancer Is Associated With Decreased Plasma Levels of Both Soluble Co-Inhibitory and Co-Stimulatory Immune Checkpoint Molecules. Front. Immunol. 2022; 13 doi:10.3389/fimmu.2022.823842
264. McHenry PR, Prosperi JR. Proteins Found in the Triple-Negative Breast Cancer Secretome and Their Therapeutic Potential. Int. J. Mol. Sci. 2023; 24(3):2100.
265. Welsh JB, Sapinoso LM, Kern SG, Brown DA, Liu T, Bauskin AR, et al. Large-scale delineation of secreted protein biomarkers overexpressed in cancer tissue and serum. Proc. Natl. Acad. Sci. U. S. A. 2003; 100(6):3410-5. doi:10.1073/pnas.0530278100
266. Lodi RS, Yu B, Xia L, Liu F. Roles and Regulation of Growth differentiation factor-15 in the Immune and tumor microenvironment. Hum. Immunol. 2021; 82(12):937-44. doi:https://doi.org/10.1016/j.humimm.2021.06.007

267. Mimeault M, Batra SK. Divergent molecular mechanisms underlying the pleiotropic functions of macrophage inhibitory cytokine-1 in cancer. J. Cell. Physiol. 2010; 224(3):626-35. doi:https://doi.org/10.1002/jcp.22196
268. Bauskin AR, Brown DA, Kuffner T, Johnen H, Luo XW, Hunter M, et al. Role of Macrophage Inhibitory Cytokine-1 in Tumorigenesis and Diagnosis of Cancer. Cancer Res. 2006; 66(10):4983-6. doi:10.1158/0008-5472.Can-05-4067
269. Joshi JP, Brown NE, Griner SE, Nahta R. Growth differentiation factor 15 (GDF15)-mediated HER2 phosphorylation reduces trastuzumab sensitivity of HER2-overexpressing breast cancer cells. Biochem. Pharmacol. 2011; 82(9):1090-9. doi:https://doi.org/10.1016/j.bcp.2011.07.082
270. He Y, Qian H, Liu Y, Duan L, Li Y, Shi G. The roles of regulatory B cells in cancer. J Immunol Res. 2014; 2014:215471. doi:10.1155/2014/215471
271. Mahon KL, Sutherland SI, Lin HM, Stockler MR, Gurney H, Mallesara G, et al. Clinical validation of circulating GDF15/MIC-1 as a marker of response to docetaxel and survival in men with metastatic castration-resistant prostate cancer. The Prostate. 2024; 84(8):747-55. doi:https://doi.org/10.1002/pros.24691
272. Di Pastena F, Pond G, Tsakiridis EE, Gouveia A, Ahmadi E, Biziotis O-D, et al. Growth differentiation factor 15 (GDF15) predicts relapse free and overall survival in unresected locally advanced non-small cell lung cancer treated with chemoradiotherapy. Radiation Oncology. 2024; 19(1):155. doi:10.1186/s13014-024-02546-y
273. Zitvogel L, Apetoh L, Ghiringhelli F, Kroemer G. Immunological aspects of cancer chemotherapy. Nature Reviews Immunology. 2008; 8(1):59-73. doi:10.1038/nri2216
274. Hagert C, Sareila O, Kelkka T, Jalkanen S, Holmdahl R. The Macrophage Mannose Receptor Regulate Mannan-Induced Psoriasis, Psoriatic Arthritis, and Rheumatoid Arthritis-Like Disease Models. Front. Immunol. 2018; 9 doi:10.3389/fimmu.2018.00114
275. Zingoni A, Fionda C, Borrelli C, Cippitelli M, Santoni A, Soriani A. Natural Killer Cell Response to Chemotherapy-Stressed Cancer Cells: Role in Tumor Immunosurveillance. Front. Immunol. 2017; 8:1194. doi:10.3389/fimmu.2017.01194
276. Wang YJ, Fletcher R, Yu J, Zhang L. Immunogenic effects of chemotherapy-induced tumor cell death. Genes Dis. 2018; 5(3):194-203. doi:10.1016/j.gendis.2018.05.003
277. Mannino MH, Zhu Z, Xiao H, Bai Q, Wakefield MR, Fang Y. The paradoxical role of IL-10 in immunity and cancer. Cancer Lett. 2015; 367(2):103-7. doi:https://doi.org/10.1016/j.canlet.2015.07.009
278. Liu C, Chu D, Kalantar-Zadeh K, George J, Young HA, Liu G. Cytokines: From Clinical Significance to Quantification. Advanced Science. 2021; 8(15):2004433. doi:https://doi.org/10.1002/advs.202004433
279. Duffy A, Bouchier-Hayes D, Harmey J. Vascular Endothelial Growth Factor (VEGF) and Its Role in Non-Endothelial Cells: Autocrine Signalling by VEGF. 2011. p. 133-44.
280. Stakheyeva M, Patysheva M, Kaigorodova E, Zavyalova M, Tarabanovskaya N, Choynzonov E, et al. Tumor Properties Mediate the Relationship between Peripheral Blood Monocytes and Tumor-Associated Macrophages in Breast Cancer. Cancer Invest. 2022; 40(5):442-56. doi:10.1080/07357907.2021.2016803
281. Esquivel-Velázquez M, Ostoa-Saloma P, Palacios-Arreola MI, Nava-Castro KE, Castro JI, Morales-Montor J. The role of cytokines in breast cancer development and progression. J. Interferon Cytokine Res. 2015; 35(1):1-16. doi:10.1089/jir.2014.0026
282. Want MY, Bashir Z, Najar RA. T Cell Based Immunotherapy for Cancer: Approaches and Strategies. Vaccines (Basel). 2023; 11(4) doi:10.3390/vaccines11040835

283. Wennhold K, Shimabukuro-Vornhagen A, von Bergwelt-Baildon M. B Cell-Based Cancer Immunotherapy. Transfus. Med. Hemother. 2019; 46(1):36-46. doi:10.1159/000496166
284. Shan F, Somasundaram A, Bruno TC, Workman CJ, Vignali DAA. Therapeutic targeting of regulatory T cells in cancer. Trends Cancer. 2022; 8(11):944-61. doi:10.1016/j.trecan.2022.06.008
285. Felcher CM, Bogni ES, Kordon EC. IL-6 Cytokine Family: A Putative Target for Breast Cancer Prevention and Treatment. Int. J. Mol. Sci. 2022; 23(3) doi:10.3390/ijms23031809
286. Lim RJ, Salehi-Rad R, Tran LM, Oh MS, Dumitras C, Crosson WP, et al. CXCL9/10-engineered dendritic cells promote T cell activation and enhance immune checkpoint blockade for lung cancer. Cell Reports Medicine. 2024; 5(4) doi:10.1016/j.xcrm.2024.101479
287. Arenberg DA, White ES, Burdick MD, Strom SR, Strieter RM. Improved survival in tumor-bearing SCID mice treated with interferon-γ-inducible protein 10 (IP-10/CXCL10). Cancer Immunol. Immunother. 2001; 50(10):533-8. doi:10.1007/s00262-001-0231-9
288. Bercovici N, Duffour MT, Agrawal S, Salcedo M, Abastado JP. New methods for assessing T-cell responses. Clin. Diagn. Lab. Immunol. 2000; 7(6):859-64. doi:10.1128/cdli.7.6.859-864.2000
289. Kouwenhoven M, Ozenci V, Teleshova N, Hussein Y, Huang YM, Eusebio A, et al. Enzyme-linked immunospot assays provide a sensitive tool for detection of cytokine secretion by monocytes. Clin. Diagn. Lab. Immunol. 2001; 8(6):1248-57. doi:10.1128/cdli.8.6.1248-1257.2001
290. Somanchi SS, McCulley KJ, Somanchi A, Chan LL, Lee DA. A Novel Method for Assessment of Natural Killer Cell Cytotoxicity Using Image Cytometry. PLoS One. 2015; 10(10):e0141074. doi:10.1371/journal.pone.0141074

Appendices

Appendix A: Appendices for Chapter 1

Figure 1: Licence details for the use of the illustrations shown in Figure 1.4 and 1.5

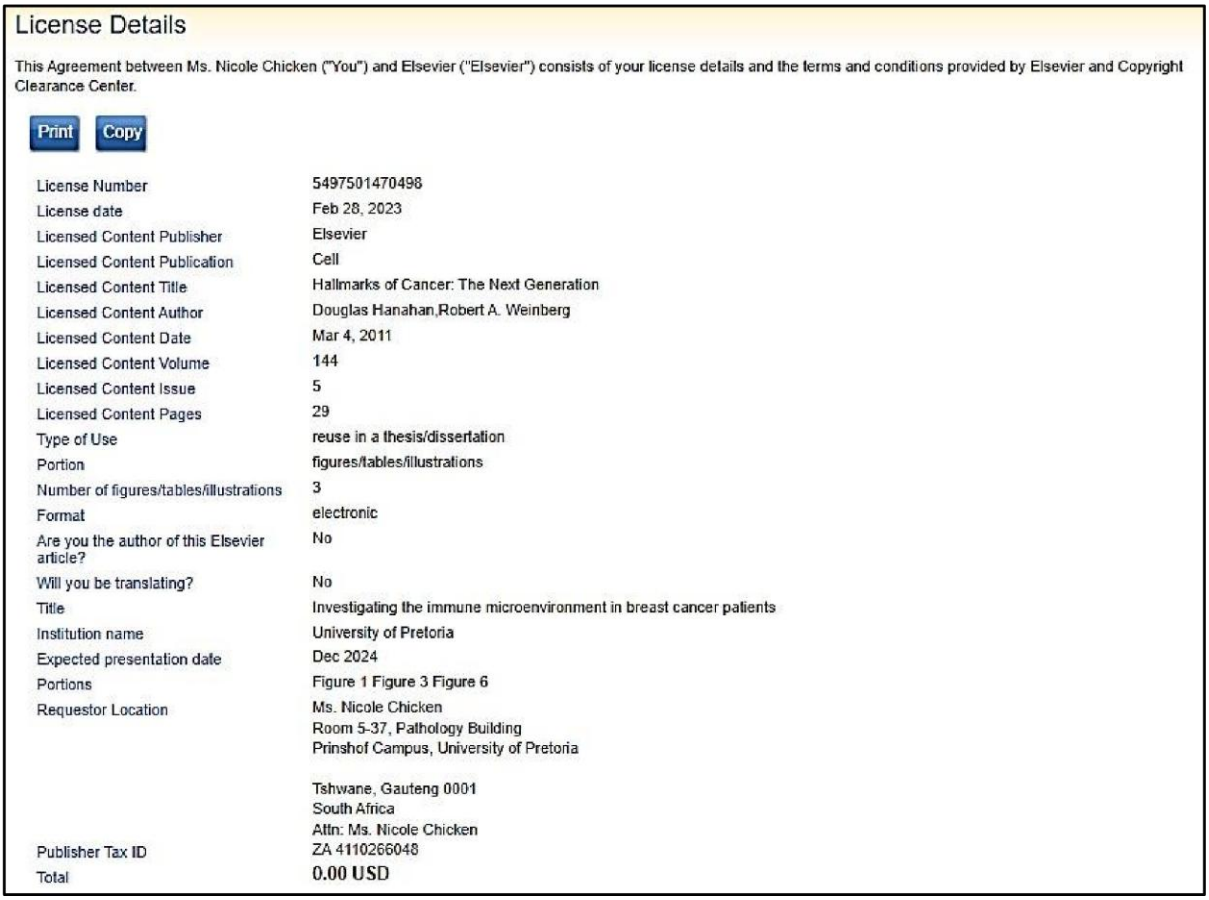

License Details

This Agreement between Ms. Nicole Chicken ("You") and Elsevier ("Elsevier") consists of your license details and the terms and conditions provided by Elsevier and Copyright Clearance Center.

Print Copy

License Number	5497501470498
License date	Feb 28, 2023
Licensed Content Publisher	Elsevier
Licensed Content Publication	Cell
Licensed Content Title	Hallmarks of Cancer: The Next Generation
Licensed Content Author	Douglas Hanahan,Robert A. Weinberg
Licensed Content Date	Mar 4, 2011
Licensed Content Volume	144
Licensed Content Issue	5
Licensed Content Pages	29
Type of Use	reuse in a thesis/dissertation
Portion	figures/tables/illustrations
Number of figures/tables/illustrations	3
Format	electronic
Are you the author of this Elsevier article?	No
Will you be translating?	No
Title	Investigating the immune microenvironment in breast cancer patients
Institution name	University of Pretoria
Expected presentation date	Dec 2024
Portions	Figure 1 Figure 3 Figure 6
Requestor Location	Ms. Nicole Chicken Room 5-37, Pathology Building Prinshof Campus, University of Pretoria Tshwane, Gauteng 0001 South Africa Attn: Ms. Nicole Chicken
Publisher Tax ID	ZA 4110266048
Total	0.00 USD

Figure 2: Licence details for the use of the illustrations shown in Figure 1.6

frontiers in Oncology

PMC full text:
Front Oncol. 2022; 12: 876451.
Published online 2022 May 13. doi: 10.3389/fonc.2022.876451

• Copyright/License Request permission to reuse

<< Prev Figure 1 Next >>

Figure 1

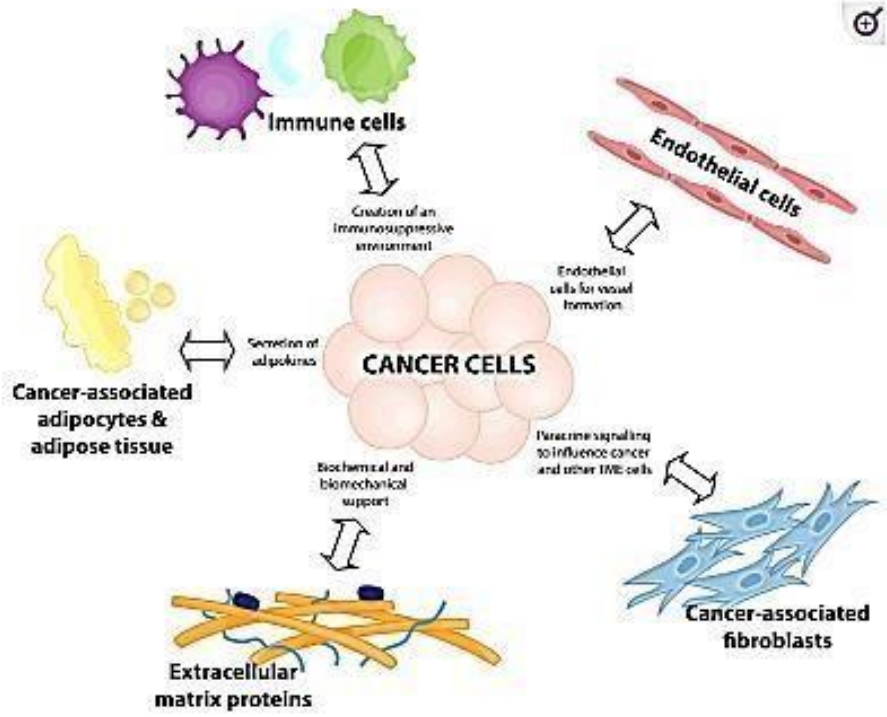

Components of a breast cancer tumor microenvironment. Breast cancer disease progression relies on a complex network of cells and interactions, termed the tumor microenvironment (TME). This consists of immune cells for the creation of an immunosuppressive environment, recruitment of endothelial cells for vessel formation, transformation of cancer-associated fibroblasts to participate in paracrine signalling to influence the cancer cells and other TME cells, release of adipokines from cancer-associated adipocytes and adipose tissue, and the biochemical and biomechanical support from extracellular matrix proteins.

Appendix B: Appendices for Chapter 2

Table 1: Inclusion and exclusion criteria for study participants

Inclusion criteria for healthy controls
Over the age of 18
No history of breast cancer
Female

Exclusion criteria for healthy controls
Under the age of 18
History of breast cancer
Male
Pregnant or breastfeeding

Inclusion criteria for breast cancer patients
Female
18 years of age or older
Patient has Eastern Cooperative Oncology Group (ECOG) Performance Status (PS) 0, 1 or 2
Histologically confirmed breast cancer
Diagnosed with clinical stage I, II, IIIa, or IIIb Breast Cancer according to the American Joint Committee on Cancer (AJCC) Breast Staging 8th Edition
Treatment naïve
Will be treated with either of the following neo-adjuvant chemotherapies: Anthracycline and Taxane based chemotherapy, platinum-based chemotherapy, or Taxotere and Cyclophosphamide-based chemotherapy

Exclusion criteria for breast cancer patients
Male
Under the age of 18
Any systemic therapy for breast cancer within the last 5 years
A history of other malignancies ≤ 5 years prior with the exception of basal cell or squamous cell carcinoma (treated with local resection only) or in situ carcinoma of the cervix
Will be treated with chemotherapeutic agents other than: Anthracycline and Taxane-based chemotherapy, platinum-based chemotherapy, or Taxotere and Cyclophosphamide-based chemotherapy
Patients with confirmed stage IV disease

Patients seropositive for the human immunodeficiency virus (HIV) and/or the Hepatitis B or C virus
Uncontrolled intercurrent illness that would limit compliance with study requirements
Patient is pregnant or breastfeeding

Figure 1: Ethical approval certificate

UNIVERSITEIT VAN PRETORIA
UNIVERSITY OF PRETORIA
YUNIBESITHI YA PRETORIA

Faculty of Health Sciences

Institution: The Research Ethics Committee, Faculty Health Sciences, University of Pretoria complies with ICH-GCP guidelines and has US Federal wide Assurance.

- FWA 00002567, Approved dd 18 March 2022 and Expires 18 March 2027.
- IORG #: IORG0001762 OMB No. 0990-0278 Approved for use through August 31, 2023.

Faculty of Health Sciences **Research Ethics Committee**

29 June 2023

Approval Certificate
New Application

Dear Miss NA Chicken

Ethics Reference No.: 302/2023
Title: Investigation of peripheral blood immune cell subsets and cytokine levels in female people living with breast cancer before and after chemotherapy

The **New Application** as supported by documents received between 2023-05-25 and 2023-06-28 for your research, was approved by the Faculty of Health Sciences Research Ethics Committee on 2023-06-28 as resolved by its quorate meeting.

Please note the following about your ethics approval:

- Ethics Approval is valid for 1 year and needs to be renewed annually by 2024-06-29.
- Please remember to use your protocol number (302/2023) on any documents or correspondence with the Research Ethics Committee regarding your research.
- Please note that the Research Ethics Committee may ask further questions, seek additional information, require further modification, monitor the conduct of your research, or suspend or withdraw ethics approval.

Ethics approval is subject to the following:

- The ethics approval is conditional on the research being conducted as stipulated by the details of all documents submitted to the Committee. In the event that a further need arises to change who the investigators are, the methods or any other aspect, such changes must be submitted as an Amendment for approval by the Committee.

We wish you the best with your research.

Yours sincerely

On behalf of the FHS REC, Professor C Kotzé
MBChB, DMH, MMed(Psych), FCPsych, Phd
Acting Chairperson: *Faculty of Health Sciences Research Ethics Committee*

The Faculty of Health Sciences Research Ethics Committee complies with the SA National Act 61 of 2003 as it pertains to health research and the United States Code of Federal Regulations Title 45 and 46. This committee abides by the ethical norms and principles for research, established by the Declaration of Helsinki, the South African Medical Research Council Guidelines as well as the Guidelines for Ethical Research: Principles Structures and Processes, Second Edition 2015 (Department of Health)

Research Ethics Committee
Room 4-60, Level 4, Tswelopele Building
University of Pretoria, Private Bag x323
Gezina 0031, South Africa
Tel +27 (0)12 356 3084
Email: deepeka.behari@up.ac.za
www.up.ac.za

Fakulteit Gesondheidswetenskappe
Lefapha la Disaense tša Maphelo

Figure 2: Protocol published online on protocols.io in January 2025

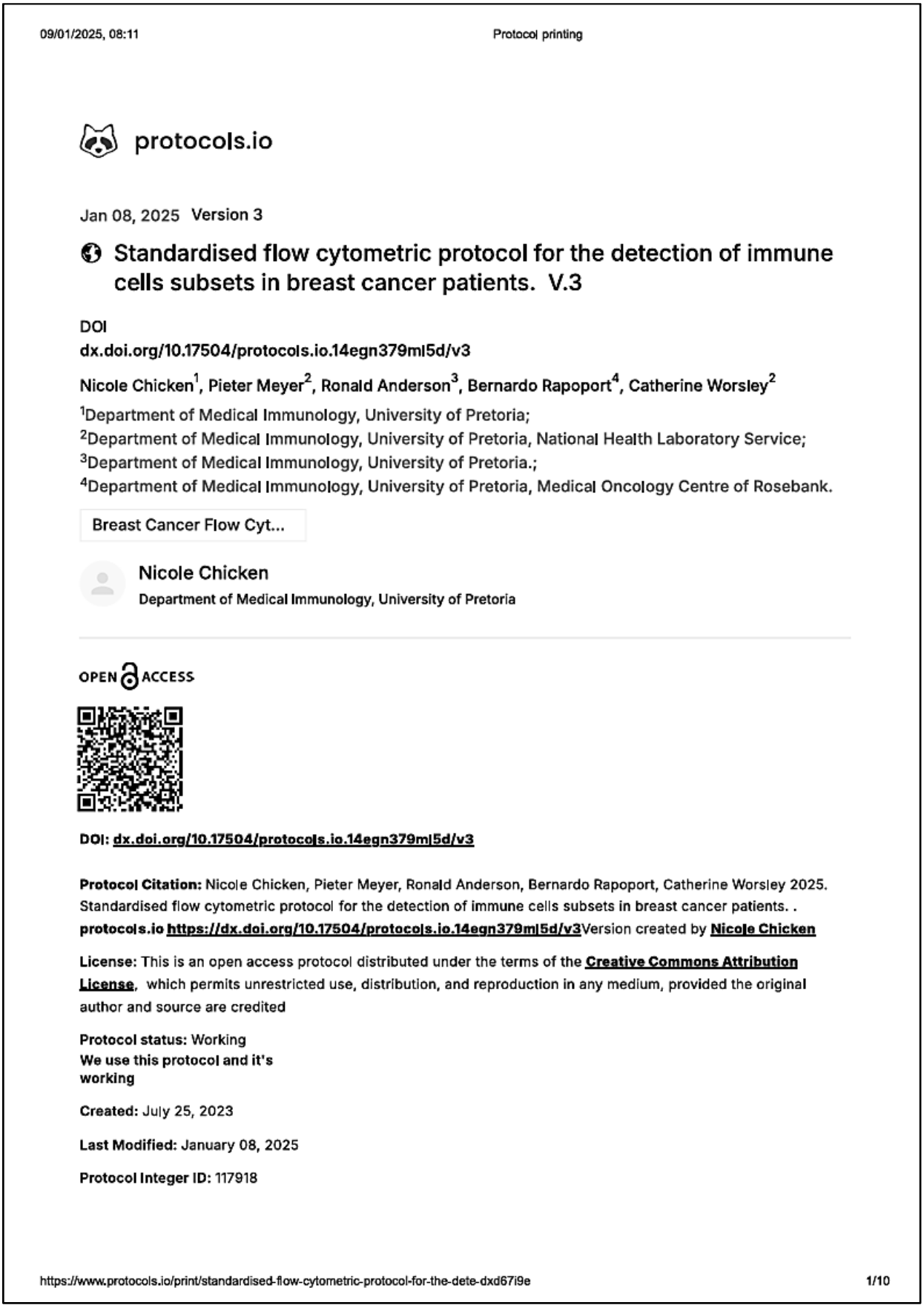

09/01/2025, 08:11 Protocol printing

protocols.io

Jan 08, 2025 Version 3

Standardised flow cytometric protocol for the detection of immune cells subsets in breast cancer patients. V.3

DOI
dx.doi.org/10.17504/protocols.io.14egn379ml5d/v3

Nicole Chicken[1], Pieter Meyer[2], Ronald Anderson[3], Bernardo Rapoport[4], Catherine Worsley[2]

[1]Department of Medical Immunology, University of Pretoria;
[2]Department of Medical Immunology, University of Pretoria, National Health Laboratory Service;
[3]Department of Medical Immunology, University of Pretoria.;
[4]Department of Medical Immunology, University of Pretoria, Medical Oncology Centre of Rosebank.

Breast Cancer Flow Cyt...

Nicole Chicken
Department of Medical Immunology, University of Pretoria

OPEN ACCESS

DOI: dx.doi.org/10.17504/protocols.io.14egn379ml5d/v3

Protocol Citation: Nicole Chicken, Pieter Meyer, Ronald Anderson, Bernardo Rapoport, Catherine Worsley 2025. Standardised flow cytometric protocol for the detection of immune cells subsets in breast cancer patients. . **protocols.io** https://dx.doi.org/10.17504/protocols.io.14egn379ml5d/v3Version created by Nicole Chicken

Protocol status: Working
We use this protocol and it's working

Created: July 25, 2023

Last Modified: January 08, 2025

Protocol Integer ID: 117918

https://www.protocols.io/print/standardised-flow-cytometric-protocol-for-the-dete-dxd67i9e 1/10

Keywords: Breast cancer, Flow cytometry, Tumour microenvironment, Tregs, Monocytes, NK cells, B-cells

Funders Acknowledgements:
National Research
Foundation Thuthuka 2023
Grant ID: TTK2203291110

Abstract

The tumour microenvironment supports tumour growth in several ways including manipulating the immune response to cancer cells. Developing accurate and reproducible assays to detect immune and characterize immune cells in cancer patients is important for understanding their impact on tumour growth and development. Multicolour flow cytometry allows for characterization of many cell populations in a single sample. In this protocol, we optimized detecting several cytotoxic and suppressive immune cell subsets that may impact on patient outcomes. In addition, this protocol can be used to monitor changes in immune cells during and after chemotherapy.

Materials

For one sample, the following is required:
1 DURAClone IM phenotyping basic kit tube (Beckman Coulter, California, USA. B53309-25 tests)
1 DURAClone IM phenotyping Treg kit tube 1 (Beckman Coulter, California, USA. B53346-25 tests)
1 DURAClone IM phenotyping Treg kit tube 2 (Beckman Coulter, California, USA. B53346-25 tests)

- 5 µL CD127-AF700 liquid antibody (BioLegend, California, USA. 351344)
- 5 µL CD206-PB liquid antibody (BioLegend, California, USA. B36119)
- 5 µL HLA-DR-BV785 liquid antibody (BioLegend, California, USA.307642)
- 30 µL Brilliant Violet stain buffer (BD Biosciences, New Jersey, USA.563794)
- 9.5 mL 1 x PBS
- 50 µL Heat-inactivated FBS (ThermoFisher Scientific, Massachusetts, USA. 16140071)
- 5 µL PerFix-nc kit buffer 1 (Beckman Coulter, California, USA. B31168)
- 400 µL PerFix-nc kit buffer 2 (Beckman Coulter, California, USA. B31168)
- 3.5 mL PerFix-nc kit buffer 3 (diluted) (Beckman Coulter, California, USA. B31168)
- 2 mL VersaLyse solution (Beckman Coulter, California, USA. A09777)

Additional requirements:
CytoFLEX Flow Cytometer (Beckman Coulter, California, USA)
CytExpert (Beckman Coulter, California, USA)
Centrifuge
Vortex
Pipettes
Clean 5 ml flow cytometry tubes
VersaComp Compensation beads (Beckman Coulter, USA)
FlowSet Pro Standardisation beads (Beckman Coulter, USA)
Ready-to-use Daily Quality Control beads (Beckman Coulter, USA)
CytoFlex Sheath Fluid (Beckman Coulter, USA)
Deionised water
FlowClean cleaning agent (Beckman Coulter, USA)
Contrad 70 cleaning solution (Beckman Coulter, USA)
FlowJo™ analysis software (Beckton Dickenson, USA)

Before start

30 minutes before running a sample, allow the following to come to room temperature:
-1x Phosphate Buffered Saline (PBS)
-Fetal Bovine Serum (FBS)
-Brilliant Violet stain buffer (BD Biosciences, New Jersey, USA)
Note:
- Samples must be centrifuged with the brake on and at room temperature.
-Samples must be incubated at room temperature.
- The reagent tubes, liquid antibodies, and other light-sensitive reagents must be kept in the dark as much as possible.

Flow cytometer start-up

1 Refill the sheath tank, empty the waste tank, and check that there is enough cleaning solution in the internal compartment of the flow cytometer.

2 Turn on the CytoFLEX flow cytometer and the PC and allow both to start up. Log in to the PC and open the CytExpert software.

3 Initiate the CytoFLEX daily start-up program and load a tube of deionised water when prompted.

Compensation set-up

4 Add two drops of positive and negative VersaComp beads into a clean 5 ml tube and to each compensation tube contained within the Basic and Treg immunophenotyping kits (Beckman Coulter, USA). If using a compensation product other than VersaComp beads, follow the product information booklet.

5 Add 10 µl of CD206, HLA-DR and CD127 liquid antibodies into separate 5 ml tubes and add two drops of the negative and positive compensation beads into each.

6 Vortex each tube and incubate in the dark for 15 minutes at room temperature (RT).

7 Add 3 ml of 1x phosphate buffered saline (PBS) and centrifuge the tubes at 500 relative centrifugal force (RCF) for 5 minutes (brake off).

8 Discard the supernatant and resuspend the pellet in 600 µl 1x PBS.

9 On the CytExpert software, select 'New Compensation' under 'File' and save. Select the channels you wish to run compensation for, select sample type and uncheck tubes not needed for the experiment. Select 'Ok'. The CytExpert software will create a list of matching empty tubes in the 'Tube' side panel as well as all required plots.

10 Load the correct unstained or single color fluorospheres as prompted and select 'Run' in the 'Acquisition' panel. Adjust the scatter gate if necessary. Use the slider scales so that the positive and negative peaks are suitably positioned, and adjust the positive and negative gates accordingly. Select 'Record'. Repeat for all tubes.

11 After running all tubes, generate the compensation matrix by selecting 'Compensation Calculation' from the toolbox or settings menu. Select 'Save As'

to export the matrix as a .comp file and to save the values to the compensation library, select 'Save to Compensation Library' . Select 'Ok' and 'Close'.

12 To save or overwrite the compensation matrix to the library, select 'Open compensation experiment' and run the compensation controls. Once completed, calculate compensation. Then save the compensation matrix to the compensation library.

13 Run a 3 minute Flow Clean cleaning solution 3 minute deionised water daily clean before proceeding.

Daily quality control

14 To run daily Quality Control (QC), make sure that the lot-specific target value file for the CytoFLEX Ready to Use Daily QC fluorophores are loaded onto the CytExpert software.

15 Open the QC/Standardisation tab and select the CytoFLEX Ready to Use Daily QC fluorophores lot number from the relevant drop-down menu. Vortex the bottle of QC fluorophores for 10 seconds before adding 10 drops into a clean 5 ml tube or 34 drops into one well of a 96-well plate. Put the tube/plate into the sample loader and initialise the instrument, then select start.

16 If the QC step fails, try re-vortexing the QC fluorphores and re-running the QC/standardisation step. If it fails again, run a daily clean, prime and re-run. If it fails again, contact Beckman Coulter.

17 Do a 3 minute FlowClean cleaning solution 3 minute deionised water Daily Clean before proceeding.

Daily standardisation

18 To set up the daily standardisation experiment, follow the instructions in your standardisation beads' product information booklet. This protocol utilises Flow-Set Pro fluorospheres from Beckman Coulter (California, USA).

19 Vortex the beads and add 10 drops into a sterile tube. Open the Standardisation tab on CytExpert, select the relevant standardisation experiment, and acquire the tube.

20 Import the results into the gain acquisition settings for the basic and Treg experiment files.

21 Plot the high voltage and/or gain values for each parameter on its respective Levey-Jennings graph.
Note: 95% of values should fall within 2 standard deviations of the high voltage and/or gain ranges for each parameter. If values move outside of this range, conduct troubleshooting.

22 Do a 3 minute FlowClean cleaning solution 3 minute deionised water Daily Clean before proceeding.

Test procedure for Treg immunophenotyping panel

23 Label a DURAClone IM Phenotyping Treg kit tube 1, and add 5 µL CD127-AF700 liquid antibody to the tube.

24 Add 50 µL whole blood to reagent tube 1, and vortex for 10 seconds. Incubate the tube in the dark for 15 minutes at room temperature (RT).

25 Add 3 mL Phosphate Buffered Saline (PBS) to reagent tube 1 and centrifuge the tube at 500 RCF for 5 minutes.

26 Discard the supernatant, and gently vortex the cell pellet for 8 seconds.

27 Resuspend the cell pellet in 50 µL 100% heat-inactivated Fetal Bovine Serum (FBS)

28 Add 5 µL PerFix-nc buffer 1 and vortex for 8 seconds. Incubate the tube in the dark for 15 minutes at RT.

29 Add 400 µL PerFix-nc buffer 2 and vortex for 8 seconds.

30 Label a DURAClone IM Phenotypic Treg kit Tube 2, and transfer the contents of reagent tube 1 into reagent tube 2 and vortex for 10 seconds.

31 Incubate the tube in the dark for 60 minutes at RT.

32 Add 3 mL PBS and incubate in the dark for 15 minutes at RT.

33 Centrifuge the tube at 500 RCF for 5 minutes. Discard the supernatant and vortex the pellet for 8 seconds.

34 Resuspend the cell pellet in 3 mL DILUTED PerFix-nc buffer 3 and centrifuge the tube at 500 RCF for 5 minutes. Discard the supernatant and vortex the pellet for 8 seconds.

35 Resuspend the pellet in 500 µL DILUTED PerFix-nc buffer 3 and acquire the results on the flow cytometer. Run a daily clean before running any DURAClone IM Phenotyping basic kit tubes.

Test procedure for basic immunophenotyping panel

36 Label a DURAClone IM Phenotyping Basic kit reagent tube, add the following, and then vortex for 8 seconds:
- 5 µL CD206-PB liquid antibody
- 5 µL HLA-DR-BV785 liquid antibody

37 Add 30 µL Brilliant Violet Stain buffer then 100 µL whole blood into the reagent tube, and vortex for 10 seconds. Incubate the tube in the dark for 15 minutes at RT.

38 Add 2 mL VersaLyse solution and vortex for 3 seconds. Incubate the tube in the dark for 15 minutes at RT.

39 Centrifuge the tube at 200 RCF for 5 minutes. Discard the supernatant, and resuspend the cell pellet in 3 mL PBS .

40 Centrifuge the tube at 200 RCF for 5 minutes, discard the supernatant, and resuspend the cell pellet in 500 µL PBS . Acquire the results on the flow cytometer.

Post-acquisition

41 Save the Flow Cytometry Standard (FCS) files onto an external storage device.

42 Run a 3 minute FlowClean cleaning solution 3 minute deionsied water and then shut down the Flow Cytometer and PC.

43 Import the FCS files into an analysis software such as FlowJo™ (Becton Dickenson, USA) and follow the gating strategies outlined in the sections below.

Gating strategy for the Treg immunophenotyping panel

44 Create a Forward Scatter height (FSC-H) vs. Forward Scatter Area (FSC-A) plot and gate singlet events (Fig. 1 A). Next, create a CD45 vs. Side Scatter (SSC) dot plot and gate the CD45+ lymphocytes (Fig. 1 B).

45 Create a CD4 vs. CD3 dot plot and gate the helper T-cells (CD3+CD4+) (Fig. 1 C).

46 Create a CD4 vs. CD25 plot, and gate the CD25+ and CD25dim helper T-cell populations (Fig. 1 D).

47 Using the gated CD25+ helper T-cells, create a FoxP3 vs. CD25 plot and gate the CD25+FoxP3+ Tregs (Fig. 1 E).

48

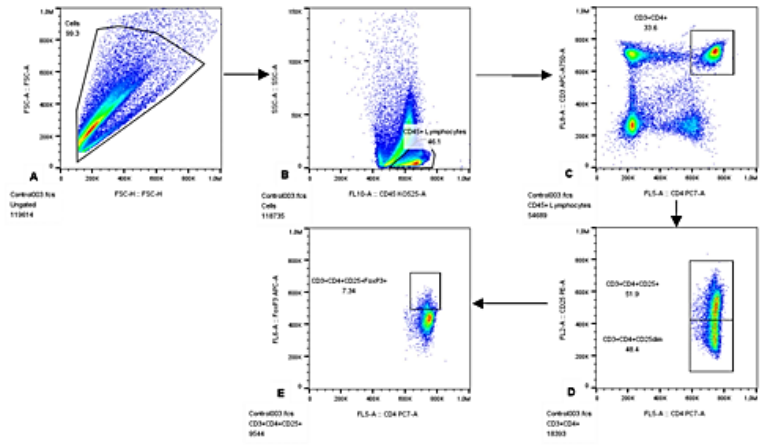

Figure 1: Gating strategy used to identify CD25+FoxP3+ Tregs in study participant peripheral blood.

49 To further improve the characterisation of CD25+FoxP3+ Tregs detected using this panel, determine the MFI of CD127, CD39, CD45RA, and Helios on these cells.

Gating strategy for the basic immunophenotyping panel

50 Create a Forward Scatter Height (FSC-H) vs. Forward Scatter Area (FSC-A) plot and gate singlet events (Fig. 2 A). Next, create a CD45 vs. side scatter (SSC) dot plot and gate the CD45+ leukocytes (Fig. 2 B).

51

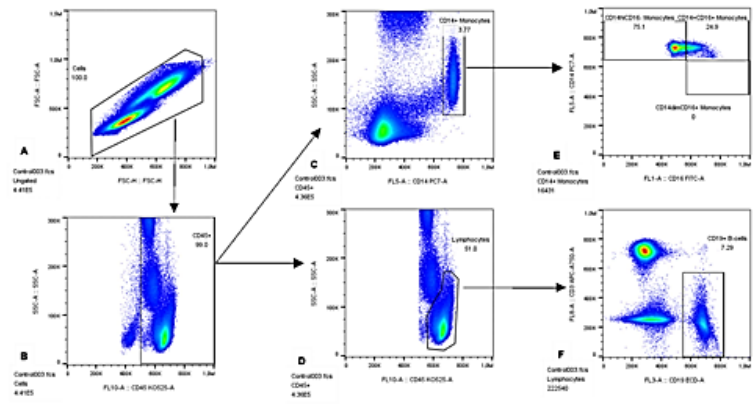

Figure 2: Gating strategy used to identify T-cell, B-cell, NK cell, and monocyte subsets in study participant whole blood.

52 Create a CD14 vs. SSC-A dot plot and gate the CD14+ cells (monocytes) (Fig. 2 C). Next, create a CD45 vs. SSC-A dot plot and gate the CD45+ lymphocytes (Fig. 2 D).

53 To identify classical (CD14+CD16-), intermediate (CD14+CD16+), and non-classical (CD14dimCD16+) monocytes, create a CD16 vs. CD14 dot plot, apply the gated CD14+ events, and gate the three subsets as shown in figure 2 plot E.

54 To identify B-lymphocytes, create a CD19 vs. CD3 dot plot, apply the CD45+ lymphocytes gate, and gate CD19+CD3- events (Fig. 2 F).

55

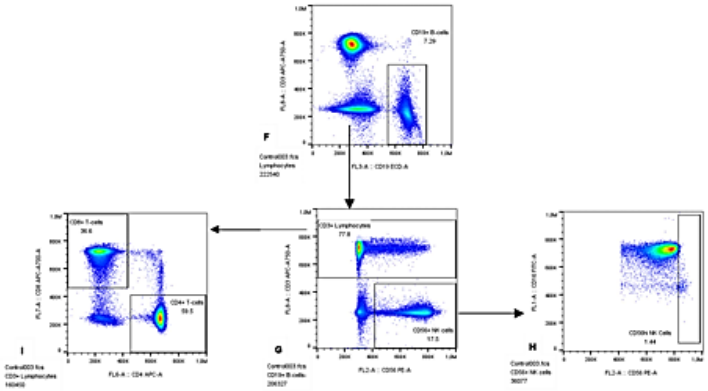

Figure 2 continued: gating strategy for the identification of T-cell, B-cell, NK cell, and monocyte subsets in participant peripheral blood.

56 Use a Boolean gate to exclude B-cells from the rest of the gating strategy, then create a CD56 vs. CD3 dot plot and gate CD3+ Lymphocytes and CD56+ NK

cells (Fig. 2 G).

57 Using the gated CD3+ lymphocytes, create a CD4 vs. CD8 dot plot and identify the cytotoxic (CD4-CD8+) and helper (CD4+CD8-) T-cells (Fig. 2 I).

58 To identify a cytokine-producing NK subset, create a CD56 vs. CD16 dot plot, apply the CD56+ NK cell population, and gate the CD56high NK cells (Fig. 2 H).

59 Record the mean fluorescence intensity (MFI) of CD206 on B-cells; CD56, CD206, and HLA-DR on monocytes; and CD16 and HLA-DR on NK cells.

Appendix C: Appendices for Chapter 3

Table 1: Participant demographics

Participant study number	Age (years)	BMI (kg/m^2)	Smoker	Ki-67% (%)	TIL% (%)	Tumour grade	Primary tumour location (left/right breast)	Treatment response at primary tumour site-PIC or PCR	Response on opposing side-benign, PIC, or PCR
Control 1	42	-	-	-	-	-	-	-	-
Control 3	24	-	-	-	-	-	-	-	-
Control 4	29	-	-	-	-	-	-	-	-
Control 5	23	-	-	-	-	-	-	-	-
Control 6	47	-	-	-	-	-	-	-	-
Control 7	23	-	-	-	-	-	-	-	-
Control 8	25	-	-	-	-	-	-	-	-
Control 9	64	-	-	-	-	-	-	-	-
Control 10	26	-	-	-	-	-	-	-	-
Control 11	23	-	-	-	-	-	-	-	-
PT270	37	23.5	No	94	-	3	Left	PCR	-
PT272	41	27.7	No	50	-	3	Left	PIC	Benign
PT273	68	-	-	15	-	3	Right	PIC	PCR
PT275	48	32	No	55	2	3	Left	PCR	Benign
PT276	34	33.8	Yes	40	-	3	Right	PCR	PIC
PT277	30	25.3	No	80	-	3	Right	PCR	Benign
PT278	60	35.6	No	52	-	2	Left	PIC	Benign
PT279	65	29.6	No	80	-	3	Right	PCR	-
PT280	56	35.1	No	50	-	3	Right	PIC	Benign
PT282	46	26.3	No	90	-	3	Right	PIC	Benign
PT283	58	22.9	No	90	-	3	Left	PCR	Benign
PT284	57	24.8	No	98	40	3	Left	PIC	Benign

PT285	49	31.5	No	20	-	3	Right	PCR	-
PT287	51	17.6	Yes	100	20	3	Right	PCR	Benign
PT288	63	28.3	Yes	38	5	2	Right	PIC	-
PT290	45	33.1	No	68	-	3	Left	PCR	Benign
PT307	60	26.1	No	73	15	3	Right	PCR	-
PT309	34	22.9	No	96	5	3	Left	PIC	Benign
PT310	64	24.1	No	58	-	3	Right	-	-
PT312	50	25	No	80	-	3	Right	-	-
PT313	60	27.7	No	75	-	3	Left	-	-
PT314	43	20.8	Yes	85	-	3	Left	-	-
PT315	59	23.6	No	66	30	3	Left	-	-
BMI: body mass index. Ki-67: Antigen Kiel-67. TIL: tumour-infiltrating lymphocyte. PCR: pathological complete response. PIC: persistent invasive carcinoma.									

Table 2: Patient full blood count results before first-phase treatment

Patient study number	Erythrocyte count (x10^12/L)	Leukocyte count (x10^9/L)	Neutrophil count (x10^9/L)	Lymphocyte count (x10^9/L)	Monocyte count (x10^9/L)	Eosinophil count (x10^9/L)	Basophil count (x10^9/L)	NLR	Platelets (x10^9/L)
PT270	4.54	7.31	4.48	2.22	0.51	0.07	0.03	2.02	309
PT272	3.99	5.38	3.53	1.56	0.25	0.03	0.01	2.26	366
PT273	4.26	9.71	7.05	2.09	0.52	0.03	0.02	3.37	296
PT275	5.23	9.49	6.37	2.41	0.52	0.15	0.04	2.64	340
PT276	4.79	11.84	6.72	4.45	0.47	0.17	0.03	1.51	274
PT277	5.5	4.75	2.59	1.69	0.29	0.15	0.03	1.53	326
PT278	4.43	4.94	2.68	1.65	0.44	0.15	0.02	1.62	290
PT279	4.51	6.33	2.88	2.9	0.41	0.12	0.02	0.99	369
PT280	5.32	7.05	4.44	1.82	0.51	0.2	0.08	2.44	327
PT282	4.38	6.18	3.74	1.54	0.59	0.28	0.03	2.43	345
PT283	4.38	6.68	3.78	2.31	0.43	0.11	0.05	1.64	198
PT284	4.8	3.93	1.33	2.18	0.31	0.04	0.07	0.61	243
PT285	4.18	6.58	3.58	2.54	0.37	0.05	0.04	1.41	302
PT287	5.1	6.79	3.89	2.43	0.37	0.05	0.05	1.6	227
PT288	4.87	7.23	3.53	2.58	0.83	0.23	0.06	1.37	175
PT290	5.35	9.55	5.84	2.22	0.89	0.52	0.08	2.63	210
PT307	4.76	7.7	4	3	0.51	0.14	0.05	1.33	269
PT309	4.57	7.82	4.92	2.15	0.44	0.25	0.06	2.29	343
PT310	5.06	8.1	4.53	2.86	0.58	0.11	0.02	1.58	289
PT312	4.39	7.57	4.65	2.32	0.46	0.08	0.06	2	250
PT313	4.61	4.91	3.3	1.07	0.35	0.17	0.02	3.08	96
PT314	3.97	6.33	2.37	3.35	0.55	0.03	0.03	0.71	199
PT315	4.74	6.93	3.75	2.49	0.57	0.08	0.04	1.51	343

NLR: neutrophil-lymphocyte ratio.

Table 3: Patient full blood count results after first-phase treatment

Patient study number	Erythrocyte count (x10^12/L)	Leukocyte count (x10^9/L)	Neutrophil count (x10^9/L)	Lymphocyte count (x10^9/L)	Monocyte count (x10^9/L)	Eosinophil count (x10^9/L)	Basophil count (x10^9/L)	NLR	Platelets (x10^9/L)
PT270	3.44	2.91	1.46	0.68	0.75	0	0.02	2.15	236
PT272	3.61	6.77	5.2	0.95	0.6	0.01	0.01	5.47	459
PT273	2.86	4.65	3.37	0.56	0.68	0.02	0.02	6.02	344
PT275	4.21	7.93	6.11	0.97	0.65	0.1	0.1	6.3	364
PT276	3.4	8.37	5.42	2.07	0.83	0.01	0.04	2.62	302
PT277	3.87	5.3	3.17	1.52	0.57	0.01	0.03	2.09	322
PT278	3.45	6.12	4.24	0.68	1.1	0.01	0.09	6.24	410
PT279	3.52	9.62	6.52	1.72	1.02	0.28	0.08	3.79	466
PT280	4.42	11.49	8.98	1.48	0.96	0.01	0.06	6.07	405
PT282	3.71	3.65	2.38	0.61	0.6	0.02	0.04	3.9	324
PT283	3.63	6.15	4.25	1.03	0.66	0.14	0.07	4.13	367
PT284	4.17	1.45	0.5	0.81	0.04	0.08	0.01	0.62	92
PT285	3.26	7.45	5.74	1.34	0.37	0	0	4.28	224
PT287	4.15	4.08	2.52	1.14	0.34	0.04	0.04	2.21	61
Pt288	4.39	6.08	3.26	1.34	1.25	0.13	0.1	2.43	430
PT290	4.81	6.69	4.24	1.1	1.13	0.15	0.07	3.85	284
PT307	3.62	3.62	2.49	0.92	0.89	0	0.03	2.71	237
PT309	3.52	7.51	5.51	1.34	0.59	0.04	0.03	4.11	360
PT310	3.75	6.12	3.5	2.08	0.49	0.04	0.01	1.68	142
PT312	3.73	6.71	4.29	1.63	0.7	0.01	0.08	2.63	326
PT313	3.16	3.25	2.14	0.58	0.51	0	0.02	3.69	61
PT314	2.69	7.52	4.76	1.95	0.78	0.01	0.02	2.44	222
PT315	3.82	5.85	3.51	1.19	1.06	0.01	0.08	2.95	345

NLR: neutrophil-lymphocyte ratio.

Table 4: CD3⁺ lymphocyte subsets detected in participant peripheral blood using the basic immunophenotyping panel

	Healthy donors (n=10)	**Pre-chemotherapy**	**After first-phase chemotherapy**	**P-value (whole group)**	**P-value (healthy donors vs. pre-chemotherapy)**	**P-value (healthy donors vs. post-first-phase-chemotherapy)**	**P-value (pre-chemotherapy vs. post-first-phase chemotherapy)**
Frequency of parent cell population; median % (range)							
CD3⁺ lymphocytes, % of "Lymphocytes" that are not CD19⁺ B-cells	79.65 (64.3-86.3)	78.8 (43.9-93.8)	77.95 (5.37-95.4)	0.4	0.3942	0.1245	0.1349
CD4⁺ T-cells, % of CD3⁺ lymphocytes	59.65 (43.2-79.7)	61.3 (30-83.5)	58.6 (27.4-75.3)	0.6426	0.4086	0.3055	0.1770
CD8⁺ T-cells, % of CD3⁺ lymphocytes	34.55 (17.4-47.7)	32.8 (12-64.3)	34.6 (21.5-66.4)	0.8756	0.3755	0.4680	0.3085
CD4 MFI; geometric mean (range)							
CD3⁺ lymphocytes	438000 (369282-559000)	460000 (308067-574000)	462000 (322602-522000)	0.6709	0.1879	0.3020	0.3202
CD8 MFI; geometric mean (range)							
CD3⁺ lymphocytes	339941 (296559-395142)	366248 (291231-552000)	384913.5 (305448-528000)	0.0508	0.0606	0.0074**	0.1369
** p≤0.01. MFI: mean fluorescence intensity.							

Table 5: CD19$^+$ B-cell subsets detected by flow cytometry in participant peripheral blood using the basic immunophenotyping panel

	Healthy donors (n=10)	**Pre-chemotherapy**	**After first-phase chemotherapy**	**P-value (whole group)**	**P-value (healthy donors vs. pre-chemotherapy)**	**P-value (healthy donors vs. post-first-phase-chemotherapy)**	**P-value (pre-chemotherapy vs. post-first-phase chemotherapy)**
Frequency of parent cell population; median % (range)							
CD19$^+$ B-cells, % of lymphocytes	9.35 (7.09-15.5)	8.23 (2.35-21)	1.105 (0.2-15.5)	0.0001****	0.2847	≤0.0001****	≤0.0001****
CD206 MFI; geometric mean (range)							
CD19$^+$ B-cells	179270.5 (137475-254922)	302214 (219962-502000)	407500 (51137-617000)	0.0001****	0.0006****	≤0.0001****	0.0103*
**** p≤0.0001, * p≤0.05. MFI: mean fluorescence intensity.							

Table 6: CD56$^+$ NK cell subsets detected in participant peripheral blood using the basic immunophenotyping panel

	Healthy donors (n=10)	**Pre-chemotherapy**	**After first-phase chemotherapy**	**P-value (whole group)**	**P-value (healthy donors vs. pre-chemotherapy)**	**P-value (healthy donors vs. post-first-phase-chemotherapy)**	**P-value (pre-chemotherapy vs. post-first-phase chemotherapy)**
Frequency of parent cell population; median % (range)							
CD56$^+$ NK cells, % of "Lymphocytes" that are not CD19$^+$ B-cells	12.85 (7.73-25)	10.4 (3.67-34.1)	11.8 (3.01-90.7)	0.5274	0.1880	0.4643	0.1579
CD56^{high} NK cells, % of CD56$^+$ NK cells	5.27 (1.44-8.86)	4.31 (0-9.1)	9.24 (0.076-28.6)	0.0107*	0.1889	0.0665	0.0014***
CD16 MFI; geometric mean (range)							
CD56$^+$ NK cells	692500 (656000-776000)	690000 (71720-752000)	667000 (403000-751000)	0.1853	0.2416	0.0428*	0.1028
CD56^{high} NK cells	545000 (497000-594000)	542000 (0-631000)	574000 (488000-747000)	0.0192*	0.2349	0.0678	0.0027***
HLA-DR MFI; geometric mean (range)							
CD56$^+$ NK cells	250575.5 (218198-287753)	238455 (216815-529000)	305042.5 (234791-633000)	0.0010***	0.4167	0.0050**	0.0002****
CD56^{high} NK cells	329829 (267738-391503)	312408 (0-367866)	335657.5 (270965-420000)	0.0155*	0.0514	0.2649	0.0023***
**** p≤0.0001, *** p≤0.001, ** p≤0.01, * p≤0.05. NK cell: natural killer cell. MFI: mean fluorescence intensity.							

Table 7: Monocyte subsets detected by flow cytometry in participant peripheral blood using the basic immunophenotyping panel

	Healthy donors (n=10)	Pre-chemotherapy	After first-phase chemotherapy	P-value (whole group)	P-value (healthy donors vs. pre-chemotherapy)	P-value (healthy donors vs. post-first-phase-chemotherapy)	P-value (pre-chemotherapy vs. post-first-phase chemotherapy)
Frequency of parent cell population; median % (range)							
CD14⁺ monocytes, % of CD45⁺ cells	6.55 (486000-616000)	4.72 (1.11-11)	9.355 (1.21-17.1)	0.0001****	0.0764	0.0258*	≤0.0001****
Intermediate monocytes, % of CD14⁺ monocytes	5.27 (3.37-95.9)	14.3 (3.45-84.8)	11.2 (2.22-90.4)	0.7786	0.2408	0.3345	0.3625
Non-classical monocytes, % of CD14⁺ monocytes	0	0	0 (0-0.47)	0.2378	0.5	0.1077	0.0607
Classical monocytes, % of CD14⁺ monocytes	94.25 (4.15-96.6)	85.7 (15.2-96.4)	88.8 (9.57-97.7)	0.7960	0.2512	0.3452	0.3644
CD56 MFI; geometric mean (range)							
Intermediate monocytes	408500 (330762-515000)	473000 (367447-556000)	527500 (422000-637000)	0.0001****	0.0247*	≤0.0001****	0.0027***
Non-classical monocytes	0	0	0 (0-547000)	0.2378	0.5	0.1077	0.0607
Classical monocytes	386717 (332776-527000)	468000 (346884-531000)	513500 (413000-573000)	0.0001****	0.0247*	≤0.0001****	0.0013***
CD206 MFI; geometric mean (range)							
Intermediate monocytes	460000 (430000-473000)	481000 (328644-544000)	492000 (450000-637000)	0.0025***	0.0023***	0.0003****	0.2507
Non-classical monocytes	0	0	0 (0-474000)	0.2378	0.5	0.1077	0.0607

Classical monocytes	449000 (417000-473000)	464000 (335937-4890000)	465000 (432000-509000)	0.0362*	0.0268*	0.0052**	0.2189
HLA-DR MFI; geometric mean (range)							
Intermediate monocytes	625000(528000-705000)	605000 (523000-721000)	614500 (402000-742000)	0.9834	0.4369	0.4308	0.4929
Non-classical monocytes	0	0	0 (0-573000)	0.2378	0.5	0.1077	0.0607
Classical monocytes	580500 (536000-618000)	5780000 (498000-651000)	574500 (467000-648000)	0.8675	0.4902	0.3424	0.3168
**** p≤0.0001, *** p≤0.001, ** p≤0.01, * p≤0.05. MFI: mean fluorescence intensity							

Appendix D: Appendices for Chapter 4

Table 1: Frequency of parent and geometric mean values for $CD4^+CD25^+FoxP3^+$ Tregs detected in participant peripheral blood using the Treg immunophenotyping panel

	Healthy donors (n=10)	**Pre-chemotherapy (n=19)**	**After first-phase chemotherapy (n=19)**	**P-value (whole group)**	**P-value (healthy donors vs. pre-chemotherapy)**	**P-value (healthy donors vs. post-first-phase-chemotherapy)**	**P-value (pre-chemotherapy vs. post-first-phase chemotherapy)**
Frequency of parent; median % (range)							
$CD4^+CD25^+FoxP3^+$, % of $CD4^+CD25^+$ lymphocytes	18.65 (10-32)	17.3 (5.83-99.9)	19.3 (11.2-98.6)	0.9618	0.3901	0.4275	0.4539
CD45RA MFI; geometric mean (range)							
$CD4^+CD25^+FoxP3^+$ lymphocytes	302395.5 (238164-400000)	296673 (232951-356678)	285334 (35788-325642)	0.2006	0.4211	0.1121	0.0443*
CD39 MFI; geometric mean (range)							
$CD4^+CD25^+FoxP3^+$ lymphocytes	413500 (361696-461000)	452000 (383723-576000)	465000 (397937-540000)	0.0024**	0.0046**	0.0003***	0.1539
CD127 MFI; geometric mean (range)							
$CD4^+CD25^+FoxP3^+$ lymphocytes	258720.5 (229427-316372)	281161 (109561-524000)	289945 (138821-314321)	0.1361	0.0692	0.0237*	0.2734
Helios MFI; geometric mean (range)							
$CD4^+CD25^+FoxP3^+$ lymphocytes	476500 (423000-489000)	470000 (408000-506000)	484000 (381271-542000)	0.2151	0.4598	0.1046	0.0511
*** p≤0.001, ** p≤0.01, * p≤0.05. FoxP3: Forkhead Box Protein 3. MFI: mean fluorescent intensity.							

Appendix E: Appendices for Chapter 5

Table 1: Analyte concentration in healthy donor and treatment-naïve TNBC patient plasma

Study number	VEGF concentration, pg/ml	IP-10 concentration, pg/ml	GDF-15 concentration, pg/ml	IL-6 concentration, pg/ml	IL-8 concentration, pg/ml	IL-10 concentration, pg/ml	GM-CSF concentration, pg/ml
Control 1	177.60	62.08	1090.47	1.21	73.35	0.58	93.19
Control 3	186.11	72.60	755.40	0.93	69.02	0.87	93.19
Control 4	693.75	284.50	645.29	0.64	67.92	0.87	93.19
Control 5	581.13	172.96	648.23	0.64	65.68	0.87	93.19
Control 6	70.07	232.61	1719.52	0.00	71.20	0.30	89.08
Control 7	1325.50	136.86	472.40	1.21	64.54	2.01	91.13
Control 8	1005.12	247.14	643.63	0.00	62.24	0.02	84.94
Control 9	391.90	293.28	1272.15	0.35	74.41	0.00	84.94
Control 10	1795.81	90.41	727.21	0.64	66.80	1.44	91.13
Control 11	930.56	29.05	1231.43	2.07	75.45	1.15	103.33
PT270	302.90	1373.66	913.27	0.93	73.35	3.73	93.19
PT277	438.12	103.71	1261.95	0.93	70.12	0.30	87.01
PT278	394.78	410.17	1677.33	0.35	77.53	0.02	103.33
PT279	1247.12	127.46	2875.50	0.64	80.57	0.30	105.34
PT280	2051.24	1322.33	783.75	0.93	87.37	1.15	91.13
PT272	531.25	360.56	1385.04	0.07	67.92	0.02	89.08
PT273	1398.22	249.18	2149.23	11.79	75.45	0.02	105.34
PT275	152.09	130.92	1110.45	0.35	67.92	0.58	91.13
PT276	368.87	15.34	1160.63	1.50	69.02	0.87	93.19
PT282	557.62	216.43	2143.92	0.64	82.55	0.30	91.13
PT283	933.65	196.91	1277.25	0.07	72.28	0.30	87.01
PT284	39.01	51.70	1190.90	0.35	67.92	0.58	89.08
PT285	58.77	230.26	561.61	0.93	66.80	0.87	99.30
PT287	101.15	581.08	1216.20	2.64	66.80	0.30	93.19

PT288	717.68	378.87	1483.51	0.07	74.41	2.87	91.13
PT290	61.59	446.83	918.13	0.35	66.80	0.30	91.13
PT307	351.62	292.17	991.42	1.21	72.28	0.58	95.23
PT309	551.75	189.20	699.18	0.35	67.92	0.02	99.30
PT310	203.15	57.52	1313.05	0.35	70.12	0.30	89.08
PT312	78.54	19.98	779.02	0.93	65.68	0.30	89.08
PT313	308.62	164.73	1130.48	3.49	82.55	0.58	95.23
PT314	197.47	138.12	2149.23	0.64	91.07	0.87	89.08
PT315	513.72	204.51	441.67	0.35	61.08	0,02	93.19
VEGF: vascular endothelial growth factor. IP-10: interferon gamma-induced protein. GDF-15: growth and differentiation factor-15. IL-6: interleukin-6. IL-8: interleukin-8. IL-10: interleukin-10. GM-CSF: granulocyte-macrophage colony stimulating factor.							

Table 2: Analyte concentration in the plasma of patients after first-phase chemotherapy

Study number	VEGF concentration, pg/ml	IP-10 concentration, pg/ml	GDF-15 concentration, pg/ml	IL-6 concentration, pg/ml	IL-8 concentration, pg/ml	IL-10 concentration, pg/ml	GM-CSF concentration, pg/ml
PT270	406.32	196.91	37412.89	1.21	109.49	1.44	93.19
Pt277	1981.98	728.65	3047.16	0.93	81.56	1.15	99.30
PT278	432.33	1361.55	4157.18	1.50	97.28	0.30	87.01
PT279	4273.69	1469.47	2698.72	2.07	80.57	1.44	93.19
PT280	1394.89	311.47	1672.06	0.93	74.41	1.44	91.13
PT272	1318.93	1405.03	1788.24	1.50	85.46	0.87	95.23
PT273	4377.48	929.12	3751.92	14.78	100.67	0.30	87.01
PT275	231.58	268.13	1431.58	0.64	72.28	0.87	91.13
PT276	389.02	197.26	1703.69	1.21	75.45	1.15	95.23
PT282	522.48	431.04	3690.98	1.21	114.01	0.87	95.23
PT283	844.61	154.71	1714.24	2.07	66.80	0.02	84.94
PT284	10.79	13.33	2611.36	1.50	87.37	0.58	93.19
PT285	123.77	250.88	2005.81	1.5	80.57	1.15	97.27
PT287	120.95	106.57	3567.30	3.49	82.55	0.87	99.30
PT288	856.83	1468.37	3356.89	0.35	94.66	4.30	89.08
PT290	115.29	464.34	2626.84	0.93	85.46	0.58	123.12
PT307	200.31	611.06	2037.69	1.21	81.56	0.87	97.27
PT309	357.37	311.47	1379.88	1.78	76.49	0.58	99.30
PT310	257.21	142.67	2080.20	0.64	79.56	0.00	82.86
PT312	50.30	136.86	2387.13	0.64	77.53	0.87	107.34
PT313	146.42	722.13	3559.29	3.20	94.66	14.83	97.27
PT314	386.14	139.78	4164.19	1.21	98.14	0.87	97.27
PT315	631.31	879.14	1323.30	0.00	78.55	1.72	95.23

VEGF: vascular endothelial growth factor. IP-10: interferon gamma-induced protein. GDF-15: growth and differentiation factor-15. IL-6: interleukin-6. IL-8: interleukin-8. IL-10: interleukin-10. GM-CSF: granulocyte-macrophage colony stimulating factor.

Table 3: Circulating VEGF, IP-10, GM-CSF, GDF-15, IL-6, IL-8, IL-10 levels in healthy donors and TNBC patients detected using ELISAs

	Healthy donors (n=10)	Pre-chemotherapy (n=23)	After first-phase chemotherapy (n=23)	p-value (whole group)	p-value (healthy donors vs. pre-chemotherapy)	P-value (healthy donors vs. post-first-phase-chemotherapy)	P-value (pre-chemotherapy vs. post-first-phase chemotherapy)
VEGF, median pg/ml (range)	637.44 (70.07-1795.81)	368.87 (39.01-2051.24)	389.02 (10.79-4377.48)	0.5307	0.1307	0.2330	0.3063
IP-10, median pg/ml (range)	154.91 (29.05-293.28)	204.51 (15.34-1373.66)	311.47 (13.33-1469.47)	0.0193*	0.1476	0.0047**	0.0231*
GM-CSF, median pg/ml (range)	92.16 (84.94-103.33)	91.13 (87.01-105.34)	95.23 (82.86-123.12)	0.2753	0.2464	0.0643	0.1241
GDF-15, median pg/ml (range)	741.30 (472.4-1719.52)	1190.9 (441.67-2875.50)	2611.36 (1323.30-37412.9)	0.0001****	0.0822	≤0.0001****	≤0.0001****
IL-6, median pg/ml (range)	0.64 (0-2.07)	0.64 (0.07-11.79)	1.21 (0-14.78)	0.0136*	0.4616	0.0151*	0.0039**
IL-8, median pg/ml (range)	68.47 (62.24-75.45)	70.12 (61.08-91.07)	81.56 (66.80-114.01)	0.0001****	0.1115	≤0.0001****	0.0001****
IL-10, median pg/ml (range)	0.87 (0-2.01)	0.30 (0.017-3.73)	0.87 (0-14.83)	0.0275*	0.1022	0.2901	0.0038**
**** p≤0.0001, ** p≤0.01, * p≤0.05. VEGF: vascular endothelial growth factor. IP-10: interferon gamma-induced protein. GM-CSF: granulocyte-macrophage colony stimulating factor. GDF-15: growth and differentiation factor-15. IL-6: interleukin-6. IL-8: interleukin-8. IL-10: interleukin-10.							

Figure 1: VEGF ELISA kit standard curve

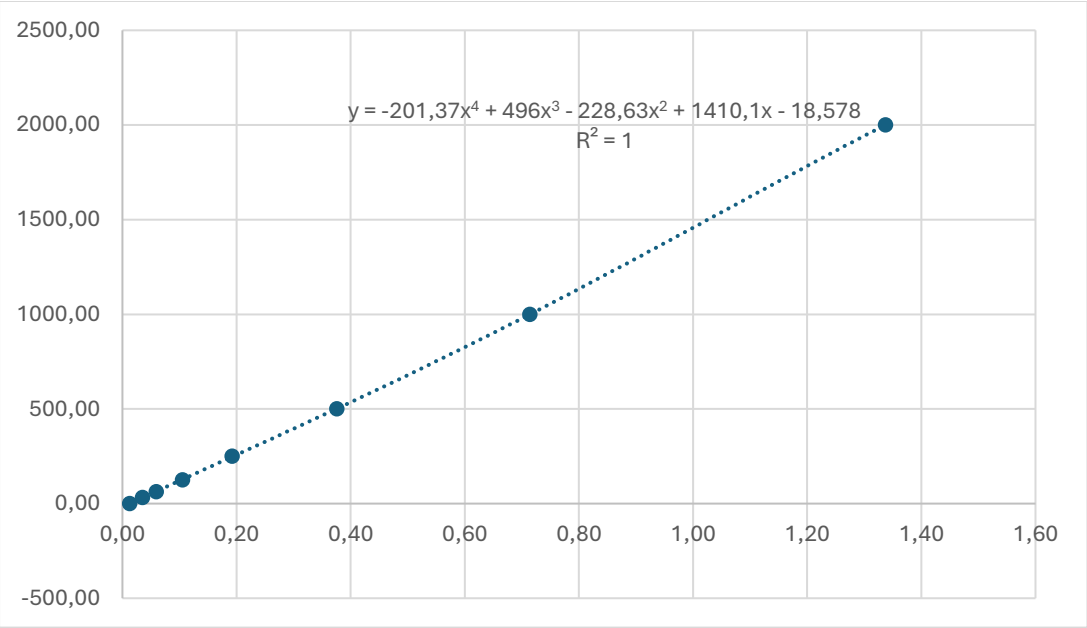

Standard number	Concentration* (pg/ml)	Optical density (optical density units (ODU))
Standard 1	2000.00	1.34
Standard 2	1000.00	0.71
Standard 3	500.00	0.38
Standard 4	250.00	0.19
Standard 5	125.00	0.11
Standard 6	62.5	0.06
Standard 7	31.25	0.04
Blank	0.00	0.01
*Standard concentration values are derived from the product information booklet.		

Figure 2: IP-10 ELISA kit standard curve

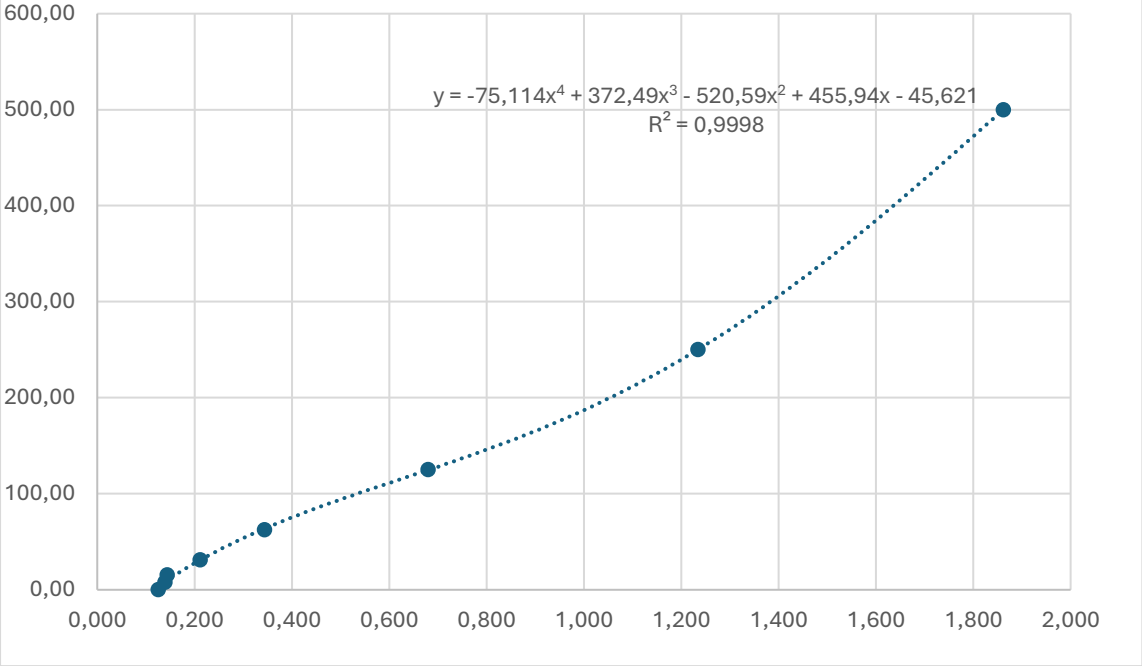

Standard number	Concentration* (pg/ml)	Optical density (ODU)
Standard 1	500.00	1.862
Standard 2	250.00	1.234
Standard 3	125.00	0.680
Standard 4	62.50	0.344
Standard 5	31.25	0.212
Standard 6	15.63	0.144
Standard 7	7.81	0.139
Blank	0.00	0.126
*Standard concentration values are derived from the product information booklet.		

Figure 3: GDF-15 ELISA kit standard curve

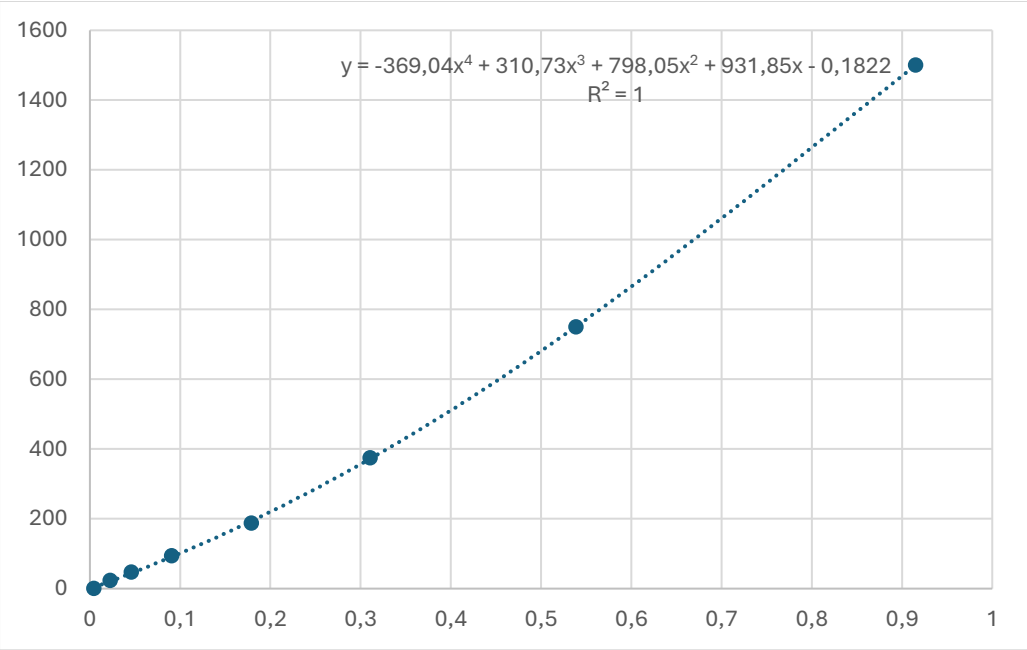

Standard number	Concentration* (pg/ml)	Optical density (ODU)
Standard 1	1500.00	0.915
Standard 2	750.00	0.5385
Standard 3	375.00	0.3105
Standard 4	187.5	0.179
Standard 5	93.75	0.0905
Standard 6	46.88	0.046
Standard 7	23.44	0.0225
Blank	0.00	0.0045
*Standard concentration values are derived from the product information booklet.		

Figure 4: IL-10 ELISA kit standard curve

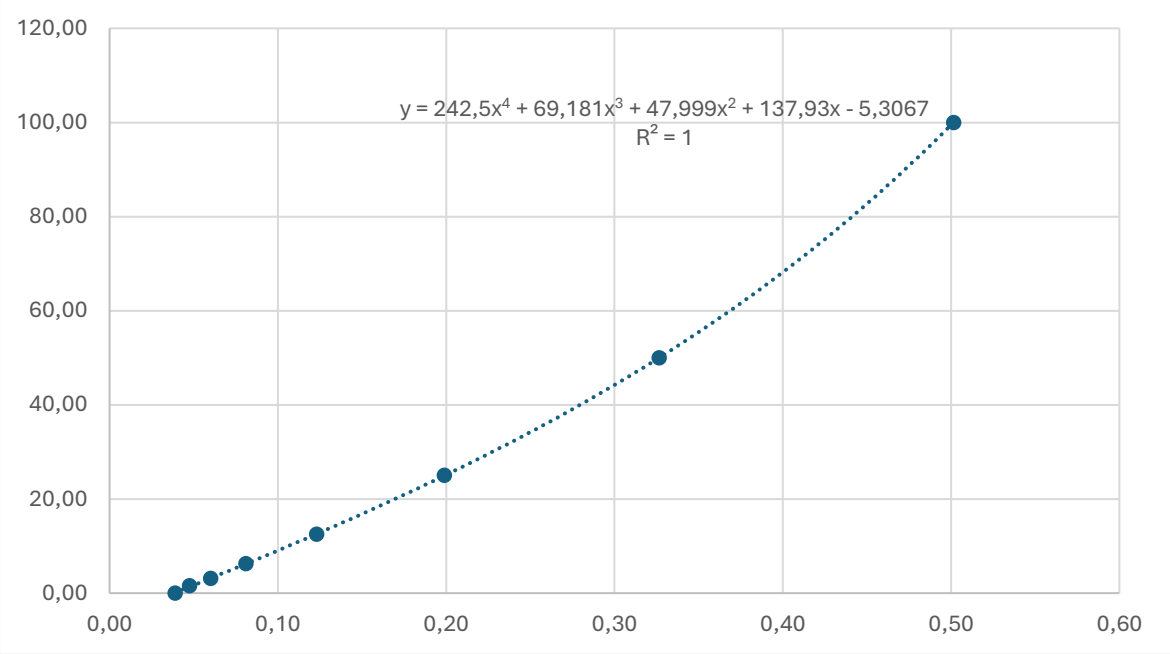

Standard number	Concentration* (pg/ml)	Optical density (ODU)
Standard 1	100.00	0.50
Standard 2	50.00	0.33
Standard 3	25.00	0.20
Standard 4	12.50	0.12
Standard 5	6.25	0.08
Standard 6	3.13	0.06
Standard 7	1.56	0.05
Blank	0.00	0.04
*Standard concentration values are derived from the product information booklet.		

Figure 5: IL-6 ELISA kit standard curve

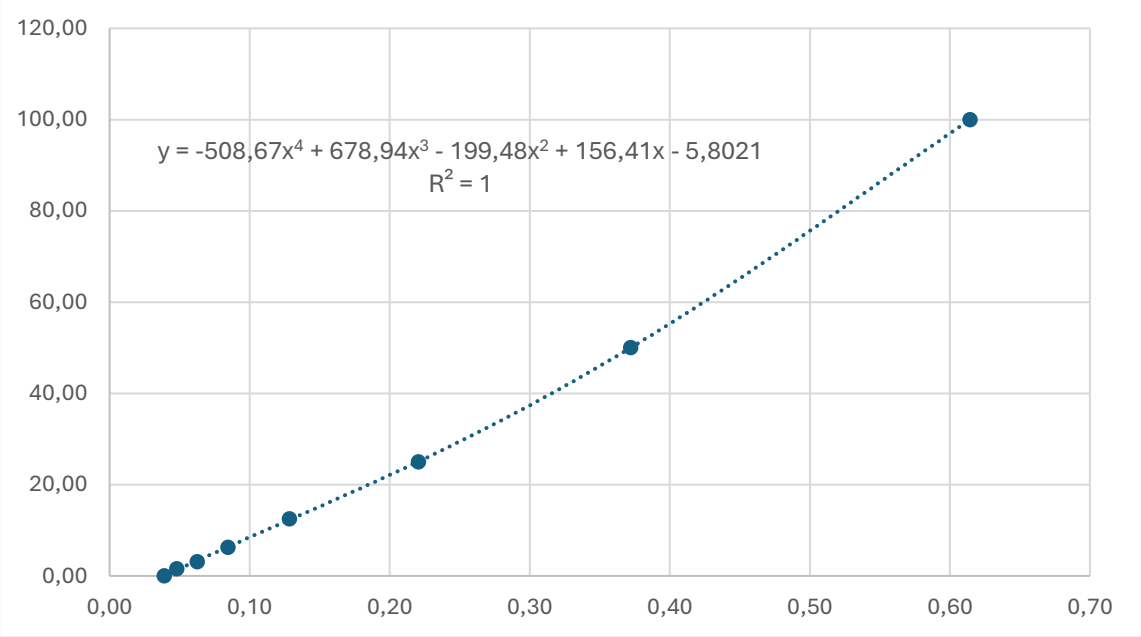

Standard number	Concentration* (pg/ml)	Optical density (ODU)
Standard 1	100.00	0.61
Standard 2	50.00	0.37
Standard 3	25.00	0.22
Standard 4	12.50	0.13
Standard 5	6.25	0.08
Standard 6	3.13	0.06
Standard 7	1.56	0.05
Blank	0.00	0.04
*Standard concentration values are derived from the product information booklet.		

Figure 6: IL-8 ELISA kit standard curve

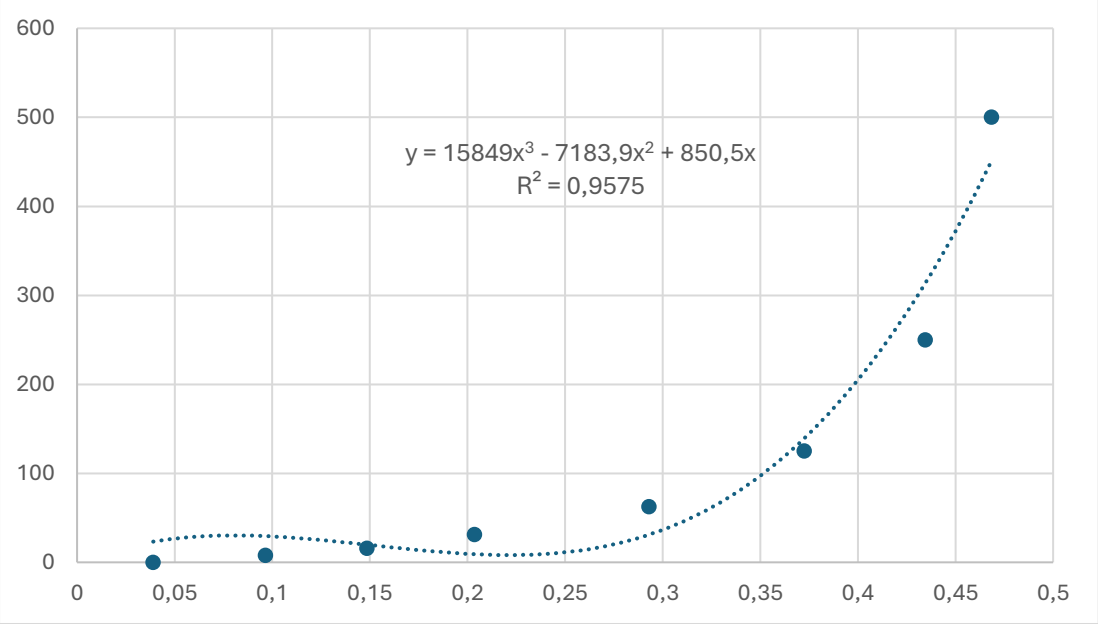

Standard number	Concentration* (pg/ml)	Optical density (ODU)
Standard 1	500.00	0.4685
Standard 2	250.00	0.4345
Standard 3	125.00	0.3725
Standard 4	62.50	0.293
Standard 5	31.25	0.2035
Standard 6	15.63	0.1485
Standard 7	7.81	0.0965
Blank	0.00	0.039
*Standard concentration values are derived from the product information booklet.		

Figure 7: GM-CSF ELISA kit standard curve

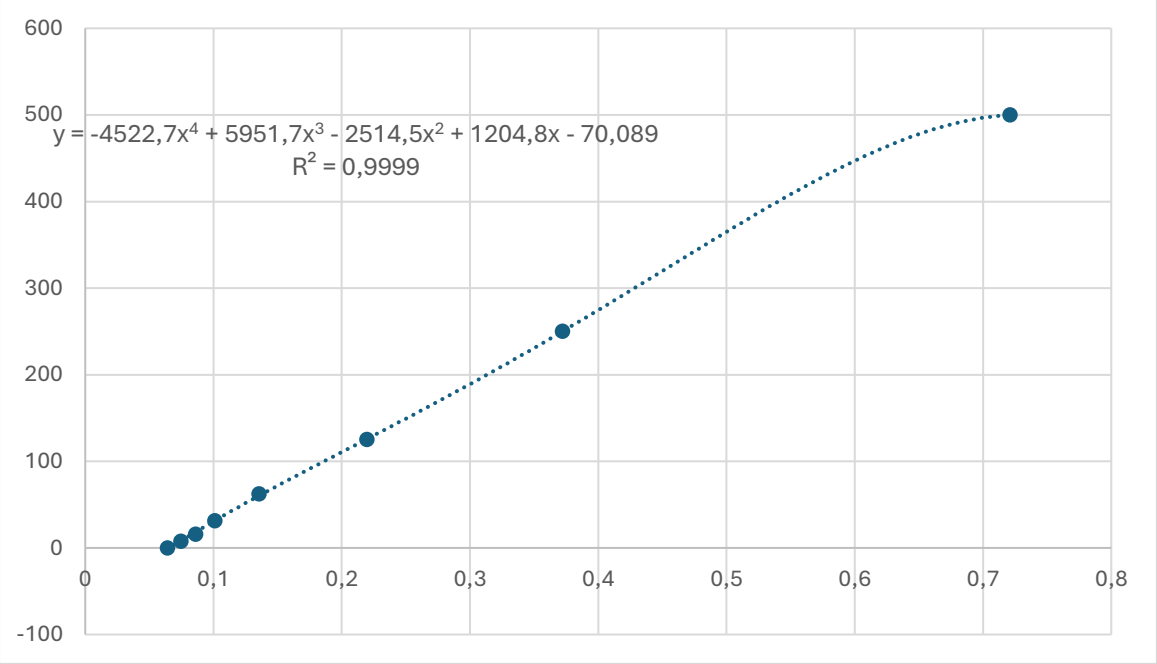

Standard number	Concentration* (pg/ml)	Optical density (ODU)
Standard 1	500.00	0.721
Standard 2	250.00	0.372
Standard 3	125.00	0.2195
Standard 4	62.50	0.1355
Standard 5	31.25	0.101
Standard 6	15.63	0.086
Standard 7	7.81	0.0745
Blank	0.00	0.064
*Standard concentration values are derived from the product information booklet.		